Shell variability in the basal turtles *Proterochersis* spp. (#29084)

First submission

Editor guidance

Please submit by **14 Jul 2018** for the benefit of the authors (and your $200 publishing discount).

Structure and Criteria
Please read the 'Structure and Criteria' page for general guidance.

Author notes
Have you read the author notes on the guidance page?

Raw data check
Review the raw data. Download from the materials page.

Image check
Check that figures and images have not been inappropriately manipulated.

Privacy reminder: If uploading an annotated PDF, remove identifiable information to remain anonymous.

Files
Download and review all files from the materials page.

10 Figure file(s)
2 Other file(s)

Structure and Criteria

Structure your review

The review form is divided into 5 sections. Please consider these when composing your review:

1. **BASIC REPORTING**
2. **EXPERIMENTAL DESIGN**
3. **VALIDITY OF THE FINDINGS**
4. General comments
5. Confidential notes to the editor

You can also annotate this PDF and upload it as part of your review

When ready submit online.

Editorial Criteria

Use these criteria points to structure your review. The full detailed editorial criteria is on your guidance page.

BASIC REPORTING

- Clear, unambiguous, professional English language used throughout.
- Intro & background to show context. Literature well referenced & relevant.
- Structure conforms to PeerJ standards, discipline norm, or improved for clarity.
- Figures are relevant, high quality, well labelled & described.
- Raw data supplied (see PeerJ policy).

EXPERIMENTAL DESIGN

- Original primary research within Scope of the journal.
- Research question well defined, relevant & meaningful. It is stated how the research fills an identified knowledge gap.
- Rigorous investigation performed to a high technical & ethical standard.
- Methods described with sufficient detail & information to replicate.

VALIDITY OF THE FINDINGS

- Impact and novelty not assessed. Negative/inconclusive results accepted. *Meaningful* replication encouraged where rationale & benefit to literature is clearly stated.
- Data is robust, statistically sound, & controlled.
- Speculation is welcome, but should be identified as such.
- Conclusions are well stated, linked to original research question & limited to supporting results.

Standout reviewing tips

The best reviewers use these techniques

Tip	*Example*
Support criticisms with evidence from the text or from other sources	*Smith et al (J of Methodology, 2005, V3, pp 123) have shown that the analysis you use in Lines 241-250 is not the most appropriate for this situation. Please explain why you used this method.*
Give specific suggestions on how to improve the manuscript	*Your introduction needs more detail. I suggest that you improve the description at lines 57- 86 to provide more justification for your study (specifically, you should expand upon the knowledge gap being filled).*
Comment on language and grammar issues	*The English language should be improved to ensure that an international audience can clearly understand your text. Some examples where the language could be improved include lines 23, 77, 121, 128 – the current phrasing makes comprehension difficult.*
Organize by importance of the issues, and number your points	*1. Your most important issue* *2. The next most important item* *3. …* *4. The least important points*
Please provide constructive criticism, and avoid personal opinions	*I thank you for providing the raw data, however your supplemental files need more descriptive metadata identifiers to be useful to future readers. Although your results are compelling, the data analysis should be improved in the following ways: AA, BB, CC*
Comment on strengths (as well as weaknesses) of the manuscript	*I commend the authors for their extensive data set, compiled over many years of detailed fieldwork. In addition, the manuscript is clearly written in professional, unambiguous language. If there is a weakness, it is in the statistical analysis (as I have noted above) which should be improved upon before Acceptance.*

Shell variability in the basal turtles *Proterochersis* spp.

Tomasz Szczygielski Corresp., [1] , **Justyna Słowiak** [1] , **Dawid Dróżdż** [1]

[1] Department of Evolutionary Paleobiology, Institute of Paleobiology, Polish Academy of Sciences, Warsaw, Poland

Corresponding Author: Tomasz Szczygielski
Email address: t.e.szczygielski@gmail.com

Background. Turtle shells tend to exhibit frequent and substantial variability, both in bone and scute layout. Aside from secondary changes, caused by diseases, parasites, and trauma, this variability appears to be inherent and result from stochastic or externally-induced flaws of developmental programs. It is, thus, expected to be present in fossil turtle species at least as prominently, as in modern populations. Descriptions of variability and ontogeny are, however, rare for fossil turtles, mainly due to rarity, incompleteness, damage, and post-mortem deformation of their remains. This paper is an attempt at description and interpretation of external shell variability in representatives of the oldest and most basal true turtles, *Proterochersis robusta* and *P. porebensis* (Proterochersidae) from the Late Triassic (Norian) of Germany and Poland.

Methods. All the available shell remains of *Proterochersis robusta* (13 specimens) and *P. porebensis* (270 specimens) were studied morphologically in order to identify any ontogenetic changes, intraspecific variability, sexual dimorphism, and shell abnormalities. To test the inferred sexual dimorphism, the shape analysis was performed for two regions (gular and anal) of the plastron.

Results. *Proterochersis* spp. exhibits large shell variability, and at least some of the observed changes seem to be correlated with ontogeny (growth of gulars, extragulars, caudals, and marginals, disappearance of middorsal keel on the carapace) or possible sexual dimorphism (morphology of caudal processes and extragulars). Several specimens show abnormal layout of scute sulci, several others unusual morphologies of vertebral scute areas, one has an additional pair of plastral scutes, and one extraordinarily pronounced, likely pathological, growth rings on the carapace. Both species are represented in a wide spectrum of sizes, from hatchlings to old, mature individuals. The largest fragmentary specimens of *P. porebensis* allow estimation of its maximal carapace length at approximately 80 cm, while *P. robusta* appears to reach lower maximal sizes.

Discussion. This is the second contribution describing variability among numerous specimens of Triassic turtles, and the first to show evidence of unambiguous shell abnormalities. Presented data supplement the sparse knowledge of shell scute development in the earliest turtles and suggest that at least some aspects of the developmental programs governing scute development were already similar in the Late Triassic to these of modern forms.

Shell variability in the basal turtles *Proterochersis* spp.

Tomasz Szczygielski[1], Justyna Słowiak[1], Dawid Dróżdż[1]

[1]Institute of Paleobiology, Polish Academy of Sciences, Warsaw, Poland

Corresponding Author:

Tomasz Szczygielski

Email address: t.szczygielski@twarda.pan.pl

Abstract

Background. Turtle shells tend to exhibit frequent and substantial variability, both in bone and scute layout. Aside from secondary changes, caused by diseases, parasites, and trauma, this variability appears to be inherent and result from stochastic or externally-induced flaws of developmental programs. It is, thus, expected to be present in fossil turtle species at least as prominently, as in modern populations. Descriptions of variability and ontogeny are, however, rare for fossil turtles, mainly due to rarity, incompleteness, damage, and post-mortem deformation of their remains. This paper is an attempt at description and interpretation of external shell variability in representatives of the oldest and most basal true turtles, *Proterochersis robusta* and *P. porebensis* (Proterochersidae) from the Late Triassic (Norian) of Germany and Poland.

Methods. All the available shell remains of *Proterochersis robusta* (13 specimens) and *P. porebensis* (270 specimens) were studied morphologically in order to identify any ontogenetic changes, intraspecific variability, sexual dimorphism, and shell abnormalities. To test the inferred sexual dimorphism, the shape analysis was performed for two regions (gular and anal) of the plastron.

Results. *Proterochersis* spp. exhibits large shell variability, and at least some of the observed changes seem to be correlated with ontogeny (growth of gulars, extragulars, caudals, and marginals, disappearance of middorsal keel on the carapace) or possible sexual dimorphism (morphology of caudal processes and extragulars). Several specimens show abnormal layout of scute sulci, several others unusual morphologies of vertebral scute areas, one has an additional pair of plastral scutes, and one extraordinarily pronounced, likely pathological, growth rings on the carapace. Both species are represented in a wide spectrum of sizes, from hatchlings to old, mature individuals. The largest fragmentary specimens of *P. porebensis* allow estimation of its maximal carapace length at approximately 80 cm, while *P. robusta* appears to reach lower maximal sizes.

Discussion. This is the second contribution describing variability among numerous specimens of Triassic turtles, and the first to show evidence of unambiguous shell abnormalities. Presented data supplement the sparse knowledge of shell scute development in the earliest turtles and

suggest that at least some aspects of the developmental programs governing scute development were already similar in the Late Triassic to these of modern forms.

Introduction

The shell of turtles, although relatively conserved structurally among taxa, tends to show considerable variation between individuals (Parker, 1901; Gadow, 1905; Newman, 1906a; Coker, 1910; Lynn, 1937; Młynarski, 1956; Zangerl & Johnson, 1957; Zangerl, 1969; McEwan, 1982; Rothschild, Schultze & Pellegrini, 2013; Cherepanov, 2015, 2016; Farke & Distler, 2015; and many others). This variation may be potentially caused by numerous factors, out of which, e.g., a suboptimal humidity (Lynn & Ullrich, 1950) or temperature (Yntema, 1970) during incubation, and a low genetic variation (inbred/bottleneck) within population (Velo-Antón, Becker & Cordero-Rivera, 2011; McKnight & Ligon, 2014) were proposed. Expressions of atavistic morphologies were frequently cited as a cause of abnormal shell variants (Gadow, 1905; Newman, 1906b; Grant, 1936a,b), but this always remained rather speculative (e.g., Coker, 1905, 1910, Cherepanov, 1989, 2006, 2014) and in most cases is easy to refute by comparison with the shell composition of basal and stem turtles (e.g., Gaffney, 1990; Li et al., 2008; Szczygielski & Sulej, 2016). In some cases, abnormal morphologies are attained during postnatal life as a result of diseases, parasites, or trauma (Rothschild, Schultze & Pellegrini, 2013, and references therein).

Shell variation affects both the bones and scutes of the plastron and carapace, and the frequency of changes within each of these domains varies between the species (e.g., Coker, 1910; Lynn, 1937; Zangerl & Johnson, 1957; Zangerl, 1969; McEwan, 1982) and may even differ between sexes within one species (Coker, 1910). Among modern turtles, Cheloniidae have especially variable shells (Kordikova, 2002; Özdemir & Türkozan, 2006; Pritchard, 2008). This unequal susceptibility of various turtles, even those inhabiting similar environments, suggests presence of some control or repair mechanisms that limit appearance of abnormal morphologies with varying efficiency in different taxa or sexes, but exact molecular or morphogenetic background of these mechanisms is little known. The developmental rules governing the appearance of supernumerary or asymmetric scutes, however, are well explained by recent studies

(Cherepanov, 1989, 2006, 2014, 2015; Moustakas-Verho et al., 2014; Moustakas-Verho & Cherepanov, 2015; Moustakas-Verho, Cebra-Thomas & Gilbert, 2017). According to them, shell scutes originate from placodes, which develop in strict correlation with body segmentation: lack of placodes, their asymmetry, improper fusion, or appearance of additional placodes on the level of vacant myosepta lead to abnormal (usually asymmetrical) development of scutes. Some scutes (most usually cervical and vertebrals) develop from fusion of initially separate, paired placodes. Some developmental information may, therefore, be obtained from the layout of scutes relative to each other (e.g., see Szczygielski, 2017, for discussion on scutation of Triassic turtles) and even from some scute abnormalities. Understanding of scute development is crucial, because shell scutes precede shell bones in development and thus determine, or at least have a large impact on, the external morphology and even layout of the shell bones (e.g., Zangerl, 1939, 1969, Cherepanov, 1989, 2006, 2016).

Various congenital changes to the typical shell structure differ in severity. Cherepanov (2016) classified them into three main categories: malformations (severe developmental flaws, usually lethal or severely detrimental), anomalies (changes to the number and layout of shell elements, not severely detrimental, possibly adaptive), and individual variation (minor changes to the number and layout of shell elements, neutral to normal function). Based on this classification, anomalies and individual variations are much more common than malformations and, out of the former two, anomalies are generally easier to spot and understand in the fossil record, because they are usually more pronounced, frequently asymmetrical, and easier to differentiate from post-mortem deformation.

Turtle shells preserve relatively easily in the fossil record, but still, many extinct turtle taxa are known from relatively few, incomplete and/or distorted specimens. For that reason, descriptions of their variability and ontogeny are rare, especially for Mesozoic forms (Gaffney, 1990; Lichtig & Lucas, 2017; Sullivan & Joyce, 2017). Here, we describe the external variability and abnormalities observed in the carapace and plastron of *Proterochersis robusta* Fraas, 1913 and *P. porebensis* Szczygielski & Sulej, 2016 (Figs 1–10, S1–S5) – representatives of the oldest and most plesiomorphic branch of true turtles (Szczygielski & Sulej, 2016).

Materials & Methods

Institutional abbreviations

CSMM. Carl-Schweizer-Museum, Murrhardt, Germany.

SMNS. Staatliches Museum für Naturkunde, Stuttgart, Germany.

ZPAL. Roman Kozłowski Institute of Paleobiology, Polish Academy of Sciences, Warsaw, Poland.

Proterochersis robusta

Proterochersis robusta (Figs 1–3, 6, 8, 9A–C, 10, S3A–C, S4A, S5A–D, Article S1, and Tables S1–S2) is known from the Late Triassic (middle Norian) Löwenstein Formation, Stuttgart neighborhood, Germany. For the geological background, see Szczygielski and Sulej (2016) and references therein. All of the existing specimens of that species (SMNS 11396, SMNS 12777, SMNS 16442, SMNS 16603, SMNS 17561, SMNS 17755, SMNS 17755a, SMNS 17756, SMNS 17930, SMNS 18440, SMNS 50917, SMNS 51441, SMNS 56606, SMNS 81917; CSMM uncat.) were studied with exception of SMNS 50918 (an internal mold of the shell). For the detailed description of these specimens see Article S1 and for the chart of scute areas preserved on each of them see Tables S1–S2.

Proterochersis porebensis

Proterochersis porebensis (Figs 4–5, 7–8, 9D–T, 10, S1–S2, S3D–N, S4B–D, S5E–M′, Article S1, and Tables S3–S4) is known from the lower part of Patoka Member of Grabowa Formation, Poręba, Poland. For geological and paleoenvironmental background, see Sulej et al. (2012), Niedźwiedzki et al. (2014), Szulc et al. (2015), Zatoń et al. (2015), and Szczygielski and Sulej (2016). All of the existing specimens (ZPAL V.39/1–28, ZPAL V.39/34, ZPAL V.39/48–72, ZPAL V.39/155–300, ZPAL V.39/331–366, ZPAL V.39/370, ZPAL V.39/272–404, and uncatalogued) were studied. For the detailed description of these specimens see Article S1 and for the chart of scute areas preserved on each of them see Tables S3–S4.

Methods

The macrophotographs of the smallest specimens, ZPAL V.39/381 and ZPAL V.39/384, were taken using Keyence Digital Microscope VHX-900F. The terminology used for the shell elements (Fig. 1) follows Zangerl (1969) with the amendment by Hutchison and Bramble (1981). To avoid confusion, we use terms "external" rather than "dorsal", "lateral", or (in case of plastron) "ventral" to describe the scute-covered surfaces of the shell, and "dorsomedial" rather than "dorsal" or "medial" when referring to the parts of the carapacial scute areas located closest to the neural row (at the middle and at the very top of the carapace), with exception of the cervical and the vertebrals, for which the term "medial" is uncontroversial, and bridge marginals in ventral aspect, for which "ventromedial" is used to indicate the direction towards the middle point of plastron. Also for clarity, for marginal scutes we use "length" for the diameter of marginal scutes measured radially from the middle to the periphery of the carapace, and "width" for the diameter measured along the edge of the carapace, regardless of the position of the scute and thus its orientation relative to anteroposterior axis of the whole carapace. The edge of the marginal scute contacting scutes other than the preceding or succeeding marginal is called "base", while its free edge is called "rim". See Article S1 for methods used for the Principal Component Analyses.

Results

Specimen sizes. Shell material of *Proterochersis robusta* consists of thirteen specimens of varying sizes and ontogenetic age spanning from young, not yet fully ossified juveniles (SMNS 81917, Fig. S4A) to large, apparently mature, individuals (e.g., SMNS 16442, Figs 2C, 3D, or SMNS 18440, Figs 2K, 3H). Shell remains of *P. porebensis* are much more numerous (270 catalogued specimens), but usually much more fragmentary, frequently consisting of parts of costals, small sections of plastron or the rim of the shell, or other uninformative elements, and only four relatively complete shells (ZPAL V.39/34, ZPAL V.39/48, ZPAL V.39/49, and ZPAL V.39/72) were found thus far (Figs 4–5).

Similarly to *P. robusta*, the collected specimens of *P. porebensis* represent a wide spectrum of sizes and ontogenetic ages. The youngest known individual appears to be a hatchling or a very

young juvenile, and is represented by a fragmentary costal (ZPAL V.39/381, Fig. S1C–D). ZPAL V.39/34 (Figs 4A–B, 5A, 9K, S2C, S3G, S5E–G) is an older juvenile (approx. 28 cm of carapace length; note that shell lengths are approximate due to damage and distortion), ZPAL V.39/48 (Figs 4C–D, 5B, 9G, S3H, S5H–J) is a sub-adult (approx. 42.5 cm of carapace length, see Szczygielski & Sulej, 2016), and ZPAL V.39/72 (Figs 4G–H, S2D, S3K) is of comparable size (approx. 44.5 cm of carapace length) and seems to be of comparable ontogenetic age. ZPAL V.39/49 (Figs 4E–F, 5C, 9D, S3I, S5K–M) is the largest complete shell found thus far (approx. 49 cm of carapace length), but some fragmentary specimens, such as ZPAL V.39/8, ZPAL V.39/57 (Fig. S1N), ZPAL V.39/60 (Fig. S1O–P), and ZPAL V.39/63 (Fig. S1A–B) indicate that this species could have reach even larger sizes. ZPAL V.39/63 (a carapace fragment with dorsal part of ilium attached) seems to be particularly large – the carapace is up to 1.5 cm thick, the sulci are very wide (see below), and the ilium is massive, being at the point of attachment to the carapace 6.3 cm broad (measured from the lateral edge of the bulge to the base of the first sacral rib), compared to 3.5 cm in ZPAL V.39/48, 4 cm in ZPAL V.39/49, and 3.7 cm in ZPAL V.39/72. Accurate measurement of ilium breadth is difficult in ZPAL V.39/34 due to damage and surrounding rock matrix, but it seems to be about 2 cm. Based on these data, it seems that there is a good correlation between the breadth of the dorsalmost end of the ilium and the length of the carapace (correlation index = 0.997 with ZPAL V.39/34 included and 0.995 with that specimen excluded; n = 4 or n = 3, respectively). Based on that, the carapace length of ZPAL V.39/63 may be estimated to be between 75 and 80 cm (depending on whether the measurement of ZPAL V.39/34 is considered). With the exception of ZPAL V.39/34, the collected complete shells of *P. porebensis* are larger than all of the known shells of *P. robusta* (possibly excluding the fragmentary specimens SMNS 16442 and SMNS 18440, as their exact size is difficult to estimate).

There is some incongruency between these large maximal sizes and the moment of shell ankylosis. Typically, shell ankylosis stops growth, because the shell grows mainly along the sutures (Pritchard, 2008). Most specimens of *Proterochersis* spp., however, are fully ankylosed, regardless of their size. Even if the prevalence of ankylosed specimens in Poręba and localities around Stuttgart may be a preservation or sorting artifact (e.g., the unankylosed specimens were typically destroyed by currents or small fragments of disarticulated unankylosed shells were buried elsewhere), the fact that ankylosis occurred even in relatively small specimens with

juvenile features (e.g., ZPAL V.39/2, ZPAL V.39/34, ZPAL V.39/66) is more troubling. Many of these small specimens are well-preserved and it is hard to imagine that the sutures were obliterated by some diagenetic processes, while minor details of shell anatomy and texture remained intact. In some turtle species the sexual dimorphism takes form of a striking difference of sizes between mature males and females (Pritchard, 2008). In such a case, specimens like ZPAL V.39/34 could be considered one of the sexes, and large specimens like ZPAL V.39/49 – the other one. This, however, seems to be refuted by a fact that there exists a full spectrum of sizes of ankylosed specimens between ZPAL V.39/34 and ZPAL V.39/49 (e.g., ZPAL V.39/48 with subadult characters). Likewise, this would preclude interpretation of small ankylosed specimens as a separate species. In lack of other likely explanations, a very broad variation in time of ankylosis is therefore provisionally accepted. Another possible solution is seasonal hypercalcifiaction and decalcification of sutures or shell bones that could increase the rigidness of the shell but also allow seasonal growth – similar mechanism of de-ossification was reported locally in the mid-section of plastron in males of some modern turtles during mating season (Wibbels, Owens & Rostal, 1991; Wyneken, 2001; Pritchard, 2008). This problem may be resolved by future histological studies.

With very few exceptions, the specimens of *Proterochersis* spp. are incomplete, and often the overlap between them is small, which makes comparisons or even reliable estimation of their size difficult – even more so, relative proportions of epidermal elements or breadth of plastral lobes may vary between individuals and sometimes even bilaterally within one individual, as evidenced by several relatively complete shells. For that reason, it is impossible to confidently estimate the shell length based on, e.g., the length of a single plastral scute. These differences in proportions are difficult to explain, and incompleteness or poor preservation of the specimens makes it currently impossible to determine if they result, e.g., from allometric growth, sexual dimorphism, or are just part of normal intraspecific variability.

Carapace

Costals. ZPAL V.39/381 (Fig. S1C–D) is a fragmentary costal of the smallest, and probably the youngest, known individual of *Proterochersis porebensis*. This costal is 8 mm wide, 2 mm thick in the peripheral sections, and 3 mm thick at the ventral ridge. It appears to lack natural edges with exception of a section of proximal (medial) rim. The gracility of that element, its smooth

external surface with subtle longitudinal striation, lack of typical rough texture indicative of contact with superficial layers of dermis, and a rounded convexity in the proximal region of the external surface (Fig. S1C) suggest, however, that it is not a part of a full-sized costal.

The widest costal with preserved sutural edges is ZPAL V.39/176 (5.1 cm wide, 5 mm–1.2 cm thick, Fig. S1E). Its width suggests that it comes from an individual similar in size to ZPAL V.39/49. The structure of the sutures is relatively uncomplicated in that specimen and the thickness is intermediate, compared to some other specimens, even if they are narrower. This probably results from the localization of the costal within the shell – as a general rule, the posterior costals seem to be narrower in *Proterochersis* spp. than the anterior ones. Thus, it is likely that the thicker costals with more developed sutural edges, such as ZPAL V.39/3 come from ontogenetically older specimens, but from more posterior section of the shell.

Vertebrae. ZPAL V.39/377 (Fig. S1H–K) is a fragment of the dorsal section of the vertebral column of a young *Proterochersis porebensis* individual, consisting of a one and a half vertebra. Besides the relatively small size (the complete vertebra is 1.9 cm long, 1.2 cm wide at the level of facets for the ribs), it differs from all other known vertebrae of *Proterochersis* spp. in lack of ankylosis and neurals. The natural bone limits are visible, proving that the dorsal ribs in proterochersids were already shifted anteriorly, to an intervertebral position typical for turtles. The facets for the ribs (Fig. S1I) are ovoid, longer than high, higher posteriorly than anteriorly, gently skewed anteroventrally in lateral view, and at least in ¾ of their length they are located in the anterior part of the centrum. Likewise, the neural spines are also inclined slightly anteriorly. The neurocentral sutures cross the articulation facets for ribs, their inclination is slightly oblique, dorsoposterior, and generally agrees with the inclination of the facets. The zygapophyses are small and roughly triangular. The centra are hourglass-shaped in ventral view (Fig. S1J). Along the long axis of the centra there continues a gentle midventral keel. As they are preserved, the vertebrae are separated by a gap approx. 3 mm wide (Fig. S1I, J), probably filled in life by the intervertebral disc or unossified, cartilaginous ends of the centra. The neural canal, exposed posteriorly, is very high and narrow, measuring up to 8 mm in height and 2.5 mm in width (Fig. S1H). The most surprising is the dorsal surface of the neural spines (Fig. S1K). Neurals are absent, but there is no sign of bone breaking, and no cancellous bone is exposed. Instead, the surface is bumpy and perforated by numerous vascular canals. This does not resemble a suture,

there are no lamellae nor spikes. For that reason, we interpret this either as a sign of a cartilaginous cap on the dorsal ends of neural spikes (albeit it is located relatively high and the neural spikes are broadened dorsally, Fig. S1H) or as incipient intramembranous ossification, just beginning the development of neurals. In either case, it indicates young ontogenetic age of the individual.

All the other specimens of *Proterochersis* spp. that preserve dorsal vertebrae, including SMNS 56606, ZPAL V.39/48 (see Szczygielski & Sulej, 2016; Szczygielski, 2017), ZPAL V/39/49 (see Szczygielski, 2017), ZPAL V.39/72 (see Szczygielski & Sulej, 2016; Szczygielski, 2017), ZPAL V.39/169 (Fig. S2E–F, comparable in size with ZPAL V.39/49), and ZPAL V.39/378 (Fig. S1F–G, comparable in size with ZPAL V.39/49) have their dorsal vertebral columns fully ankylosed, and no unambiguous intervertebral and costovertebral articulation points or sutures can be seen. In these ontogenetically older specimens the dorsal vertebrae get obviously larger and more robust, particularly at the points of articulation. The ventral surfaces of the dorsal vertebrae of ZPAL V.39/48 (with exception of the first and the last three dorsal vertebra) form a relatively sharp midventral keel (see Szczygielski & Sulej, 2016), and a less-pronounced sharpened keel can be seen on the mid-dorsal vertebra of ZPAL V.39/49, but in the remaining specimens the keel is more rounded. Given the limited sample, it is difficult to tell if this is related to ontogeny or just variable in population. It seems that this sharpened keel is more frequent in the mid-section of the dorsum than in the anterior or posterior end of the dorsal vertebral column. The neural canal of ZPAL V.39/49, ZPAL V.39/169, and ZPAL V.39/378, as exposed, is closer to circular in cross-section and measures approx. 4 mm x 5 mm in ZPAL V.39/169 and ZPAL V.39/378, and approx. 7 mm x 8 mm in ZPAL V.39/49.

Cervical scute. In adult and subadult individuals of *Proterochersis robusta* and *P. porebensis* the cervical was trapezoid to crescent-shaped (Figs 1–2, 4, 6B–C, S1N). The posterior (basal) edge, contacting the anterior edge of the first vertebral scute, was longer than the anterior. The shortest, slanted, anterolateral edges contacted the medioposterior edges of the first pair of marginal scutes. The lateral tip of the cervical scute may form a several millimeter long contact with the base of the second marginal scute (e.g., *P. porebensis* specimens ZPAL V.39/57, Fig. S1N, and ZPAL V.39/49, Fig. 4E), merely touch the second marginal (e.g., *P. porebensis* ZPAL V.39/48, Fig. 4C, and ZPAL V.39/72, Fig. 4G), or such a contact may be prevented by the first

marginal (e.g., *P. robusta* SMNS 17561, Fig. 2F, and SMNS 17930, Figs 2I, 6B–C, *P. porebensis* ZPAL V.39/22). In *P. porebensis* specimen ZPAL V.39/34 (Fig. 4A) the cervical was more rectangular, with roughly anteroposteriorly directed lateral edges. The scute grew in length and width with increasing size of the animal. In ZPAL V.39/34 (Fig. 4A) the cervical is 8 mm long, in ZPAL V.39/390 (Fig. S1L) it is 1 cm long, in ZPAL V.39/22 and ZPAL V.39/48 (Fig. 4C) it measures 1.5 cm in length, in ZPAL V.39/72 (Fig. 4G) it is 1.9 cm long, and in ZPAL V.39/49 (Fig. 4E) it is 2.2 cm long. ZPAL V.39/57 (Fig. S1N) has the longest cervical, measuring 2.4 cm. In most specimens the cervical scute breadth did not exceed 1/3 of the width of the first vertebral scute, but in ZPAL V.39/49 the cervical is wider than a half of the first vertebral (Fig. 4E).

Vertebral scutes. *Proterochersis* spp. had a single row of five broad vertebral scutes, which covered most of the dorsal surface of the carapace (Figs 1–2, 4, 6). The first vertebral was fan-shaped, with a rounded medial process directed posteriorly, which was received by an anterior medial notch of the second vertebral. Anterior edge was gently bowed, it contacted the posterior (basal) edge of the cervical, the base of the second marginal, and (usually) cranial section of the base of the third marginal (*P. porebensis* ZPAL V.39/57, Fig. S1N, being the only known exception due to the second marginal preventing such contact). In some specimens (e.g., *P. robusta* specimens SMNS 17561, Fig. 2F, and SMNS 17930, Figs 2I, 6B–C, and *P. porebensis* ZPAL V.39/22) there is a minor contact between the first vertebral and the caudal section of the base of the first marginal scute. Laterally, the first vertebral formed facets for contact with the first pair of pleurals. The length of these facets increased with the size of the animal, in large individuals (such as *P. porebensis* ZPAL V.39/49, Fig. 4E, and ZPAL V.39/57, Fig. S1N) reaching over 3.5 cm. The first vertebral in some specimens was slightly asymmetrical – in SMNS 17561 its left posterolateral margin was more concave than the right one (Fig. 2F), in ZPAL V.39/49 the scute was expanded slightly more to the right than to the left (Fig. 4E), and in ZPAL V.39/72 the posteriormost point of the posterior process seems to be shifted to the left relative to the midline (Figs 4G).

Anterior edge of the second vertebral was bow-shaped, with a rounded medial embayment which received the posterior process of the first vertebral scute. Anterolaterally, it contacted the dorsomedial edges of the first pair of pleurals, laterally it contacted about 3/5 of the dorsomedial

edge of the second pair of pleurals, and posteriorly it contacted the anterior edge of the third vertebral scute. The second vertebral is widest in its posterior part, at (or slightly posterior to) the level of the sulcus between the first and the second pleural. The remaining vertebrals were roughly trapezoid, each scute slightly narrower posteriorly than anteriorly, and had generally straight anterior edges. The third vertebral contacted the second vertebral anteriorly, the remaining part of the dorsomedial edge of the second pair of pleurals and over 2/3 of the dorsomedial edge of the third pair of pleurals laterally, and the fourth vertebral scute posteriorly. It was widest around the sulcus between the respective pleurals, and in dorsal view its width was comparable to the width of the second vertebral (although it might have been slightly larger measured along the surface due to shell curvature – this, however, in most specimens is obscured by deformation or breakage). The fourth vertebral contacted the third anteriorly, the remaining part of the dorsomedial edge of the third pair of pleurals and the whole dorsomedial edge of the fourth pair of pleurals laterally, and the fifth vertebral scute posteriorly. The widest point of that scute lied in its anterior part. The fifth vertebral was more semi-dome-shaped than the vertebrals first to fourth. It contacted the preceding vertebral anteriorly and the posterior edges of the last (fourth) pair of pleurals anterolaterally. Laterally and posterolaterally, it contacted the bases of the posteriormost marginals – usually the 12th, the 13th, and the 14th, although sometimes there was no contact with the 12th and at least in ZPAL V.39/48 the 15th pair of marginals was present (see below). Posteriorly, in *Proterochersis* spp. there was a caudal notch (Fig. S3). The variability in the vertebral scutes 2–5 is mostly evident medially.

In two small specimens of *Proterochersis porebensis* (ZPAL V.39/2, Fig. S2A–B; ZPAL V.39/34, Figs 4C, S2C, see Sulej, Niedźwiedzki & Bronowicz, 2012; Szczygielski & Sulej, 2016) a pronounced medial ridge is present crossing the area of the second, the third, and the fourth (in ZPAL V.39/34; in ZPAL V.39/2 this part is missing) vertebral scute. The ridge is rounded to triangular in cross-section, laterally symmetrical, and for most of its length surrounded laterally by deep troughs. Anteriorly, the ridge and the troughs gradually even out, they tend to nearly disappear in the posteriormost sections of the vertebral scute areas, just before the intervertebral sulci, and in ZPAL V.39/34 the ridge disappears posteriorly before the throughs do, resulting in a shallow, longitudinal, midline depression in the posterior part of the fourth vertebral scute area (Fig. S2C). The external morphology and small distance between the ribs in ZPAL V.39/2 indicate that it was similar in size to ZPAL V.39/34, which suggests that

this morphology of the midventral keel is related to the young ontogenetic age of the individuals. In *P. porebensis* specimens ZPAL V.39/1 (Fig. S2G–H), ZPAL V.39/4, ZPAL V.39/72 (Fig. S2D), and ZPAL V.39/169 (Fig. S2E–F), and on a small midcarapacial fragment of *P. robusta* specimen SMNS 11396, a much more subtle, low, and rounded midline ridge can be seen with equally subtle lateral troughs or no troughs at all. If the middorsal keel of ZPAL V.39/2 and ZPAL V.39/34 is interpreted as a juvenile character, then it seems probable that the middorsal ridges of ontogenetically older SMNS 11396, ZPAL V.39/1, ZPAL V.39/4, and ZPAL V.39/72 may represent remnants of that structure. No midline ridges can be found in ZPAL V.39/48 (slightly smaller than ZPAL V.39/72 and, judging by rib spacing, comparable in size to ZPAL V.39/1) or ZPAL V.39/49, but the carapaces of these two specimens are broken along the midline, possibly obscuring the ridges. The ridge in ZPAL V.39/1 is slightly tilted anteriorly to the left, so in the anterior part of the specimen it loses strict correlation with underlying neural processes of the vertebrae (Fig. S2G–H). This supports the view that middorsal ridges of proterochersids are not strictly induced by the position of the axial skeleton, but rather are related to epidermal scutes.

Three *P. robusta* specimens (CSMM uncat., Fig. 2A; SMNS 17561, Fig. 2F; SMNS 17930, Figs 2J, 8) exhibit various degrees of indentation along the midline of the second, the third, and the fourth vertebral scute areas. The most severe case is exhibited by CSMM uncat. (Fig. 2A). Along the midline in the anterior regions of the second and the third vertebral, deep, funnel-shaped grooves are present, as if the scute area was anteriorly split in two. These grooves are approximately as deep as the anterior vertebral sulci with which they are connected, they penetrate the vertebral fields no further than to the mid-length, and posteriorly they become noticeably shallower and narrower, ending in a sharpened point. In the posterior parts of the scute areas they continue as subtle depressions. The third vertebral lacks the deep groove, but there is a similarly shaped, shallow depression. The fifth vertebral is depressed as well, but the depression is wider and gentle. In SMNS 17930 (Figs 2I, 6) the anatomy is similar, but less pronounced – there are weak grooves in the anterior parts of the second and the third vertebral area, similar to the posterior sections of the grooves of CSMM uncat., and there is a gentle depression running along the middle of the shell. SMNS 17561 (Fig. 2F) exhibits only a weak depression along the midline, only slightly more pronounced in the anterior sections of the vertebral areas. This morphology initially resembles the midline troughs of ZPAL V.39/2 (Fig.

S2A) and ZPAL V.39/34 (Figs 4A, S2C) but there are several important differences. Firstly, in CSMM uncat., SMNS 17561, and SMNS 17930 there is no middorsal keel. Secondly, these specimens are relatively large (SMNS 17561 is approx. 35 cm long, SMNS 17930 is approx. 36 cm long, and CSMM uncat. is over 36.5 cm long; note that the damage suffered by SMNS 17930 and CSMM uncat. may cause some underestimation of their sizes and/or relative size differences). Thirdly, the middorsal keels and troughs of ZPAL V.39/2 (Fig. S2A) and ZPAL V.39/34 (Figs 4A, S2C) do not reach the anterior edge of the second vertebral and span along the full length of the third vertebral, but do not connect to intervertebral sulci, while the midline grooves or depressions of CSMM uncat. (Fig. 2A), SMNS 17561 (Fig. 2F), and SMNS 17930 (Figs 2I, 6A–C)are most pronounced near the anterior edges of the vertebral scutes and in CSMM uncat. they connect to intervertebral sulci. Considering that the vertebral scutes grew mostly in their anterior part (see below), it seems likely that these depressions and grooves developed relatively late during ontogeny, and may be evidence of scute splitting. Congruent with this hypothesis is the observed positive correlation between the severity of observed morphologies and the size of the specimens. The presence of that morphology on the vertebral scute areas of *P. robusta* specimen SMNS 16442 (Fig. 2C) is ambiguous. A shallow groove seems to be present medially, but this specimen is compacted, broken, and its surface is poorly preserved, making assessment difficult.

In *Proterochersis robusta* specimen SMNS 17930 (Figs 2I, 6) and in several specimens of *P. porebensis* (ZPAL V.39/4; ZPAL V.39/34, Figs 4A, S2C; ZPAL V.39/49, Fig. 4E; ZPAL V.39/72, Figs 4G, S2D; ZPAL V.39/169, Fig. S2E) the sulci separating the first and the second, the second and the third, and/or the third and the fourth vertebral scute area form in the middle small, ^-shaped anterior projection. In some cases (ZPAL V.39/4, ZPAL V.39/34, ZPAL V.39/72) this projection is laterally surrounded by two rounded posterior projections, resulting in a ω-shaped pattern. The presence of the anterior projection seems to be correlated with, but not exclusive to, the presence of a middorsal keel or ridge.

The intervertebral sulci of most *Proterochersis* spp. specimens, although relatively straight compared to, e.g., to circumpleural sulci, understandably are not ideally straight, but exhibit some minor irregularities. In many cases, it is difficult to evaluate whether these irregularities are an effect of post-mortem distortion. Curiously, however, the sulcus between the third and the

fourth vertebral seems to be comparatively more prone to severe irregularities. In *P. robusta* specimen CSMM uncat. (Fig. 2A) it is clearly asymmetrical in the middle section, where it spans anteriorly, and an asymmetry of the same sulcus is also profound in another *P. robusta* specimen, SMNS 17561 (Fig. 3F) – in that case the sulcus is wavy rather than straight and skewed, so it meets the third pleural more anteriorly on the right sight than on the left. Similarly to CSMM uncat., the mid-section of this sulcus is asymmetrical in *P. porebensis* specimen ZPAL V.39/34 (Fig. 4A).

Pleural scutes. *Proterochersis* spp. had paired rows of four polygonal, slightly elongated pleural scutes (Figs 1–2, 4, 6, S3). The first pleural was hexagonal. In all the specimens of *Proterochersis* spp. it contacted the first vertebral medioanteriorly via dedicated facet, and the relative length of this facet seems to increase with the size of the animal (Figs 2, 4). In this respect, *Proterochersis* spp. differed from *Keuperotersta limendorsa*, in which the sulcus between the first vertebral and the first pleural lies in the same line as the sulcus between the first vertebral and the second marginal, and nearly in the same line as the sulcus between the second vertebral and the first pleural. *K. limendorsa*, however, is currently represented by a single specimen, so it is difficult to estimate if this difference is taxonomic, ontogenetic, or an effect of intraspecific variability. Beside the first vertebral, the first pleural contacted the second vertebral dorsomedially, the second pleural posteriorly, the caudal part of the base of the second marginal (with the exception of *P. porebensis* specimen ZPAL V.39/57, Fig. S1N), the whole base of the third, and the cranial part of the base of the fourth marginal as well as the cranial part of the dorsomedial edge of the first supramarginal ventrolaterally, and the second pleural scute posteriorly. The second pleural was heptagonal and had contacts with the first pleural (anteriorly), all three supramarginals (ventrolaterally), the third pleural (posteriorly), and the second and the third vertebral scute (dorsomedially). The third pleural usually was hexagonal, contacted the second pleural (anteriorly), the third supramarginal scute and the ninth and tenth marginal (ventrolaterally), the fourth pleural (posteriorly), and the third and fourth vertebral scute (dorsomedially). In most individuals the sulcus with the ninth and tenth marginal was roughly continuous and straight, but in *P. porebensis* specimen ZPAL V.39/49 (Fig. 4E–F) the basal edges of these scutes were directed at an angle, resulting in heptagonal third pleural. Less pronounced, but similar condition can be seen also in *P. robusta* specimen SMNS 17561 (Fig. 2G) and *P. porebensis* ZPAL V.39/72 (Fig. 4G–H). The fourth (last) pleural was hexagonal and

contacted the third pleural (anteriorly), the bases of the tenth, 11th, and 12th marginal (in some specimens, such as *P. robusta* SMNS 17561, Figs 2F–G, S3B, and *P. porebensis* ZPAL V.39/48, Figs 4C–D, S3H, the posteriormost tip of the last pleural may also touch the cranial tip of the 13th marginal), and the fourth (dorsomedially) and fifth (posteriorly) vertebral scute. Usually, the interpleural sulci lack pronounced curvature, but in some specimens (e.g., *P. robusta* SMNS 17561, Fig. 2F–G, *P. porebensis* ZPAL V.39/48, Fig. 4C–D, and ZPAL V.39/49, Fig. 4E–F) the posterior edges of pleurals 1–3 are slightly concave and form posterior processes in their dorsomedial parts, at the level of pleural tubercles.

Supramarginal scutes. On each side of the carapace there were three elongated supramarginal scutes (Figs 1–2, 4, 6A). The first supramarginal was pentagonal and had its longest tip directed cranially. Posteriorly, this scute contacted the second supramarginal, and its dorsomedial tip was tucked between the first and the second pleural scute. The second supramarginal was rectangular and contacted the first supramarginal (anteriorly), the third supramarginal (posteriorly), and the ventrolateral edge of the second pleural (dorsomedially). The third supramarginal was pentagonal and shaped roughly the same as the first, but with its longest tip directed caudally. This scute contacted the second supramarginal anteriorly and its dorsomedial tip was tucked between the third and the fourth pleural scute. The row of three supramarginals always contacted the bases of the fifth to ninth marginal ventrolaterally. The intersupramarginal sulci are located roughly at the same level as the sulci separating the sixth, seventh, and eight marginal scute areas, but some several millimeter misalignment frequently occurs – the intermarginal sulci usually are shifted slightly anteriorly in relation to the intersupramarginal sulci (*Proterochersis robusta* specimens SMNS 17561, Fig. 2G, SMNS 17755, and SMNS 18440, Fig. 2K; *P. porebensis* specimens ZPAL V.39/8; ZPAL V.39/48, Fig. 4C–D, ZPAL V.39/49, Fig. 4E–F, right side of ZPAL V.39/72, Fig. 4G, ZPAL V.39/160, and, possibly, in ZPAL V.39/34, although the shell margin of that individual is damaged in that region) but in some cases they may be shifted slightly posteriorly (left side of ZPAL V.39/72, Fig. 4G–H, ZPAL V.39/168). *P. porebensis* specimen ZPAL V.39/48 is closest to have these sulci coinciding with only few millimeter anterior shift of intermarginal sulci (Fig. 4C–D). Other than that, no meaningful variability or clear allometry was observed in the supramarginals. They seem to increase their sizes more or less linearly with the carapace. The largest found supramarginal is the first supramarginal of *Proterochersis porebensis* specimen ZPAL V.39/8, which was 8 cm long and

5.5 cm high – slightly larger than in ZPAL V.39/49 (7.7 cm x 5 cm) and significantly larger than in ZPAL V.39/48 (6.6 cm x 4.2 cm) and ZPAL V.39/72 (6.7 x 4.2 cm). Unfortunately, the first supramarginal is too severely damaged in ZPAL V.39/34 to allow precise measurement, but the probable outline of this scute on the right side of the specimen suggests the length of approx. 4.2 cm. This would mean that, even more so than for the ninth marginal, there is a good correlation between the length of the shell and the length of the first supramarginal (correlation index = 0.994 for n = 4). Based on that, the shell of ZPAL V.39/8 may be estimated to be over 50 cm long.

Marginal scutes. There were two rows of marginals spanning from the anterolateral region of the cervical scute to the posterolateral limits of the caudal notch (Figs 1–5, S3). Typically, each row included fourteen scutes. Besides some minor random variations in shape and relative size, which are usually difficult to grasp, the marginal scutes of *Proterochersis* spp. exhibited variability in three main ways.

Firstly, their number was variable – variants of 15 marginals (ZPAL V.39/48) and 14 marginals (all the other specimens with complete marginal series) are known (see Szczygielski & Sulej, 2016). There are at least 12 marginals identifiable in the juvenile ZPAL V.39/34, but their exact number is uncertain due to preservation, so it is probable that the typical number of 14 marginals was present. The layout relative to pleurals and supramarginals suggests that one intermarginal sulci is likely to be undetected in the bridge region, below the supramarginal row, and this area is heavily damaged on both sides of ZPAL V.39/34. Another likely missing sulcus should be located anterolateral to the cervical scute and should delineate the first marginal. This area, however, is well-preserved in ZPAL V.39/34. It is, nonetheless, possible that the scute was there, but its sulcus is too subtle to be identified (many sulci on that specimen are very weak, see below) or that in such a young animal the scute was very small and located at the very edge of the carapace – possibly the first marginal exhibited allometry during development. This option seems plausible mainly because there is no nuchal notch in ZPAL V.39/34 (the anterior edge of the carapace is flush – Fig. 4A–B, see also Sulej, Niedźwiedzki & Bronowicz, 2012; Szczygielski & Sulej, 2016) in some specimens (particularly SMNS 17561, Fig. 2F, ZPAL V.39/48, Fig. 4C, ZPAL V.39/49, Fig. 4E, and on the right side of ZPAL V.39/72, Fig. 4G) the first marginal scute was almost entirely anterior to the cervical scute (and, optionally, to the

second marginal), having very little or no contact with the first vertebral scute. This leaves two possibilities – either the first marginal scute was in some individuals "crowded out" during ontogeny by the cervical and the second marginal or, at least in some individuals, it started to develop on the very margin of the shell. Alternatively, some variability in the number of marginal scutes is possible. Note that this condition is different from the missing first marginal of *Keuperotesta limendorsa* Szczygielski & Sulej, 2016 – in *K. limendorsa* the lateral contact between the cervical scute and the marginal series is very narrow or nonexistent (Szczygielski & Sulej, 2016), while in ZPAL V.39/34 it is wide. The smallest fragmentary specimen with the first marginal anterolateral to the cervical scute is ZPAL V.39/390 (Fig. S1L–M).

The second type of marginal variability of *Proterochersis* spp. affects the layout of the intermarginal sulci relative to the sulci of remaining scutes, resulting in (usually minor) differences of contacts between these scutes and variation of their shape. The first marginal in dorsal aspect always contacted the cervical posteromedially, was subtriangular or trapezoid, depending on whether it was prevented from the contact with the first vertebral by the lateral tips of the cervical scute (as in *P. porebensis* ZPAL V.39/48, Fig. 4C, ZPAL V.39/49, Fig. 4E, ZPAL V.39/57, Fig. S1N, and ZPAL V.39/72, Fig. 4G) or not (as in *P. robusta* SMNS 17561, Fig. 2F, and SMNS 17930, Figs 2I, 6B–C, and *P. porebensis* ZPAL V.39/22), respectively, and had a rounded craniomedial tip. In ventral aspect, it was subtriangular and had a concave sulcus at its base. In this aspect, the intermarginal sulci of this and the following nine marginals as well as the basal sulci of all except the first marginal are gently convex. The second marginal was subrectangular to trapezoid both in dorsal and in ventral aspect, always contacted the first vertebral, in some specimens its tip touched the cervical (*P. porebensis* ZPAL V.39/48, ZPAL V.39/49, ZPAL V.39/57, and ZPAL V.39/72), and in ZPAL V.39/57 (Fig. S1N) it also touched the first pleural. Consequently, in most *Proterochersis* spp. specimens the third marginal scute was pentagonal in dorsal aspect (subrectangular in ventral aspect) and contacted both the first pleural and the first vertebral scute (Figs 2, 4), but ZPAL V.39/57 (Fig. S1N) is the only known exception – the sulcus between the second and the third marginal scute in that specimen is continuous with the sulcus between the first vertebral and the first pleural scute, and the third marginal was subrectangular in dorsal aspect. The fourth marginal was always subrectangular in both aspects and contacted the first pleural in dorsal aspect and cranial part of the axillary in ventral aspect. The fifth marginal was always pentagonal both in dorsal ventral aspect, and

contacted both the first pleural and the first supramarginal dorsomedially, and the axillary and the first inframarginal scute ventromedially. In dorsal aspect, the marginals sixth to eighth always contacted the row of three supramarginals and were subrectangular to weakly pentagonal (depending on how much their intermarginal sulci are offset from the intersupramarginal sulci, see above). In ventral aspect, they are usually pentagonal and contact the row of four inframarginals. The posterior sulcus of the sixth marginal in this aspect is located around the level of the sulcus between the first and the second inframarginal – in *P. robusta* specimen SMNS 17561 (Fig. 3F) and *P. porebensis* specimen ZPAL V.39/48 (Fig. 5B) it is slightly posterior, but seems to be slightly anterior in ZPAL V.39/49 (although the exact morphology is obscured in that individual by damage, Fig. 5C), and it falls on a gap between the inframarginals in *P. robusta* SMNS 18440 (Fig. 3H) and in *P. porebensis* ZPAL V.39/21 (see below). The posterior sulci of the seventh and the eighth marginal fall around the midsections of the third and the fourth inframarginal, respectively. The ninth marginal was pentagonal in dorsal aspect and subpentagonal in ventral aspect, gradually increasing its size posteriorly. It contacted the third supramarginal dorsomediocranially, and the third pleural dorsomedially. The ventromedial edge was gently curved rather than angular, it contacted the fourth (last) inframarginal and formed the caudal end of the bridge. The tenth marginal was pentagonal in dorsal aspect and subrectangular in ventral aspect. Dorsomedially, it contacted the third and the fourth pleural. In most cases, the dorsomedial sulcus of the tenth marginal is roughly continuous with the dorsomedial sulcus of the ninth marginal, although in *P. porebensis* specimen ZPAL V.39/49 (Fig. 4E–F) these sulci are set at an angle, and similar, but less pronounced break in sulcus direction is also present in *P. robusta* specimen SMNS 17561 (Fig. 2G) and *P. porebensis* ZPAL V.39/72 (Fig. 4G–H). The 11th marginal was always subrectangular both in dorsal and in ventral aspect and dorsomedially it contacted the fourth pleural. The 12th marginal was either trapezoid (dorsomedial contact with fourth pleural only – *P. robusta* SMNS 17561, Figs 2F–G, S3B, *P. porebensis* ZPAL V.39/48, Figs 4C–D, S3H) or pentagonal (dorsomedial contact with the fourth pleural and the fifth vertebral – remaining specimens, Figs 2, 4, S3) in dorsal aspect due to the varied position of the sulcus between the 12th and the 13th marginal relative to the sulcus between the fourth pleural and the fifth vertebral scute area (see Szczygielski & Sulej, 2016). In SMNS 17561 (Figs 2F–G, S3B), ZPAL V.39/48 (Figs 4C–D, S3H), ZPAL V.39/72 (Figs 4G–H, S3K), and ZPAL V.39/386 (Fig. S3N) these sulci are located nearly in the same line (the intermarginal sulcus usually only

548 slightly posterior, but on the left side of SMNS 17651 even slightly anterior), while in SMNS
549 17755a (Figs 2H, S3C) and ZPAL V.39/49 (Fig. S3I) the pleurovertebral sulcus falls close to the
550 middle of the 12th marginal, and the intermarginal sulcus is located clearly more posteriorly. This
551 is also the configuration of sulci in the corresponding region of ZPAL V.39/34 (Figs 4A–B,
552 S3G), regardless of the number of marginals in that specimen. In SMNS 17930 (Figs 2I–J, 6A),
553 the sulcus between the last pleural and the last vertebral lies approximately in the same line as
554 the intermarginal sulcus between the 12th and the 13th marginal but the pleurovertebral sulcus in
555 that specimen is fully contained in the area restored with plaster and has an unusual layout (it is
556 continuous with the sulcus between the last pleural and the fourth vertebral instead of creating an
557 angle, as in other specimens – compare Figs 2 and 4), so it seems more plausible that in life it
558 met the 12th marginal in the middle. Given the limited sample which still exhibits some variance
559 in the relative position of sutures, it is possible that these two morphologies are not the only
560 possibilities, but a full spectrum of intermediate morphologies existed in the population.
561 Regardless of the shape of the 12th marginal, the 13th marginal was always subtrapezoid in dorsal
562 aspect, had a convex rim, and contacted the fifth vertebral dorsomedially (in SMNS 17561, Figs
563 2F–G, S3B) and ZPAL V.39/48 (Figs 4C–D, S3H) additionally touching the caudal end of the
564 fourth pleural). Both the 12th and the 13th were subrectangular in ventral aspect. In most
565 specimens, the 14th marginal is the last of the series and in subadult and adult specimens it had a
566 rounded or spiky rim, the end of which was free from the preceding marginal. In ZPAL V.39/48
567 this morphology is exhibited by the 15th marginal, while 14th is intermediate between the 15th and
568 the 13th (Figs 4C–D, S3H). In some specimens (ZPAL V.39/6, Fig. S3D, ZPAL V.39/18, Fig.
569 S3E, ZPAL V.39/48, Fig. S3H) the sulcus between the last and second-to-last marginal is
570 sinuous. The notch between the last two marginals in most specimens (except ZPAL V.39/23,
571 Fig. S3D, ZPAL V.39/72, Fig. S3K, and ZPAL V.39/380, Fig. S3M) is rounded and the bone
572 around the level of the sulcus or just posterior to it is thinner than in the middle of the marginal
573 areas. Dorsomedially, the 14th and the 15th marginal (if present) contacted only the fifth vertebral.

574 The posteriormost marginals (be it the 14th or the 15th) grew in a characteristic manner. In
575 *Proterochersis porebensis* specimen ZPAL V.39/34 (Fig. S3G) and in *P. robusta* specimen
576 SMNS 17561 (Fig. S3B) the last pair of marginals was small and triangular (they lacked a
577 posteroventral tip on their rims), broader then long (in ZPAL V.39/34 2.1 cm wide, measured
578 along the sulcus with the last vertebral and 1 cm long in the longest place; not measured in

SMNS 17561), and their edge was continuous with the edge of the preceding pair, resulting in lack of serration (see also Szczygielski & Sulej, 2016). *P. porebensis* ZPAL V.39/23 (Fig. S3F) is the smallest last marginal that has a tip, resulting in its roughly rhomboidal shape. It is 1.6 cm wide, its maximal size (measured across from the tip to the corner of the sulci with the fifth vertebral and preceding marginal) is 1.9 cm, and length (from the sulcus with the fifth vertebral to the tip, parallel to the posterior edge) is 1.4 cm (although the tip is broken, so these measurements should probably be about 1 mm larger). Slightly larger (last marginal 2.1 cm wide, 2 cm long, 2.4 cm max. size) *P. porebensis* individual, ZPAL V.39/18 (Fig. S3E), exhibits a transitional morphology linking these small specimens and the more adult-like morphology – there is a small but distinct tip and a shallow but noticeable rounded notch separates it from the rim of the preceding marginal. In larger (and, supposedly, older) individuals, the last marginals were becoming spikier, and longer than wide. The largest last marginal found thus far is in *Proterochersis porebensis* specimen ZPAL V.39/59 (Fig. S3J; its width is 3.2 cm, maximal size is 5.1 cm, and length is 3.9 cm). The remaining posterior marginals in large specimens, as evidenced by ZPAL V.39/6 (Fig. S3D) and ZPAL V.39/59 (Fig. S3J), also tended to increase their sizes towards the periphery of the shell, but lacked the serration and spikiness of the last marginal.

One of the largest fragmentary *Proterochersis porebensis* specimens, ZPAL V.39/60 (Fig. S1O–P), has the ninth marginal 7.8 cm long (measured on the external side of carapace, close to the edge). ZPAL V.39/34 has this marginal approximately 3.5 cm long, ZPAL V.39/48 – 5.2 cm long, ZPAL V.39/49 – 6.5 cm long, and ZPAL V.39/72 – 6 cm long. There seems to be reasonably good correlation between the length of carapace (see above) and the length of that element (correlation index = 0.986 for n = 4). Based on that, the shell of ZPAL V.39/60 may be estimated to reach up to about 60 cm in length.

Scute sulci and surface. The morphology and size of sulci in carapaces of *Proterochersis* spp. is dependent on their ontogenetic age, as inferred from shell size. There is a positive correlation between the ontogenetic age of the animal and the depth and breadth of sulci. In ZPAL V.39/34 (Figs 4A–B, S2C, S3G) the sulci on the carapace are less than 1 mm wide and in some cases one edge of the sulcus (e.g., the posterior edge of the vertebral scute area in intervertebral sulci) is slightly curled externally, creating a characteristic lip and making it a bit higher than the other

edge (rarer is the situation when both the edges are raised, as in ZPAL V.39/2, Fig. S2A). Also in ZPAL V.39/34, some sulci (e.g., between some lateral marginals) are very poorly defined or seem to be convex rather than concave (e.g., between the cervical and the anterior marginals or between the supramarginals) – the latter morphology may be a combination of the two former, i.e., the sulcus proper (the groove) is too weak to be seen, but the lip around the periphery of one of the scutes is visible. In larger specimens the sulci are broader (up to over one centimeter in ZPAL V.39/63, Fig. S1B) and universally concave. The intervertebral and intermarginal sulci usually have their anterior edge (formed by the preceding scute area) slightly higher than the posterior one (formed by the succeeding scute area), but the edges are usually rounded and rarely form a curled lip (e.g., ZPAL V.39/169, Fig. S2E).

Most scute sulci on the carapace of *Proterochersis* spp. are sinuous. This, however, seems to be at least partially determined by the ontogenetic age of the individual – in juveniles, such as SMNS 16603 (Fig. 2D–E) and ZPAL V.39/34 (Figs 4A–B, S2C, S3G), the sulci appear to be straight, and with age their undulation increases. It is most prominent around the supramarginals and pleurals. The undulation is also related to the radial striation on the surface of the scutes, which is frequently visible (although usually faint) as imprints on the bone surface. The surficial striation and the undulation of sulci are most prominent in the carapaces of the largest specimens, such as SMNS 16442, ZPAL V.39/49 (Fig. 4E–F), ZPAL V.39/59 (Fig. S3J), and ZPAL V.39/63 (Fig. S1B), because the length of the undulations and depth of striations seems to increase with growth. The striation on the pleurals is most prominent along their anterior and pleuromarginal sulci, where the grooves are longer than along the posterior and pleurovertebral sulci. Most marginals of not very large individuals exhibit weak undulation of sulci and striation, with the exception of the ninth marginal, in which these characters are strongly expressed along the sulcus with the third supramarginal. Usually, the intervertebral sulci do not undulate (even though the pleurovertebral sulci and the anterolateral sulcus of the first vertebral scute are clearly sinuous and, especially the latter, frequently exhibit striation), but in very large individuals (e.g., ZPAL V.39/63, Fig. S1B) the intervertebral sulci are becoming slightly uneven. Separate from the radial striation are the bowed, concentric growth marks. These marks are located in the same areas as the radial striation (most notably on pleurals along the anterior pleural and pleuromarginal sulci and on vertebrals along the pleurovertebral sulci and along the anterolateral sulcus of the first pleural), but are parallel rather than perpendicular to the scute sulci, usually

fainter, broader, and less densely packed. They do not reach the borders of the scute, and thus are not correlated with the undulation of the sulci. Their relatively large breadth and shallowness makes them difficult to spot on supramarginals and on the posterior and dorsomedial parts of the pleurals. Together with their low number even in large specimens (no more than several growth marks per scute) and their absence in young specimens, this also indicates that they do not exhibit strict seasonal (annual) iterativity, but rather developed as a result of long-term (polyseasonal) changes of environmental conditions. Both the radial striations and the growth marks seem to originate near the posterodorsomedial region of the pleurals, where the bone is thickened to a boss. This agrees with the observed pattern of scute growth (see below). Similar boss is also present in some specimens in the posterodorsomedial region of the first supramarginal, near the dorsomedial edge of the second supramarginal, and in the anterodorsomedial region of the third supramarginal.

Proterochersis robusta specimen SMNS 17930 (Figs 2I, 6) is unique in its accentuated growth marks of its vertebral and pleural scutes. There are two generations of these abnormal growth marks per scute and they are bilaterally symmetrical. In breadth and position they resemble typical growth marks of other *Proterochersis* spp. specimens (such typical growth marks are also present between and above the abnormal ones in SMNS 17930, Fig. 6) but they are deeper (in that respect approximating sulci) and have sharper edges. Along the anterior edges of the first and the third vertebral scute the growth marks of the older, higher positioned generation are bilaterally continuous and take form of "fake sulci" by copying the shape of true sulci in front of them (albeit in smaller scale, as evidenced by the first vertebral). They, however, do not reach the edges of the scutes and do not connect to true sulci. Based on the fact that this morphology is present only in this one, middle-sized specimen, we interpret it as pathological.

Plastron

Young specimens. Several fragmentary specimens of plastral bones on early stages of development are known from the *Proterochersis* spp.-yielding localities of Murrhardt and Poręba – SMNS 81917 (Fig. S4A), ZPAL V.39/165, ZPAL V.39/197 (Fig. S4C), ZPAL V.39/277 (Fig. S4B), ZPAL V.39/383, ZPAL V.39/384 (Fig. S4D), and several other specimens from Poręba.

Given their size (several centimeters each), it is likely that they belong to young juveniles, older than hatchlings but younger than ZPAL V.39/34, which has its shell completely ossified. Other than the typical characteristics of developing plastral bones – jagged edges with fingerlike projections and minute striation indicative of progressing intramembranous ossification (e.g., Gilbert et al., 2001) – they exhibit little surficial characters, no identifiable sulci, and only ZPAL V.39/165 and ZPAL V.39/197 (Fig. S4C) can be identified with relative confidence as hyoplastra, based on the shape of their incipient axillary buttresses. SMNS 81917 (Fig. S4A) is up to 2 mm thick and has a rounded notch, which indicates that it is either a hyoplastron or a hypoplastron. Unfortunately, it is exposed only in visceral view and flattened, therefore it is difficult to establish which one of its lobes represents a buttress, and which one the main plate of the bone. For that reason, it is also difficult to identify it more precisely. A lip along one of the edges of the notch and gentle thickening along the other edge differentiate this specimen from ZPAL V.39/165 and ZPAL V.39/197, potentially hinting that it is a hypoplastron, but these differences may be specific or ontogenetic. Based on the overall shape and relatively large thickness (5 to 8 mm, compared to 1 to maximally 5 mm of ZPAL V.39/165 and ZPAL V.39/197), ZPAL V.39/277 is likely a xiphiplastron (compare to, e.g., Zangerl, 1939; Gilbert et al., 2001; Rice et al., 2016) or may be one of the mesoplastra – it is thicker than ZPAL V.39/165 and ZPAL V.39/197, even though they are larger and relatively well-developed, so it is unlikely that this element represents an earlier stage of hyoplastron formation, and for the same reason its identity as a hypoplastron may be likely refuted. Overall, the developing plastral bones which may be attributed to *Proterochersis* spp. are already more similar to plastral bones of derived turtles than to fusing gastralia, from which the plastron probably originated (Schoch & Sues, 2015, 2017).

Gular and extragular scutes. *Proterochersis* spp. had a pair of gular (roughly pentagonal in ventral view) and extragular (roughly trapezoid in ventral view) scutes located at the cranial end of the plastron (Figs 1, 3, 5, 7, S5), contacting the anterior edges of the humeral scutes (the exception being *P. porebensis* ZPAL V.39/385, see below). The posterior sulci of the gulars are roughly straight or gently concave and skewed anterolaterally, while the posterior sulci of the extragulars are gently convex and skewed posterolaterally. Usually, the gulars are separated from the extragulars by a tilted, anterolaterally directed sulcus, but the angle of tilting varies between specimens and in SMNS 16603 the sulcus is directed craniocaudally. It appears that the size of

gulars relative to extragulars is variable – e.g., in ZPAL V.39/48 they are, respectively, 2.6 cm and 3.2 cm wide, while in ZPAL V.39/385, 1.9 cm and 3.9 cm wide (measured anteriorly).

A trend may be observed concerning the growth of the gulars and extragulars. In young specimens, such as SMNS 16603 (Figs 3E, S5B) and ZPAL V.39/34 (Figs 5A, S5E–G) these scutes were completely flat and the cranial edge of the anterior plastral lobe was flush (see Szczygielski & Sulej, 2016). In larger, older specimens, these scutes formed tubercles. It seems that their growth was slightly faster dorsally than ventrally, so at first they pointed primarily in cranial direction and were relatively flat ventrally (e.g., SMNS 17561, Figs 3F, S5C–D; ZPAL V.39/388, S5K′–M′), but with time in some individuals they curled and were becoming more and more pronounced downwards (e.g., ZPAL V.39/48, Figs 5B, S5H–J; ZPAL V.39/49, Figs 5C, S5K–M; ZPAL V.39/186, Fig. S5N–Q; ZPAL V.39/379, Fig. S5B′–D′; ZPAL V.39/385, Fig. S5E′–G′; ZPAL V.39/387, Fig. S5H′–J′). Advanced stages of curling are visible only in *P. porebensis* specimens (but only four specimens of *P. robusta* have this region preserved, including juvenile SMNS 16603), and there is some variation when it comes to the degree of curling relative to size – e.g., in ZPAL V.39/387 (Fig. S5H′–J′) the extragular is more curled downwards than in ZPAL V.39/187 (Fig. S5R–T) and ZPAL V.39/333 (S5Y–A′), even though the former is significantly smaller (3.5 vs 4.8 cm and 4 cm wide, respectively). Similarly, in ZPAL V.39/189 (Fig. S5U–X) the gular is thick and large (3 cm wide) but relatively short and nearly flat ventrally, while the curling is already evident e.g. in ZPAL V.39/385 (1.8 cm wide gular, Figs 7, S5E′–G′) and ZPAL V.39/48 (2.6 cm wide gular, Figs 5B, S5H–J). Also CSMM uncat., despite its relatively large size, has ventrally flat gulars (Figs 3A, S5A). Herein, the degree of curling was analyzed using the shape analysis as it may potentially be a form of sexual dimorphism (see Shape analysis below, Fig. 8A–B). In SMNS 16442 (Fig. 3D) the preserved medial parts of gulars are nearly flat and do not show clear ventral inclination despite the large size of that specimen, but (in addition to potential dimorphism) it is possible that this is caused by the compaction or that the curling was mostly expressed in the lateral parts of gulars, which were supported by epiplastra and are now missing. Finally, it is possible that better development of gular and extragular scutes in mature specimens is an autapomorphy of *P. porebensis.*

In ZPAL V.39/385 (Figs 7, S5E′–G′) the gulars are rounded ventrally, but in most specimens they are slightly spiky (Fig. S5). In ZPAL V.39/49 (Fig. 5C, S5K–M) the gulars are laterally

asymmetrical (the right one is 2.7 cm wide while the left one is 2.4 cm wide) even though the intergular sulcus is located on the midline of the anterior plastral lobe. In CSMM uncat. (Fig. 3A, S5A) and SMNS 16603 (Fig. 3E, S5B) this sulcus is slightly moved to the left. Only the right gular is preserved in these two specimens, but it may be hypothesized that this also caused some minor asymmetry.

No significant clustering was seen on the PCA plots as well as on the regression analysis (p-value > 0.1) of gulars and extragulars in ventral view (Fig. 8A–B). The PCA plots for the vertical cross-section of extragulars separate the analyzed sample in two groups (Fig. 8C–D). The principal component 1 (62.3% of total variance) clusters one group of adults (I) in the post positive values, and the second (II) in the negative values. The only juvenile in that analysis, ZPAL V.39/34, is closer to the second adult group. In the case of principal component 2 (27.9% of total variance) the first and the second group are placed along the whole spectrum of PC2 values, the same occurs along PC3 (7.4% of total variance). The results of the regression analysis also show separation between these two groups, however not statistically significant (p-value > 0.1).

Abnormal scute set. *Proterochersis porebensis* specimen ZPAL V.39/385 (Fig. 7, S5E′–G′) exhibits a scute abnormality. In this specimen, between the row of gulars and intergulars and the set of humerals, there were paired, roughly triangular supernumerary scutes. The right one was slightly smaller than the left one, and did not reach the lateral edge of plastron, allowing partial contact between the right extragular and humeral. The left, larger supernumerary scute did reach the edge of the plastron, and thus separates the extragular from the humeral completely. The sulci separating these two additional elements from the humerals have slightly raised edges, are deepest medially, and become less clear laterally. At first sight, their layout resembles the posterolateral suture of the entoplastron, as visible in *P. robusta* specimen SMNS 16442 (Fig. 3D), but upon closer inspection, they cannot be mistaken for this suture – their edges are smooth, they lack interdigitation and other macro- and microscopic characteristic of sutures but instead their morphology is consistent with that of other sulci in that specimen, they are located more posterolaterally than the entoplastral suture and do not enter area of gulars (nor extragulars), and there is no sign of sutures on the visceral surface of that specimen.

Humeral scutes. *Proterochersis* spp. had a set of two humerals (Figs 1, 3, 5, 7, S5) located behind the gulars and extragulars (except ZPAL V.39/385, see above) and in front of the pectorals. The posterior sulci of the humeral set have a characteristic appearance – their lateral ends are turned anteriorly, and medial ends are usually turned more or less posteriorly, forming a variously pronounced tip (best visible in *P. robusta* specimens CSMM uncat., Fig. 3A, and SMNS 17561, Fig. 3F, as well as in *P. porebensis* specimen ZPAL V.39/49, Fig. 5C). Beside ZPAL V.39/385, which had the anteromedial edges of the humerals misshaped due to presence of additional abnormal scute pair, there is no clear variability in humeral shape.

Axillary scutes. There was a pair of elongated, hexagonal axillary scutes present in *Proterochersis* spp. Each contacted the ventromedial bases of the fourth and fifth marginal, the cranial border of the first inframarginal, and the cranial edge of the lateral part of the pectoral scute. Best preserved in *Proterochersis robusta* SMNS 17561 (Fig. 3F) and *P. porebensis* ZPAL V.39/48 (Fig. 5B), these scutes do not exhibit visible variation.

Pectoral scutes. There was a pair of pectoral scutes present in *Proterochersis* spp. (Figs 3, 5, 7). Anteriorly, they contacted the humerals, their lateral ends contacted with the axillaries and the first two pairs of inframarginals, and posteriorly they contacted the first pair of abdominal scutes. The only specimen with an unusual shape of the pectorals is *P. robusta* specimen SMNS 17561 (Fig. 3F), in which the scutes were abnormally elongated posteriorly in the middle section (see below).

Abdominal scutes. There were two pairs of wide and short, strap-like abdominals in *Proterochersis* spp. (Figs 1, 3, 5). The first pair was located between the pectorals (anteriorly), the second and the third inframarginal (laterally), and the second pair of abdominals (posteriorly). The latter, beside the first abdominal pair, contacted the third and fourth inframarginal and the ninth marginal laterally, and the femoral scutes posteriorly. Both abdominal pairs gradually increased in length towards the ventromedial end of the bridge, at which level their anterior sulci are characteristically bent. From that point towards the lateral ends of the bridge, the length of the first abdominal remained roughly constant and the length of the second abdominal slightly decreased. Typically, abdominals of both pairs met medially. In *P. robusta* specimen SMNS 17561 (Fig. 3F), however, the first pair of abdominals lacked medial contact. These scutes gradually decreased in length towards the midline and disappeared

completely just before reaching it. Their place in the mid-section of the plastron seems to be partially taken by the posterior expansions of the pectorals and partially by the second pair of abdominals, which seem to retain roughly constant length instead of tapering medially, as typical (compare Figs 3, 5, 7). Based on available evidence (at least five other specimens of *P. robusta* and several specimens of *P. porebensis*) this morphology is unlikely to be part of normal variability, and pretty confidently may be considered abnormal. SMNS 15479 (a double external mold of proterochersid plastron found in Reichenbach, Germany, figured but not described by Gaffney, 1990, fig. 68 therein) lacks characters that would allow its precise identification as *P. robusta*, but such an identity is possible, in which case it would further support the medial contact of the first pair of abdominals as the norm.

Inframarginal scutes. *Proterochersis* spp. had four polygonal or rounded inframarginal scutes on each side (Figs 1, 3, 5). Dorsolaterally, they contacted the marginal row (fourth to eighth marginal, see above). Anteriorly, the first inframarginal contacted the axillary scute. Ventromedially, the inframarginals contacted the lateral ends of the pectoral (first and second inframarginal), the first abdominal (second and third inframarginal), and the second abdominal (third and fourth inframarginal) scute. In ZPAL V.39/34 (Fig. 5A), the inframarginals were relatively narrow, elongated, and comma-shaped. In larger specimens (SMNS 17561, Fig. 3F; SMNS 17755, Fig. 3G; SMNS 18440, Fig. 3H; ZPAL V.39/48, Fig. 5B; ZPAL V.39/49, Fig. 5C) they increasingly gained girth, becoming relatively flatter. In *Proterochersis robusta* specimen SMNS 17755 (Fig. 3G) the third and the fourth inframarginal is separated by a small gap. In *P. robusta* specimen SMNS 18440 (Fig. 3H) there is a triangular gap between the anterior part of the third inframarginal and the seventh marginal, and possibly there was a gap between the first inframarginal, the sixth and the seventh marginal, and (maybe) the second inframarginal, but the posterior part of the first marginal is damaged, making this uncertain. In *P. porebensis* ZPAL V.39/21 there also is an apparent gap between the first and the second inframarginal, around the level of the sulcus between the fifth and the sixth marginal. These gaps seem to lack any pores inside, so they likely were interplates covered by skin rather than housed Rathke's glands, especially that there is no evidence of similar gaps in the remaining specimens of *Proterochersis* spp.

Femoral scutes. The femorals in *Proterochersis* spp. were located behind the bridge, between the second pair of the abdominal scutes and the anals (Figs 1, 3, 5). Typically, the abdominofemoral sulcus is gently bowed posteriorly, and in most specimens (the exceptions being *P. robusta* SMNS 16442, Fig. 3C, and *P. porebensis* ZPAL V.39/48, Fig. 5B) this is also true for the femoroanal sulcus. Both of these sulci are always directed posterolaterally – the femoroanal sulcus more profoundly than the abdominofemoral. No clear variability is observed in these scutes.

Anal scutes. Contacting the femorals anteriorly and the intercaudal and caudal scutes posteriorly, the anals of *Proterochersis* spp. were the longest scutes in the posterior plastral lobe (Figs 1, 3, 5). They gradually decreased in width posteriorly. No clear variability was observed for these scutes.

Intercaudal and caudal scutes. The posteriormost part of the plastron, presenting a set of two caudal and one intercaudal scute, seems to be the most variable section of the shell in *Proterochersis* spp. (Figs 1, 3, 5, 9). In the youngest specimens, such as ZPAL V.39/34 (Figs 5A, 9K) and ZPAL V.39/66 (Fig. 9J), the caudal processes are small, wider than long, and are entirely (ZPAL V.39/34) or almost entirely (ZPAL V.39/66) covered dorsally by the posterior plate of ischium. In larger specimens, the variation is expressed in several ways. Firstly, the caudal processes may be relatively short and rounded distally (CSMM uncat., Figs 3A, 9A; SMNS 17561, Figs 3F, 9C; ZPAL V.39/69, Fig. 9F) or relatively long and spiky (SMNS 12777, Figs 3C, 9B; ZPAL V.39/48, Figs 5B, 9G; ZPAL V.39/49, Figs 5C, 9D; ZPAL V.39/56, Fig. 9L–N; ZPAL V.39/68, Fig. 9H; ZPAL V.39/70, Fig. 9I; ZPAL V.39/71, Fig. 9E; ZPAL V.39/199, Fig. 9O–Q). Secondly, the lateral edges of the caudal processes are generally thinner than the medial edges, but in ZPAL V.39/56 (Fig. 9N) and SMNS 12777 (apparently – the process is not preserved, but it left an imprint in the rock matrix; Figs 3C, 11B) the lateral edge is sharpened, while in the remaining specimens it is more rounded. In some cases, this may be an artifact of preservation (the edges are frequently damaged), but some well-preserved and seemingly undamaged specimens (most notably ZPAL V.39/68, Fig. 9H, and ZPAL V.39/199, Fig. 9Q) show that the edge indeed was rounded in some individuals. Thirdly, in some large specimens (ZPAL V.39/69, Fig. 9F; ZPAL V.39/70, Fig. 9I; ZPAL V.39/71, Fig. 9E; *P. robusta* specimens are not prepared sufficiently to validate whether this is the case) the ischium is visible

in ventral view between the caudal processes, but in most specimens it is not exposed. The degree of this exposure varies from minor (ZPAL V.39/70) to major (ZPAL V.39/69, ZPAL V.39/71). Fourthly, the angle between the caudal processes varies – e.g., in ZPAL V.39/68 (Fig. 9H) it is low, in ZPAL V.39/49 (Figs 5C, 9D) and ZPAL V.39/70 (Fig. 9I) it is intermediate, and in ZPAL V.39/48 (Figs 5B, 9G) and ZPAL V.39/69 (Fig. 9F) it is larger. Finally, the size and the proportions (length to width) of the intercaudal scute is varied – e.g., in ZPAL V.39/68 (Fig. 9H) it is very elongated craniocaudally (2.2 cm in length x 1.2 cm in width), in ZPAL V.39/69 (Fig. 9F) it is nearly as wide as long (2.3 in length x 2.2 cm in width), while in SMNS 56606 (Fig. 3J) it seems to be wider than long (but unfortunately damaged). Because there is no clear correlation between these morphologies and size of the specimen, we decided to use shape analysis in search of possible sexual dimorphism (see the section shape analysis below, Fig. 9C–F).

Based on the width of the posterior plastral lobe, *Proterochersis robusta* specimen SMNS 17561 (Figs 3F, 9C) appears to be of roughly comparable size to *P. porebensis* specimen ZPAL V.39/66 (Fig. 9J), but the former has a well-developed, adult-like shell, while the latter appears to be a juvenile, more similar to ZPAL V.39/34 (Figs 5A, 9K) than to larger specimens, suggesting that *P. robusta* achieved adult-like features (and, supposedly, sexual maturity) at smaller sizes than *P. porebensis*. This is congruent with larger average and maximal sizes of *P. porebensis* specimens found thus far compared to *P. robusta* specimens.

ZPAL V.39/200 (Fig. 9R–T) is a curious, thorn-like element with lamellar sutural surface at its base. It may represent an isolated caudal plastral process, although it is small compared to other specimens. Otherwise, it may be interpreted as a part of a complex cervical or caudal osteoderm, similar to those described by Gaffney (1990) for *Proganochelys quenstedti* Baur, 1887, and suggested by Lucas et al. (2000) and Joyce et al. (2009) for *Chinlechelys tenertesta* Joyce et al., 2009, but no other evidence of such osteoderms is known from Poręba.

In the in the PCA plots of the caudal processes and intercaudal scute (Fig. 10A–B) the principal component 1 (65.4% of total variance) clusters one group of adults (II) in the most positive values, the juvenile ZPAL V.39/34 in the most negative, and the second adult group (I) between them. The small individual ZPAL V.39/66 is placed close to the group I, it may indicate that it already can be classified there. The specimens do not cluster according to their taxonomical affiliation. The principal component 2 (19.8% of total variance) shows that the individuals of

878 group I are placed along the whole value spectrum of PC2 values, while the specimens of group
879 II are clustered around 0. The juvenile ZPAL V.39/34 lies around the PC2 value 0, while ZPAL
880 V.39/66 has a negative value. The juvenile ZPAL V.39/34 occupies the 0 value also on principal
881 component 3 (5.5% of total variance). Here the specimens of group I are clustered around 0,
882 however, while the individuals of group II are placed along the negative values of the PC3. The
883 second juvenile, ZPAL V.39/66, is positioned in the most positive values of PC3.

884 A multivariate analysis of variance (MANOVA), which was performed on the groups identified
885 by the PCA plot, showed that they differ significantly in shape ($F = 2.51$, p-value < 0.01) but not
886 in (centroid) size ($F = 4.15$, p-value > 0.2; Table S6). Therefore, the difference in shape but not
887 in size indicates that the dimorphism is not ontogenetic, but rather sexual. There is no significant
888 distinction in the shape of caudal process between species (Table S6).

889 To better distinguish the dimorphism in the caudal plastral region of *Proterochersis* spp., we
890 used CVA analysis (Fig. 10D). The canonical variate 1 (80% of variation) separates juveniles
891 from adults, while canonical variate 2 (20% of variation) separates group I from II. The group I
892 occupies negative values of canonical variate 2, the individuals of group II find themselves in the
893 positive values, and the juveniles ZPAL V.39/34 and ZPAL V.39/66 are placed between them
894 (Fig. 10D). The Mahalanobis distance (Mardia, Kent & Bibby, 1979) between group I and II is
895 4.2 and it is statistically significant (p-value < 0.02; Table S7).

896 The results of the regression analysis (pooled by species, Fig. 10C) of two *Proterochersis* taxa
897 show that 49.5% (p-value = 0.001) of the total shape variability can be explained by size
898 variation. The results show, that the individuals from group I occur different regression scores
899 than the specimens from group II, even if they are similar in size (ZPAL V.39/69 and SMNS
900 12777, Fig. 10C).

901 **Scute sulci and proportions.** Like in carapace, the width and depth of sulci increase with the
902 ontogenetic age of the animal. Unlike in carapace, the sulci in plastron never seem to undulate
903 and there is no scute striation. In large specimens, however, the sulci do exhibit some minor
904 irregularities, while in small ones they are usually very straight (compare Figs 3, 5). As in
905 modern turtles, there is typically some bilateral asymmetry when it comes to the sulci layout on
906 the plastron – most notably, the scutes in corresponding pairs (humerals, pectorals, abdominals,

907 etc.) differed slightly in length, so the points in which their anterior and posterior sulci meet the
908 midline are shifted slightly cranially or caudally relative to each other (this is best visible in
909 CSMM uncat., Fig. 3A). This shift is random, so there is no clear alteration (i.e., the sulci on one
910 side do not always precede the sulci on the other side).

911 **Plastron thickness.** The plastron in proterochersid is not equally thick throughout, but rather it is
912 thinnest in the bridge area and around midline, and thickest in the lateral sections of femoral
913 scute area, where it forms a bulbous expansion. In ZPAL V.39/34 the femoral is 18 cm thick, in
914 ZPAL V.39/48 it is 2.1 cm thick, and in ZPAL V.39/49 it is 2.5 cm thick. The thickest plastron
915 found thus far is ZPAL V.39/157, with femoral scute region 2.7 cm thick in the lateral part and
916 about 0.5 cm thick at the medial anterior section of the anal scute area.

917

918 Discussion

919 Ontogeny

920 The shell of proterochersids changed during ontogeny in several ways. The most notable is the
921 expansion of gular, extragular, and caudal processes, and projections of anterior and posterior
922 marginals. In young specimens these elements were short and lack pronounced tips, while in
923 older specimens they were becoming proportionally larger. The nuchal notch formed by
924 expansion of anterior marginals relative to cervical scute. Furthermore, the depth and width of
925 shell sulci increased with ontogenetic age. This is linked to increase of sulci undulation and
926 radial striation of scute areas. In some subadult and adult specimens, bow-shaped growth marks
927 appeared on the scutes. As discussed above, a middorsal keel was apparently present in juveniles
928 and reduced or lost in older specimens. The dorsal vertebrae were ankylosed in subadults and
929 adults, and the axial skeleton mostly expanded at the points of rib head attachments. The neural
930 canal changed its shape from vertically elongated to oval.

931

932 Scute surface

Radial striation. Radial striation and sinuous sulci, similar to those observed in *Proterochersis* spp., are present in numerous Triassic (de Broin et al., 1982; Gaffney, 1990) and Jurassic (Broin, 1994; Anquetin & Joyce, 2014; Anquetin, Püntener & Billon-Bruyat, 2014; Jansen & Klein, 2014; Anquetin, Püntener & Joyce, 2017; Sullivan & Joyce, 2017) turtles. The same surficial characters are also present in *Keuperotesta limendorsa* specimen SMNS 17757, including clear striation and growth marks along the anterior and lateral edges of the last vertebral scute, and unlike *Proterochersis* spp. the sulcus between the fifth and fourth vertebral scute of *K. limendorsa* is clearly sinuous. In that specimen, these characters are more pronounced in the posterior part of the shell than in the anterior part, but this may be a preservation artifact. Due to small sample, it is unknown whether this is taxonomically important, or just related to an old ontogenetic age of SMNS 17757. The ecology of early turtles is controversial, but currently no clear adaptive value is apparent for these low, radial ridges, and given their widespread occurrence in early taxa, they are likely plesiomorphic. Moreover, a delicate striation is present on scutes of some turtles, and possibly in older specimens it may leave imprints on underlying bones.

Growth marks. The presence of bow-shaped scute growth marks is most typical for the turtle species in which the scutes are not shed (Zangerl, 1969; Alibardi, 2005). This most usually means terrestrial turtles, but there are also some examples of scute shedding terrestrial box-tortoises or non-shedding aquatic emydids (Alibardi, 2005). The non-pathological growth marks in *Proterochersis* spp. and *Keuperotesta limendorsa* are, however, very subtle, and more comparable to those seen in some specimens of scute-shedding aquatic turtles (pers. obs.), therefore it is not clear whether proterochersids shed their scutes. Furthermore, if scute shedding is an adaptation to aquatic environment (e.g., by lowering drag during swimming thanks to smoother shell surface), it is likely that this mechanism developed with some delay, some time after turtles invaded the aquatic environment, and thus might have been absent in the earliest aquatic testudinates. Conversely, if scute shedding is plesiomorphic for turtles and was repressed as an adaptation to terrestrial life (by thickening the durable, keratinous layer protecting the epidermis and shell bones), it might have developed in more advanced terrestrial turtles. For that reason, the correlation between the scute shedding and life environment may not be strict for the Triassic turtles.

Middorsal ridges and keels. A low middorsal ridge was thus far reported among Triassic turtles only in *Proganochelys quenstedti* in the anterior sections of its vertebral scutes (Gaffney, 1990). A subtle ridge is also present crossing the area of the vertebral scutes (including the fifth vertebral) of *Keuperotesta limendorsa* specimen SMNS 17757. Similar low midline ridges are also present in numerous modern turtles (Pritchard, 2008). Much more enigmatic are pronounced keels surrounded by deep troughs of young *Proterochersis porebensis* specimens. Given current data, it seems that they are unique to young stages of shell development of *Proterochersis* spp. Their genesis and relationship to vertebral scutes, however, are problematic. Certainly, they are not caused by any post-mortem, mechanical folding, because they are symmetrical, their morphology is virtually the same in both specimens, and there is no sign of folding or cracking on the ventral surface of ZPAL V.39/2 (Fig. S2A–B). It would be tempting to conclude that in life they were covered by normal, unpaired vertebral scutes, and that the troughs were initially filled by dermis, connective tissue, or rudimentary muscles, and subsequently by developing bone of neurals. The walls of the troughs, including the lateral edges of the midline keel, bear, however, the same rough texture as the remaining, scute-covered surfaces of carapacial bones (contrary to some deeper-located or visceral surfaces), suggesting that they were lined by keratinous elements as well. On the other hand, the scutes of older specimens do not show any remnants of deep troughs in their older parts. This is problematic, because turtle scutes grow from the bottom (Alibardi, 2005) and the heavily cornified and stiff outer scute layers hardly seem to be susceptible to remodeling. This would call out either for local, temporal scute decornification of mid-sections of proterochersid vertebral scutes, as in plastra of breeding male chelonioids (Wibbels, Owens & Rostal, 1991; Wyneken, 2001; Pritchard, 2008), or for scute shedding in proterochersids, at least when young. Even with help of scute shedding, though, filling of the scute-lined troughs with bone still appears tricky, because the shape of the younger, deeper, and less cornified layer of the scute, which would potentially allow some flexibility and space for bone apposition, would still be determined by the older, stiffer, external layer. It seems, nonetheless, possible that uneven thickness of cornifying epidermis (thicker below the flat parts and thinner at the points of penetration into the troughs) would, with every generation of shed scutes, result in shallower troughs, and eventually in their disappearance. Less probable seems the hypothesis that the newer generations of scutes of *Proterochersis* spp. attained their stiffness some time after the older scutes were shed, and until then they were pliable enough to allow

gradual filling of the troughs, or that the troughs are pathological and developed independently in two specimens of similar sizes from the same locality. Possibly, this conundrum will be solved by future histological studies. Until then, these interpretations remain speculative.

Plastron scutes. The scutes of the plastron in proterochersids (but also in *Proganochelys quenstedti*) generally lacked undulating edges, surficial striation, and growth marks, in which they differ from the carapacial scutes. In agreement with this, the molecular background of plastral and carapacial scute development is divergent (Cherepanov, 1989; Moustakas-Verho et al., 2014; Moustakas-Verho & Cherepanov, 2015). These differing characteristics may result from different evolutionary history of plastron and carapace – they developed separately and the former appeared before the latter (Li et al., 2008; Schoch & Sues, 2015, 2017) – and possibly are rooted in varied (primaxial vs abaxial) environment of morphogenesis (Burke, 1989; Nowicki & Burke, 2000; Burke & Nowicki, 2003; Shearman & Burke, 2009).

Scute anomalies and growth

Anomalies in scute layout, shape, and number are relatively frequent in turtles (Parker, 1901; Coker, 1905, 1910; Grant, 1936b; Młynarski, 1956; Zangerl & Johnson, 1957; Zangerl, 1969; Cherepanov, 2006, 2014, 2015; Farke & Distler, 2015; Sullivan & Joyce, 2017; Lichtig & Lucas, 2017). Thus far, however, no unambiguous scute anomalies were reported in the Triassic turtles. The only possible exception is the missing first marginal in one of *Proganochelys quenstedti* specimens but interpretation of that case is uncertain (Gaffney, 1990; Szczygielski, 2017). Some of the morphologies described here were previously noted by Karl and Tichy (Karl & Tichy, 2000), but not considered in wider populational or developmental context, but rather glanced over as a part of normal intraspecific variation of their "*Murrhardtia staeschei*". The data on *Proterochersis* spp. presented here reveals, therefore, the first uncontroversial evidence of scute abnormalities in the Triassic turtle taxa.

The most obvious cases concern additional scutes and improper scute shape. The asymmetry of the lateral parts of the first vertebral scute in ZPAL V.39/49, as well as the asymmetrical intervertebral sulci of *Proterochersis robusta* specimens CSMM uncat. and SMNS 17561, and *P. porebensis* specimens ZPAL V.39/34 and ZPAL V.39/72 are minor and may be easily explained

as effects of uneven tempo of scute growth in its contralateral parts, and most likely are not caused by improper development (skipped segment or additional placode in vacant myoseptum) and fusion of scute placodes (Cherepanov, 1989, 2006, 2014, 2015; Moustakas-Verho et al., 2014; Moustakas-Verho & Cherepanov, 2015; Moustakas-Verho, Cebra-Thomas & Gilbert, 2017). Likewise, the medial separation of the first pair of abdominal scutes in *P. robusta* specimen SMNS 17561 appears to be caused by simple overgrowth of the preceding and the succeeding pair of scutes. As noted by, e.g., Zangerl and Johnson (1957), abnormalities in the abdominals are relatively frequent. The supernumerary prehumeral scutes of *P. porebensis* specimen ZPAL V.39/385 are, on the other hand, a handbook example of an effect of additional pair of scute placodes. This specimen is even more interesting due to relative rarity of additional scutes in the plastron in many taxa (e.g., Newman, 1906b; Lynn, 1937), and rarity of bilateral additional scutes in general (e.g., Newman, 1906b; Coker, 1910; Młynarski, 1956; Moustakas-Verho & Cherepanov, 2015).

Proterochersis robusta specimen SMNS 17930 differs from all the other *Proterochersis* spp. specimens in its abnormally deep growth lines which form “false sulci” along the anterior limits of vertebral scutes. They are well-visible on pleural and vertebral scute areas, and on the latter they are bilaterally symmetrical, which excludes trauma or post-mortem damage from the list of potential causes. Renal hyperparathyroidism (improper bone formation caused by calcium deficiency related to impeded vitamin D metabolism) was reported to cause accentuated ‘interplates’ and growth lines (Frye, 1994; Rothschild, Schultze & Pellegrini, 2013). The morphology of SMNS 17930 may therefore be tentatively interpreted as resulting from this condition, but further studies will validate this diagnosis. Alternatively, if proterochersids did normally shed their scutes, the morphology of SMNS 17930 may be an effect of dysecdysis (scute retention). In any case, this specimen informs about the growth of scutes in *Proterochersis* spp.

In modern turtles, newly cornified layers of the shell develop below the old scutes (Alibardi, 2005). The scutes typically do not grow with equal speed in all directions, resulting in an off-center position of the oldest (embryonic) part relatively to whole scute area (Zangerl, 1969; Cherepanov, 2015). Based on the growth rings on the scute areas of *Proterochersis* spp. (including very clear abnormal growth marks of SMNS 17930) and *Keuperotesta limendorsa*, it

can be inferred that in proterochersids this growth characteristics were also present. The vertebral scutes grew fastest anteriorly, moderately fast laterally, and slowest posteriorly. This is also true for the odd-shaped first vertebral, which apparently grew mainly cranially, while its posterior process retained throughout life the same general shape and size. The pleurals grew fastest anteriorly and lateroventrally, and their oldest areas were likely located close to (or on) the posterodorsomedial bosses. Based on the layout of striation (Gaffney, 1990), vertebrals and pleurals of *Proganochelys quenstedti* also grew predominantly anteriorly (not in a radially symmetrical way, contra Cherepanov, 2015). No growth marks are visible on supramarginals and marginals, but the striation of the first and the third supramarginal suggests that the embryonic areas were located, respectively, in the posterior and in the anterior region of the scute area (possibly slightly above the midline). Little can be said about the plastral bones, with the exception of gulars and extragulars, which apparently grew faster dorsally than ventrally, resulting in their ventral curling (see above).

In the light of the above, the deep, sulci-like grooves in the anterior parts of vertebral scutes of *Proterochersis robusta* specimen CSMM uncat. and shallower, but similar positionally and morphologically depressions of SMNS 17930 and (even less pronounced) SMNS 17561 (Figs 2F–G, 8) are best interpreted as appearing late in ontogeny. As stated above (see Results section), there is a positive correlation between the severity of this morphology and size of the specimen. It is highly unlikely that virtually the same (albeit pronounced with various strength) morphologies appeared ideally medially on several vertebrals of three individuals as a result of trauma or post-mortem damage. For that reason, we interpret this as a developmentally-driven scute splitting. Occurrences of splitting (i.e., partially divided) scutes were reported in modern turtles (e.g., Parker, 1901; Coker, 1910; Grant, 1936b; Zangerl & Johnson, 1957) and the split usually occurs in the youngest parts of the affected scutes (Coker, 1910; Grant, 1936a; Zangerl & Johnson, 1957). In some cases, this phenomenon may be explained as a result of damage to interscutal epidermis, which leads to scar formation and loss of proper cornification ability. In many cases, however, the splitting occurs in regions of asymmetry apparently caused, e.g., by pairing of vertebral scute primordia, originating from asymmetrically located scute placodes or just in the middle of a vertebral, and the split divides the areas of particular placodes (Coker, 1910; Grant, 1936b; see Cherepanov, 1989, 2006, 2014, 2015; Moustakas-Verho et al., 2014; Moustakas-Verho & Cherepanov, 2015; Moustakas-Verho, Cebra-Thomas & Gilbert, 2017).

Therefore, it seems that in some cases during postnatal life, due to unknown factors, the primarily fused scute placodes may lose connection and start to produce separate scutes. It is, nonetheless, possible, that the lateral integration between the vertebral placodes was relatively weak in early turtles such as *P. robusta* (it may be hypothesized that huge size of vertebrals may be partially responsible, e.g., by causing some signaling difficulties in large specimens; a mid-section loss of coordination of cornification front may be also responsible for the asymmetry of the sulcus between the third and the fourth vertebral scute in CSMM uncat.), and for that reason the medial split was relatively common. Curiously, there is no sign of anterior vertebral scute splitting in any specimen of *P. porebensis* or *Keuperotesta limendorsa*, but the sample is too small to reliably decide whether the anterior scute splitting in large specimens may be treated as autapomorphy of *P. robusta*. The interpretation of this morphology as abnormality, part of a normal intraspecific variability, or a specific character is, therefore, impossible.

Sexual dimorphism

A wide array of sexually dimorphic characters is known in turtles (see Table S8 for examples). Many of these characters, unfortunately, are either unavailable for study in fossil material (cloacal position, hindlimb callosities) or impossible to check in currently collected *Proterochersis* spp. material due to its incompleteness (e.g., tail length, paw morphology) or damage and distortion (morphometry of the shell). Among the Triassic taxa, probable dimorphism was proposed for *Proganochelys quenstedti* in form of two morphotypes of hypoischium (Gaffney, 1990).

As noted above (see Results section), there is a very wide spectrum of sizes, within which the shells of *Proterochersis* spp. are ankylosed. It appears that all of the individuals possessed a ventral plastral concavity, and while size dimorphism may be present in *Proterochersis* spp., as the specimens of group II are generally larger than the specimens of group I (Fig. 10C), this difference in size does not explain the presence of ankylosis in even smaller specimens, such as ZPAL V.39/34. It appears that all of the individuals possessed a ventral plastral concavity, and while it is possible that the dimorphism was expressed in varied depth or area of this concavity, the breakage and possible compaction of specimens prevent from using sensitive numerical

methods, such as the Principal Component Analysis, to reliably check this. Similarly, the incompleteness, crushing, and possible compaction preclude utility of these methods to identify subtle dimorphisms in the carapace. The gular and extragular processes of the anterior plastral lobe and the caudal processes of the posterior plastral lobe, on the other hand, are relatively well-preserved and apparently not deformed in numerous specimens, and these regions of the shell are known to be dimorphic in some Testudines (Brophy, 2006; Pritchard, 2008; Cadena, Jaramillo & Bloch, 2013; Leuteritz & Gantz, 2013; Sullivan & Joyce, 2017).

The tubercles in the gular plastral region are usually larger in males of modern turtles, especially those with combat-based mating behaviors (Pritchard, 2008). It would be therefore likely that specimens of *Proterochersis* spp. with large, pronounced processes would represent males. The dimorphism might have also been expressed in the degree of ventral curling in extragular scutes. As can be seen on the PCA plots (Fig. 8) the adults can be separated into two groups with extragulars curled downwards (group II; ZPAL V.39/48, ZPAL V.39/49, ZPAL V.39/379, ZPAL V.39/385, ZPAL V.39/387) or straight (group I; ZPAL V.39/187; ZPAL V.39/333; ZPAL V.39/388). We suggest that this may be a result of sexual dimorphism, especially that the segregation is not influenced by size. Unfortunately, the sample is still too small to test it statistically.

Although we did not perform the test on the gular scutes, the specimens with ventrally flat extragulars also bear wide and thick but relatively short and ventrally flat gulars, such as ZPAL V.39/189 or SMNS 17561 (and possibly SMNS 16442), while the specimens with extragulars curled downward have comparably wide but long and curled gulars, such as ZPAL V.39/49 or ZPAL V.39/186 (see above). Currently, there are no known exceptions from that correlation. Lack of ventral gular and extragular curling in known *P. robusta* specimens leaves a possibility that this character is an autapomorphy of *P. porebensis*, but this area is preserved in only three non-juvenile specimens of the former species, which may potentially either be too young to have well-developed gulars and extragulars (SMNS 17561), be too strongly compacted or lack the sections of gulars in which the curling was present (SMNS 16442), or just be females (SMNS 17561, SMNS 16442, and/or CSMM uncat.). The latter interpretation seems to be supported by the shape of the caudal processes in SMNS 17561 and CSMM uncat.

The variability of the caudal processes (Figs 9–10) is seemingly much larger in *Proterochersis* spp. than the variability in the gular region. Typically, the depth, width, and shape of anal notch is correlated with sex (Brophy, 2006; Pritchard, 2008; Cadena, Jaramillo & Bloch, 2013; Leuteritz & Gantz, 2013; Sullivan & Joyce, 2017). Usually, males have deeper notches than females, to facilitate movement of cloaca-supporting tail during copulation (Brophy, 2006; Cadena, Jaramillo & Bloch, 2013; Sullivan & Joyce, 2017), but there are taxa in which females have deeper notches, possibly to facilitate oviposition (Leuteritz & Gantz, 2013). The structure of cloaca and penis is, obviously, unknown for the Triassic turtles, but it may be hypothesized, that in any case an increased ventral movement of tail would be beneficial to males. Furthermore, it seems that the hypoischium of Triassic turtles, which was located just behind the usually had two fingerlike caudal processes (Gaffney, 1990; Sterli, de la Fuente & Rougier, 2007; Li et al., 2008) was dimorphic and likely it played a role during copulation (Gaffney, 1990). The shape analysis confirmed that the specimens with long, spiky, widely spread caudal processes, such as SMNS 12777, ZPAL V.39/48, or ZPAL V.39/49 (presumably males), cluster together in separation to those with short, rounded caudal processes (arguably females), such as CSMM uncat., SMNS 17561, or ZPAL V.39/69 (consistently with long posterior process of ischium of ZPAL V.39/69, which blocks the space between the caudal processes and would likely get in the way of male tail). The clustering based on the morphology of the posterior plastral lobe seems to be congruent with the division based on the morphology of the gular region. Although many of the tested specimens preserve only one of these sections, the individuals with both the anterior and posterior plastral lobe (ZPAL V.39/48, ZPAL V.39/49, CSMM uncat. and SMNS 17561) fall clearly into one of two groups. The presumed males ZPAL V.39/48 and ZPAL V.39/49 bear both the long, spiky caudal processes and the ventrally curled extragulars, while SMNS 17561 and CSMM uncat. have short, rounded caudals and ventrally flat gulars and extragulars. This picture is, however, distorted by odd specimens – ZPAL V.39/68 (long caudal processes, but very close together) and ZPALV.39/71 (long, widely spread caudal processes, but the space between them is at least partially blocked by ischium). According to our analysis, ZPALV.39/71 is classified as a representative of group II (speculated male), and its pronounced posterior ischial plate may be linked to its large size (Fig. 10), but it must be kept in mind that this is the worst preserved specimen in the tested group and its edges are worn, so the exact extent of its posterior ischial plate and exact length of the caudal processes may be

misrepresented. Unfortunately, ZPAL V.39/69 is too fragmentary to include it in the shape analysis. Thus far, all available and complete caudal processes separate subadults and adults of *Proterochersis* spp. into two distinct groups and the best explanation for it seems to be the sexual dimorphism.

Conclusions

The observations of shell variation in Proterochersidae reveals, as could be anticipated, that these oldest and most basal true turtles exhibited a mix of characters – some clearly derived (e.g., development of plastral bones, patterns of scute growth, intervertebral position of dorsal ribs), but some either plesiomorphic (radial striation of carapacial scutes) or difficult to assess (unique middorsal keel surrounded laterally by deep troughs in young individuals, seemingly common medial splitting of vertebral scutes). The presence of growth marks and shell abnormalities comparable to those occurring in modern turtles suggest that the scute system of *Proterochersis* spp. was already controlled by similar developmental mechanism as in crown group taxa. The anteriormost and posteriormost regions of the plastron are hypothesized to be sexually dimorphic in *Proterochersis* spp. No clustering was found on the PCA analysis of gular and extragular tubercles, indicating a population variability (Fig. 8A–B). We noticed separation into two groups in extragular curling, which may potentially indicate some sexual dimorphism (Fig. 8C–D). Nonetheless, a statistically significant separation between the specimens with spiky and rounded caudal processes was detected and implies that they represent males and females of *Proterochersis* spp., respectively (Fig. 10A–B). Therefore, it seems that the sexual dimorphism in the anal region of the plastron, which can be observed in some species of extant turtles (most notably pleurodires, but also some cryptodires; see, e.g., Brophy, 2006; Pritchard, 2008; Cadena, Jaramillo & Bloch, 2013; Leuteritz & Gantz, 2013; Sullivan & Joyce, 2017) was present also in the beginning of their evolution, in the oldest and most basal true turtles, around 215 million years ago.

Acknowledgements

We thank Rainer Schoch for access to SMNS collection, Carl Schweizer for granting access to CSMM collection, Łucja Fostowicz-Frelik for the macrophotographs of ZPAL V.39/381 and ZPAL V.39/384, Marco Marzola for 3D models of ZPAL V.39/34 and ZPAL V.39/48, Tomasz Sulej for discussion, and Piotr Bajdek for additional preparation work, as well as the Editor, the Reviewers, and the Production Office for their work needed to process and improve this manuscript.

References

Alibardi L. 2005. Proliferation in the epidermis of chelonians and growth of the horny scutes. *Journal of Morphology* 265:52–69. DOI: 10.1002/jmor.10337.

Anquetin J., Joyce WG. 2014. A reassessment of the Late Jurassic turtle Eurysternum wagleri (Eucryptodira, Eurysternidae). *Journal of Vertebrate Paleontology* 34:1317–1328. DOI: 10.1080/02724634.2014.880449.

Anquetin J., Püntener C., Billon-Bruyat J-P. 2014. A taxonomic review of the Late Jurassic eucryptodiran turtles from the Jura Mountains (Switzerland and France). *PeerJ* 2:e369. DOI: doi: 10.7717/peerj.369.

Anquetin J., Püntener C., Joyce WG. 2017. A review of the fossil record of turtles of the clade Thalassochelydia. *Bulletin of the Peabody Museum of Natural History* 58:317–369. DOI: 10.3374/014.056.0203.

Baur G. 1887. Ueber den Ursprung der Extremitäten der Ichthyopterygia. *Berichte über Versammlungen des Oberrheinischen Vereines* 20:17–20.

Broin F de. 1994. Données préliminaires sur les chéloniens du Tithonien inférieur des calcaires lithographiques de Cajuers (Var, France). *Geobios* 16:167–175.

de Broin F., Ingavat R., Janvier P., Sattayarak N. 1982. Triassic turtle remains from northeastern Thailand. *Journal of Vertebrate Paleontology* 2:41–46.

Brophy TR. 2006. Allometry and sexual dimorphism in the snail-eating turtle *Malayemys*

1227 *macrocephala* from the Chao Phraya River Basin of central Thailand. *Chelonian*
1228 *Conservation and Biology* 5:159–165. DOI: 10.2744/1071-
1229 8443(2006)5[159:AASDIT]2.0.CO;2.

1230 Burke AC. 1989. Development of the turtle carapace: Implications for the evolution of a novel
1231 bauplan. *Journal of Morphology* 199:363–378. DOI: 10.1002/jmor.1051990310.

1232 Burke AC., Nowicki JN. 2003. A new view of patterning domains in the vertebrate mesoderm.
1233 *Developmental Cell* 4:159–165. DOI: 10.1016/S1534-5807(03)00033-9.

1234 Cadena EA., Jaramillo CA., Bloch JI. 2013. New material of the platychelyid turtle *Notoemys*
1235 *zapatocaensis* from the Early Cretaceous of Colombia; Implications for understanding
1236 Pleurodira evolution. In: Brinkman DB, Holroyd PA, Gardner JD eds. *Morphology and*
1237 *Evolution of Turtles*. Dordrecht: Springer Science+Business Media, 105–120.

1238 Cherepanov GO. 1989. New morphogenetic data on the turtle shell: discusion on the origin of
1239 the horny and bony parts. *Studia Geologica Salmanticensia* 3:9–24.

1240 Cherepanov GO. 2006. Ontogenesis and evolution of horny parts of the turtle shell. *Fossil Turtle*
1241 *Research* 1:19–33.

1242 Cherepanov GO. 2014. Patterns of scute development in turtle shell: Symmetry and asymmetry.
1243 *Paleontological Journal* 48:1275–1283. DOI: 10.1134/S0031030114120028.

1244 Cherepanov GO. 2015. Scute's polymorphism as a source of evolutionary development of the
1245 turtle shell. *Paleontological Journal* 49:1–10.

1246 Cherepanov GO. 2016. Nature of the turtle shell: Morphogenetic causes of bone variability and
1247 its evolutionary implication. *Paleontological Journal* 50:1641–1648. DOI:
1248 10.1134/S0031030116140033.

1249 Coker RE. 1905. Orthogenetic variation? *Science* 22:873–875.

1250 Coker RE. 1910. Diversity in the scutes of Chelonia. *Journal of Morphology* 21:1–75.

1251 Farke CM., Distler C. 2015. Ontogeny and abnormalities of the tortoise carapace: A computer
1252 tomography and dissection study. *Salamandra* 51:231–244.

1253 Fraas E. 1913. *Proterochersis*, eine pleurodire Schildkröte aus dem Keuper. *Jahreshefte des*
1254 *Vereins für Vaterlandische Naturkunde in Württemberg* 69:13–30.

1255 Frye FL. 1994. Diagnosis and surgical treatment of reptilian neoplasma with a compilation of
1256 cases 1966–1993. *In Vivo* 8:885–892.

1257 Gadow H. 1905. Orthogenetic variation. *Science* 22:637–640.

1258 Gaffney ES. 1990. The comparative osteology of the Triassic turtle *Proganochelys*. *Bulletin of*
1259 *the American Museum of Natural History* 194:1–263.

1260 Gilbert SF., Loredo GA., Brukman A., Burke AC. 2001. Morphogenesis of the turtle shell: The
1261 development of a novel structure in tetrapod evolution. *Evolution & Development* 3:47–58.
1262 DOI: 10.1046/j.1525-142X.2001.003002047.x.

1263 Grant C. 1936a. The "midventral keel" in Testudinata. *Proceedings of the Indiana Academy of*
1264 *Science*:246–252. DOI: 10.1007/s10641-007-9325-3.

1265 Grant C. 1936b. Orthogenetic variation. *Proceedings of the Indiana Academy of Science* 46:240–
1266 245.

1267 Hutchison JH., Bramble DM. 1981. Homology of the plastral scales of the Kinosternidae and
1268 related turtles. *Herpetologica* 37:73–85.

1269 Jansen M., Klein N. 2014. A juvenile turtle (Testudines, Eucryptodira) from the Upper Jurassic
1270 of Langenberg Quarry, Oker, Northern Germany. *Palaeontology* 57:743–756. DOI:
1271 10.1111/pala.12085.

1272 Joyce WG., Lucas SG., Scheyer TM., Heckert AB., Hunt AP. 2009. A thin-shelled reptile from
1273 the Late Triassic of North America and the origin of the turtle shell. *Proceedings of the*
1274 *Royal Society of London B: Biological Sciences* 276:507–513. DOI:
1275 10.1098/rspb.2008.1196.

1276 Karl H-V., Tichy G. 2000. *Murrhardtia staeschei* n. gen. n. sp. – eine neue Schildkröte aus der
1277 Oberen Trias von Süddeutschland. *Joannea Geologie und Paläontologie* 2:57–72.

1278 Kordikova EG. 2002. Heterochrony in the evolution of the shell of Chelonia. Part 1:

1279 Terminology, Cheloniidae, Dermochelyidae, Trionychidae, Cyclanorbidae and
1280 Carettochelyidae. *Neues Jahrbuch für Geologie und Paläontologie - Abhandlungen*
1281 226:343–417.

1282 Leuteritz TEJ., Gantz DT. 2013. Sexual Dimorphism in Radiated Tortoises (*Astrochelys*
1283 *radiata*). *Chelonian Research Monographs* 6:105–112. DOI: 10.3854/crm.6.a18p105.

1284 Li C., Wu X-C., Rieppel OC., Wang L-T., Zhao L-J. 2008. An ancestral turtle from the Late
1285 Triassic of southwestern China. *Nature* 456:497–501. DOI: 10.1038/nature07533.

1286 Lichtig AJ., Lucas S. 2017. Sutures of the shell of the Late Cretaceous-Paleocene baenid turtle
1287 *Denazinemys*. *Neues Jahrbuch für Geologie und Paläontologie - Abhandlungen* 283:1–8.
1288 DOI: 10.1127/njgpa/2017/0622.

1289 Lucas SG., Heckert AB., Hunt AP. 2000. Probable turtle from the Upper Triassic of east-central
1290 New Mexico. *Neues Jahrbuch für Geologie und Paläontologie - Monatshefte* 5:287–300.

1291 Lynn WG. 1937. Variation in scutes and plates in the box-turtle, *Terrapene carolina*. *The*
1292 *American Naturalist* 71:421–427.

1293 Lynn WG., Ullrich MC. 1950. Experimental production of shell abnormalities in turtles. *Copeia*
1294 1950:253–262.

1295 Mardia K., Kent J., Bibby J. 1979. *Multivariate analysis*. Academic Press.

1296 McEwan B. 1982. Bone anomalies in the shell of *Gopherus polyphemus*. *Florida Scientist*
1297 45:189–195.

1298 McKnight DT., Ligon DB. 2014. Shell and pattern abnormalities in a population of western
1299 chicken turtles (*Deirochelys reticularia miaria*). *Herpetology Notes* 7:89–91.

1300 Młynarski M. 1956. Studies on the morphology of the shell of recent and fossil tortoises. I-II.
1301 *Acta Zoologica Cracoviensia* 1:1–19.

1302 Moustakas-Verho JE., Cebra-Thomas J., Gilbert SF. 2017. Patterning of the turtle shell. *Current*
1303 *Opinion in Genetics & Development* 45:124–131. DOI: 10.1016/j.gde.2017.03.016.

1304 Moustakas-Verho JE., Cherepanov GO. 2015. The integumental appendages of the turtle shell:
1305 An evo-devo perspective. *Journal of Experimental Zoology Part B: Molecular and*
1306 *Developmental Evolution* 324:221–229. DOI: 10.1002/jez.b.22619.

1307 Moustakas-Verho JE., Zimm R., Cebra-Thomas JA., Lempiäinen NK., Kallonen A., Mitchell
1308 KL., Hämäläinen K., Salazar-Ciudad I., Jernvall J., Gilbert SF. 2014. The origin and loss of
1309 periodic patterning in the turtle shell. *Development* 141:3033–3039. DOI:
1310 10.1242/dev.109041.

1311 Newman HH. 1906a. The significance of scute and plate "abnormalities" in Chelonia. A
1312 contribution to the evolutionary history of the chelonian carapace and plastron. Part II.
1313 *Biological Bulletin* 10:99–114.

1314 Newman HH. 1906b. The significance of scute and plate "abnormalities" in Chelonia. A
1315 contribution to the evolutionary history of the chelonian carapace and plastron. Part I.
1316 *Biological Bulletin* 10:68–98.

1317 Niedźwiedzki G., Brusatte SL., Sulej T., Butler RJ. 2014. Basal dinosauriform and theropod
1318 dinosaurs from the mid-late Norian (Late Triassic) of Poland: Implications for Triassic
1319 dinosaur evolution and distribution. *Palaeontology* 57:1121–1142. DOI:
1320 10.1111/pala.12107.

1321 Nowicki JN., Burke AC. 2000. *Hox* genes and morphological identity: Axial versus lateral
1322 patterning in the vertebrate mesoderm. *Development* 127:4265–4275.

1323 Özdemir B., Türkozan O. 2006. Carapacial scute variation in green turtle, *Chelonia mydas*
1324 hatchlings in Northern Cyprus. *Turkish Journal of Zoology* 30:141–146.

1325 Parker GH. 1901. Correlated abnormalities in the scutes and bony plates of the carapace of the
1326 sculptured tortoise. *The American Naturalist* 35:17–24. DOI: 10.1525/tph.2001.23.2.29.

1327 Pritchard PCH. 2008. Evolution and structure of the turtle shell. In: Wyneken J, Godfrey MH,
1328 Bels V eds. *Biology of Turtles*. Boca Raton, London & New York: CRC Press, 46–83.

1329 Rice R., Kallonen A., Cebra-Thomas JA., Gilbert SF. 2016. Development of the turtle plastron,
1330 the order-defining skeletal structure. *Proceedings of the National Academy of Sciences of*

the United States of America 113:5317–5322. DOI: 10.1073/pnas.1600958113.

Rothschild BM., Schultze H-P., Pellegrini R. 2013. Osseous and other hard tissue pathologies in turtles and abnormalities of mineral deposition. In: Brinkman DB, Holroyd PA, Gardner JD eds. *Morphology and Evolution of Turtles*. Dordrecht: Springer Science+Business Media, 501–534.

Schoch RR., Sues H-D. 2015. A Middle Triassic stem-turtle and the evolution of the turtle body plan. *Nature* 523:584–587. DOI: 10.1038/nature14472.

Schoch RR., Sues H-D. 2017. Osteology of the Middle Triassic stem-turtle *Pappochelys rosinae* and the early evolution of the turtle skeleton. *Journal of Systematic Palaeontology*:1–39. DOI: 10.1080/14772019.2017.1354936.

Shearman RM., Burke AC. 2009. The lateral somitic frontier in ontogeny and phylogeny. *Journal of Experimental Zoology Part B: Molecular and Developmental Evolution* 312:603–612. DOI: 10.1002/jez.b.21246.The.

Sterli J., de la Fuente MS., Rougier GW. 2007. Anatomy and relationships of *Palaeochersis talampayensis*, a Late Triassic turtle from Argentina. *Palaeontographica Abteilung A* 281:1–61.

Sulej T., Niedźwiedzki G., Bronowicz R. 2012. A new Late Triassic vertebrate fauna from Poland with turtles, aetosaurs, and coelophysoid dinosaurs. *Journal of Vertebrate Paleontology* 32:1033–1041. DOI: 10.1080/02724634.2012.694384.

Sullivan PM., Joyce WG. 2017. The shell and pelvic anatomy of the Late Jurassic turtle *Platychelys oberndorferi* based on material from Solothurn, Switzerland. *Swiss Journal of Palaeontology* 136:323–343.

Szczygielski T. 2017. Homeotic shift at the dawn of the turtle evolution. *Royal Society Open Science* 4:160933. DOI: http://dx.doi.org/10.1098/rsos.160933.

Szczygielski T., Sulej T. 2016. Revision of the Triassic European turtles *Proterochersis* and *Murrhardtia* (Reptilia, Testudinata, Proterochersidae), with the description of new taxa from Poland and Germany. *Zoological Journal of the Linnean Society* 177:395–427. DOI:

10.1111/zoj.12374.

Szulc J., Racki G., Jewuła K., Środoń J. 2015. How many Upper Triassic bone-bearing levels are there in Upper Silesia (Southern Poland)? A critical overview of stratigraphy and facies. *Annales Societatis Geologorum Poloniae* 85:587–626. DOI: 10.14241/asgp.2015.037.

Velo-Antón G., Becker CG., Cordero-Rivera A. 2011. Turtle carapace anomalies: The roles of genetic diversity and environment. *PLoS ONE* 6:e18714. DOI: 10.1371/journal.pone.0018714.

Wibbels T., Owens DW., Rostal DC. 1991. Soft plastra of adult male sea turtles: An apparent secondary sexual characteristic. *Herpetological Review* 22:47–49.

Wyneken J. 2001. *The anatomy of sea turtles*. U.S. Department of Commerce NOAA Technical Memorandum NMFS-SEFSC-470.

Yntema CL. 1970. Extirpation experiments on embryonic rudiments of the carapace of *Chelydra serpentina*. *Journal of Morphology* 132:235–244. DOI: 10.1002/jmor.1051320209.

Zangerl R. 1939. The homology of the shell elemests in turtles. *Journal of Morphology* 65:383–409.

Zangerl R. 1969. The turtle shell. In: Gans C ed. *Biology of the Reptilia*. London & New York: Academic Press, 311–339.

Zangerl R., Johnson RG. 1957. The nature of shield abnormalities in the turtle shell. *Fieldiana Geology* 10:341–362. DOI: 10.1017/CBO9781107415324.004.

Zatoń M., Niedźwiedzki G., Marynowski L., Benzerara K., Pott C., Cosmidis J., Krzykawski T., Filipiak P. 2015. Coprolites of Late Triassic carnivorous vertebrates from Poland: An integrative approach. *Palaeogeography, Palaeoclimatology, Palaeoecology* 430:21–46. DOI: 10.1016/j.palaeo.2015.04.009.

Figure 1

Nomenclature of turtle scutes shown on the reconstruction of the shell of *Proterochersis robusta* in (A) dorsal, (B) lateral left, and (C) ventral view, and the legend of color and pattern codes used.

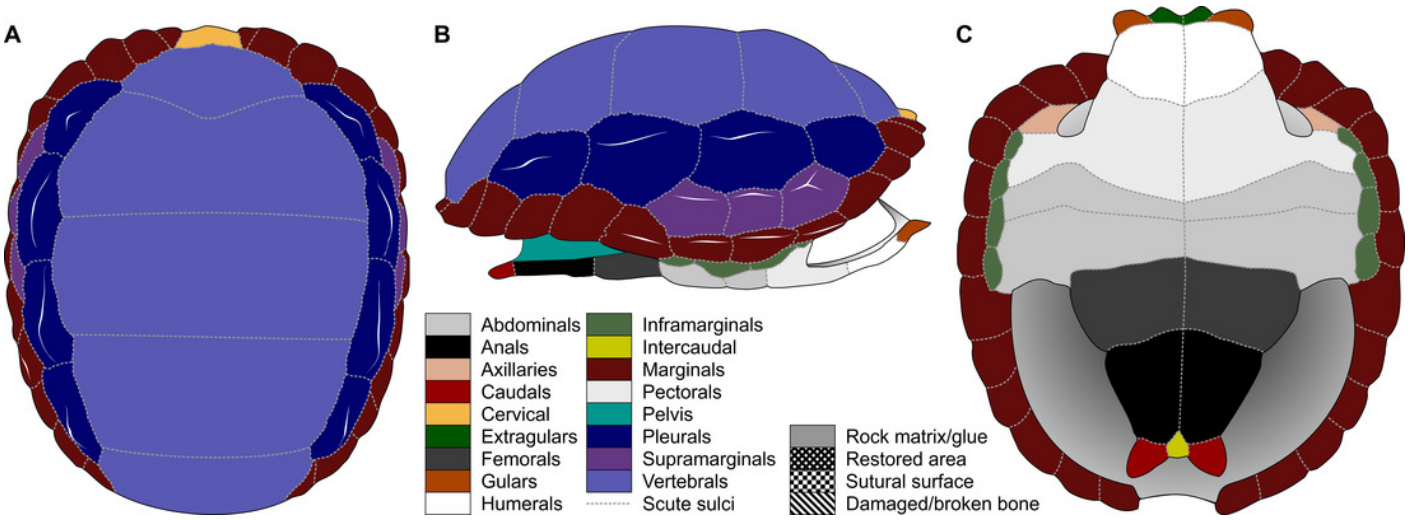

Figure 2

External carapace morphology of *Proterochersis robusta*.

(A, B) CSMM uncat. in (A) dorsal and (B) lateral right view; (C) SMNS 16442, carapace in dorsal view; (D, E) SMNS 16603 in (D) dorsal and (E) lateral right view; (F, G) SMNS 17561 in (F) dorsal and (G) lateral left (mirrored) view; (H) SMNS 17755a in dorsal view; (I, J) 17930 in (I) dorsal and (J) lateral right view. (K) SMNS 18440 in lateral left (mirrored) view. Restored area not shown for SMNS 17561 (F, G) due to difficulties in evaluation. Minor damage and restorations not shown for clarity.

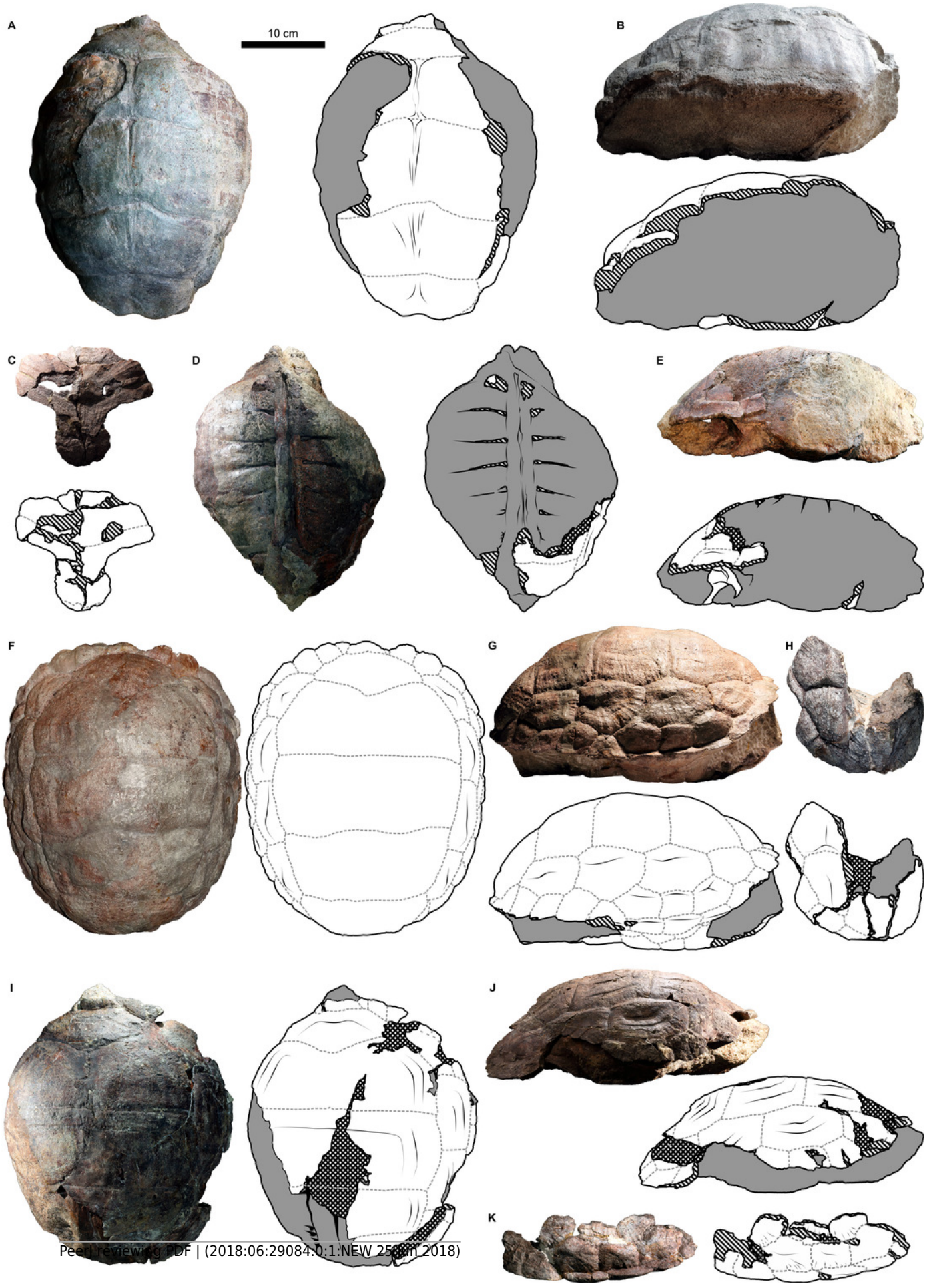
A
10 cm
B
C
D
E
F
G
H
I
J
K

Figure 3

External plastron morphology of *Proterochersis robusta*.

(A) CSMM uncat. in ventral view; (B) SMNS 11396, plastron in ventral view; (C) SMNS 12777 in ventral view; (D) SMNS 16442, plastron in ventral view; (E) SMNS 16603, plastron in ventral view; (F) SMNS 17561 in ventral view; (G) SMNS 17755, plastron in ventral view; (H) SMNS 18440 in ventral view; (I) SMNS 50917 in ventral view; (J) SMNS 56606 in ventral view. Scute sulci are represented by dashed grey lines. Restored area not shown for SMNS 17561 (F) due to difficulties in evaluation. Minor damage and restorations not shown for clarity.

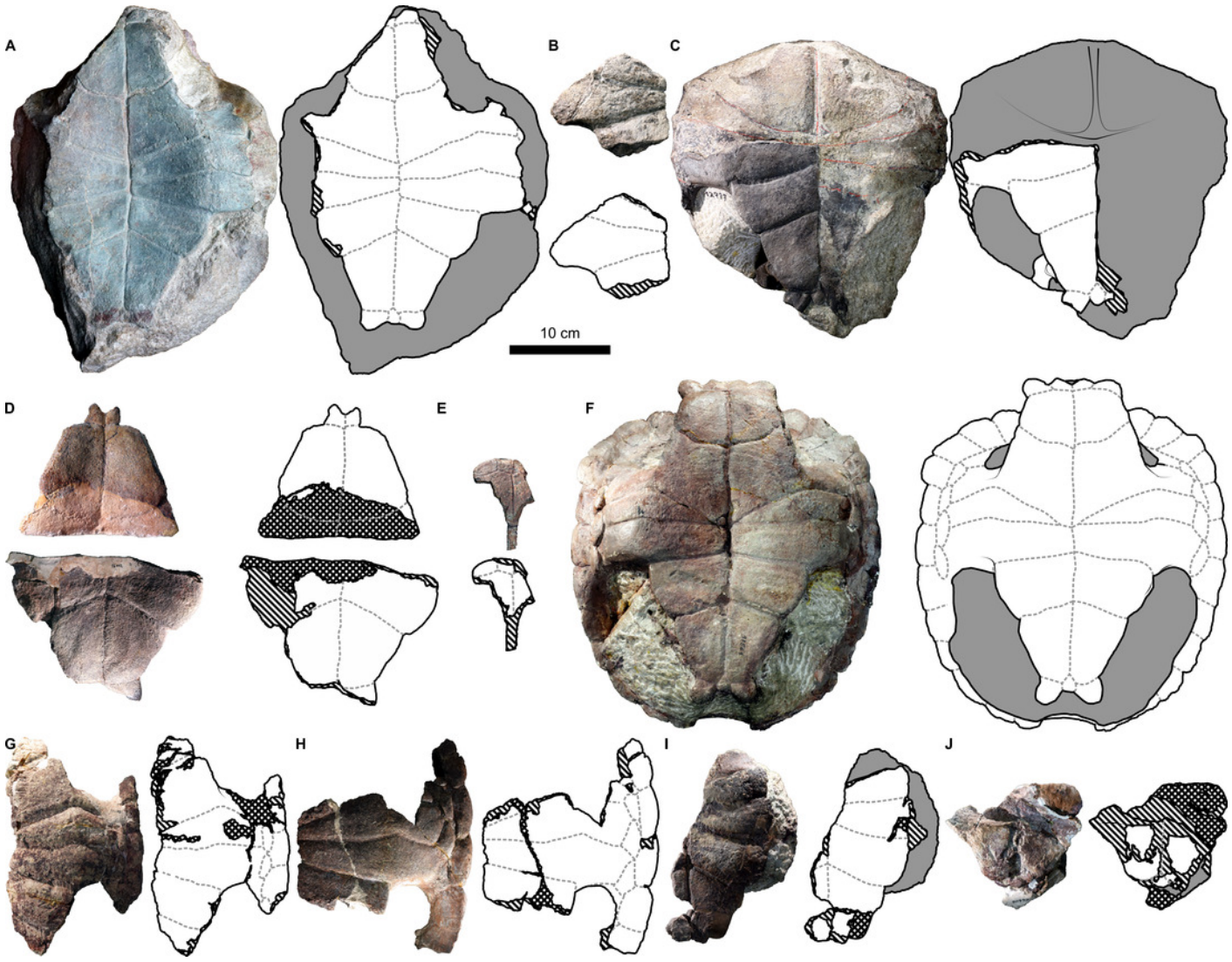

Figure 4

External carapace morphology of *Proterochersis porebensis*.

(A, B) ZPAL V.39/34 in (A) dorsal and (B) lateral left (mirrored) view; (C, D) ZPAL V.39/48, (C) carapace in dorsal and (D) lateral right view; (E, F) ZPAL V.39/49, (E) carapace in dorsal and (F) lateral right view; (G, H) ZPAL V.39/72 in (G) dorsal and (H) lateral left (mirrored) view. Minor damage and restorations not shown for clarity.

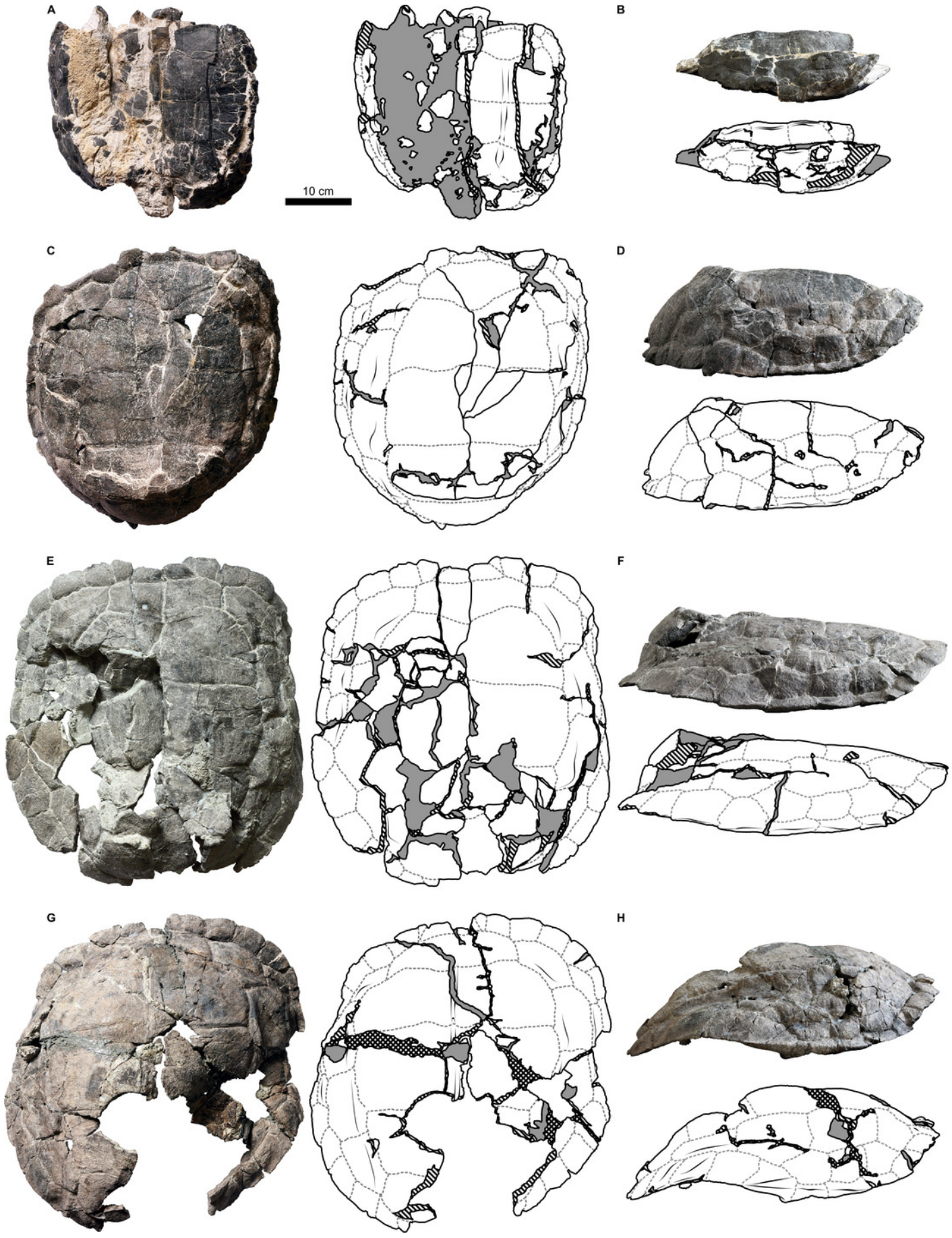
A
10 cm
B
C
D
E
F
G
H

Figure 5

External plastron morphology of *Proterochersis porebensis*.

(A) ZPAL V.39/34 in ventral view; (B) ZPAL V.39/48 in ventral view; (C) ZPAL V.39/49 in ventral view. Minor damage and restorations not shown for clarity.

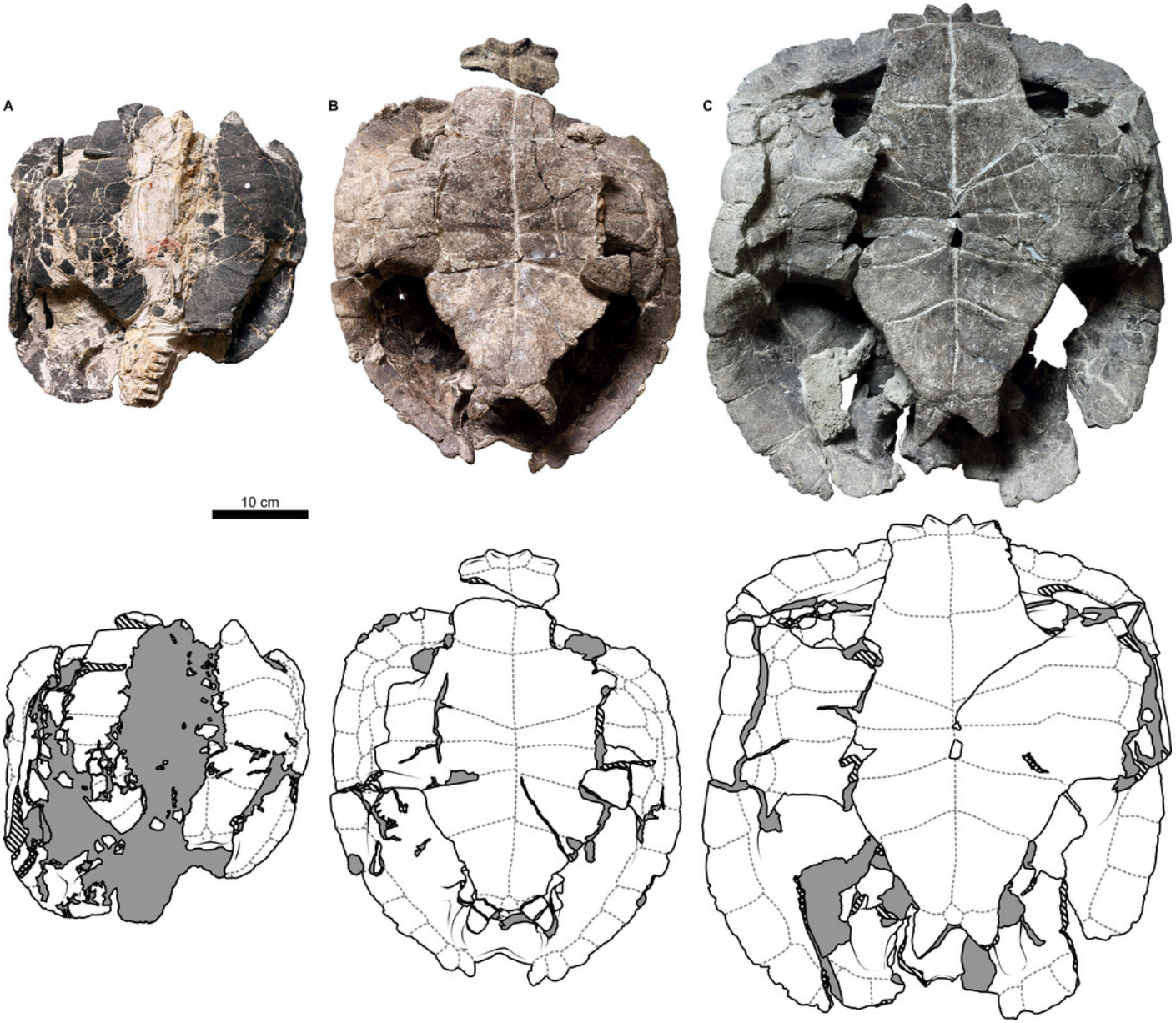

Figure 6

Proterochersis robusta, SMNS 17930, carapace in (A) lateral right, (B) laterodorsoanterior, and (C) dorsoanterior view.

Note pronounced growth marks.

**Note: Auto Gamma Correction was used for the image. This only affects the reviewing manuscript. See original source image if needed for review.*

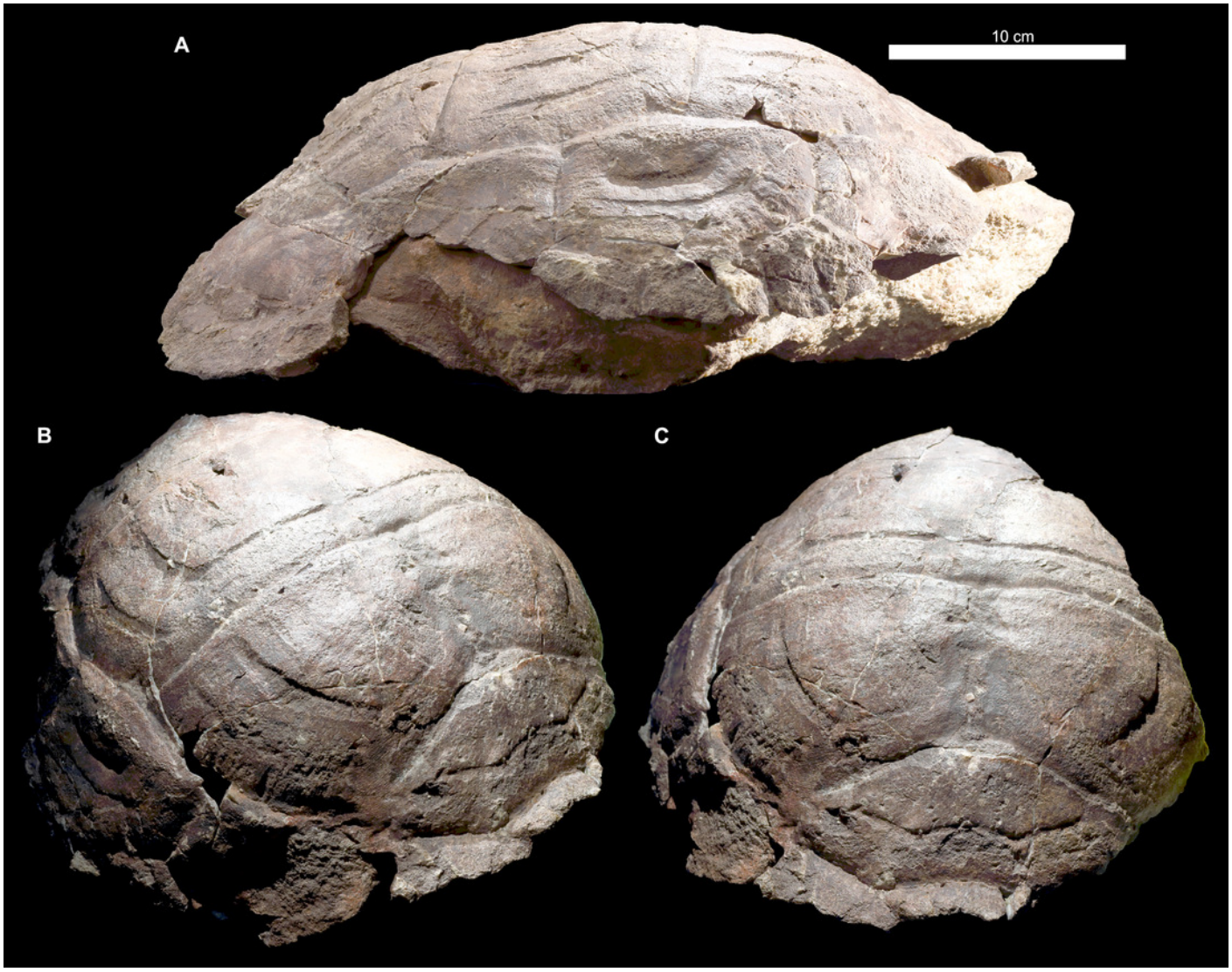

Figure 7

Proterochersis porebensis, ZPAL V.39/385, anterior plastral lobe with supernumerary scutes (*) in (A) visceral and (B) external view.

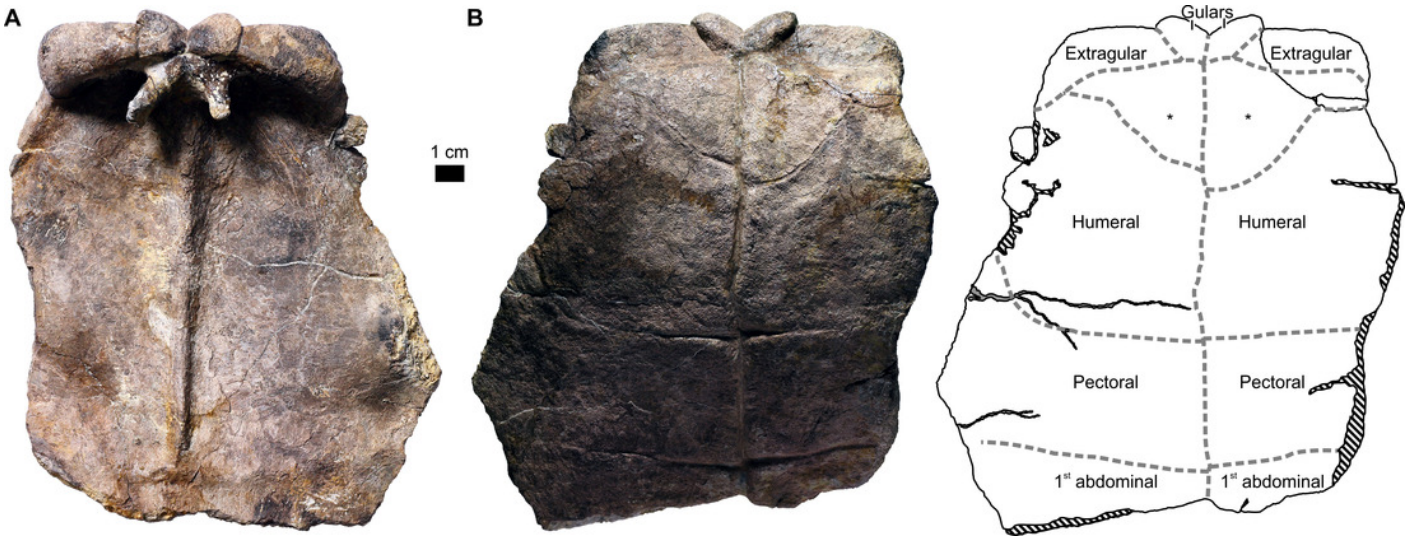

Figure 8

Results of the Principal Component Analysis of the gular plastral region in (A, B) ventral view and (C–F) vertical cross-section of extragulars.

Proterochersis robusta is represented by stars, *P. porebensis* by dots. Juvenile specimens are represented by green points, sex groups are indicated by blue and red points, black points indicate specimens of an unknown sex. Representations of scute shapes not to scale.

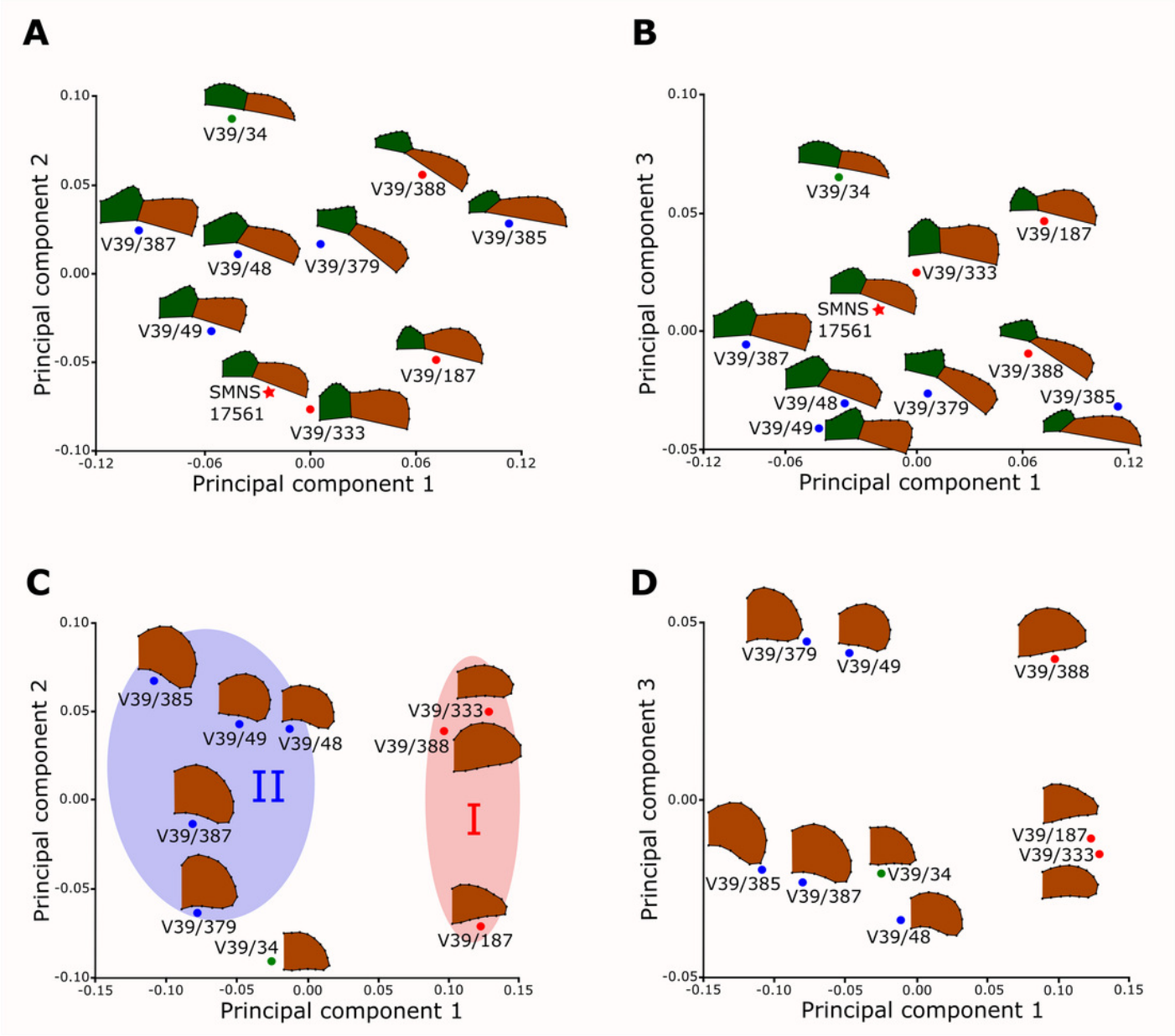

Figure 9

Variability of caudal region of plastron of (A–C) *Proterochersis robusta* and (D–T) *P. porebensis*.

(A) CSMM uncat.; (B) SMNS 12777; (C) SMNS 17561; (D) ZPAL V.39/49; (E) ZPAL V.39/71; (F) ZPAL V.39/69; (G) ZPAL V.39/48; (H) ZPAL V.39/68; (I) ZPAL V.39/70; (J) ZPAL V.39/66; (K) ZPAL V.39/34; (L–N) ZPAL V.39/56, left caudal process in (L) dorsal, (M) ventral, and (N) lateral view; (O–Q) ZPAL V.39/199, left caudal process in (O) dorsal, (P) ventral, and (Q) lateral view; (R–T) ZPAL V.39/200, (?)left caudal process in (R) dorsal, (S) ventral, and (T) lateral view. A–K in ventral view, in the same scale, ordered roughly by decreasing size. L–T in the same scale.

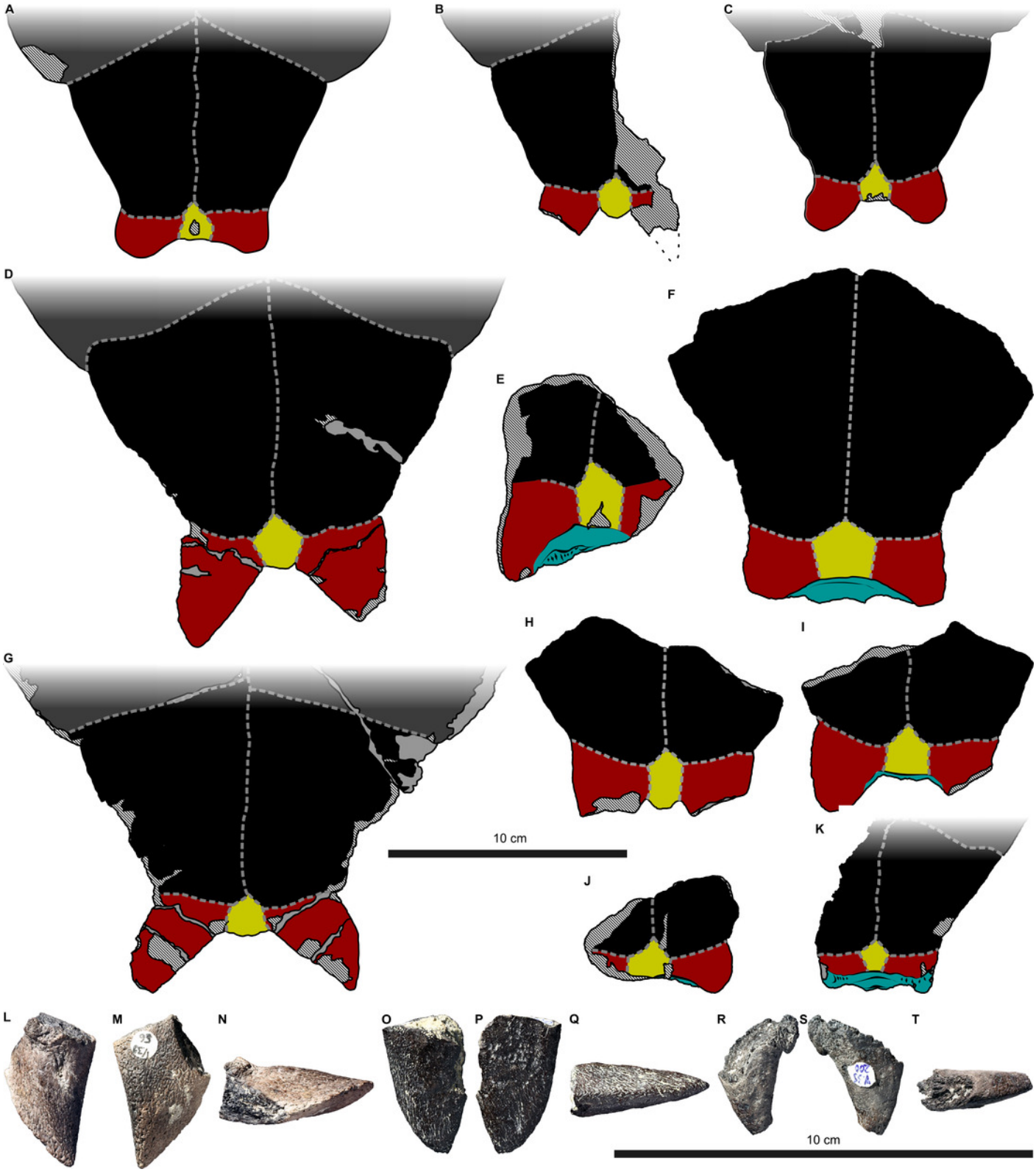
A
B
C
D
E
F
G
H
I
J
K
10 cm
L
M
N
O
P
Q
R
S
T
10 cm

Figure 10

Results of the Principal Component Analysis of the caudal plastral region.

Principal Plots showing (A) the first against second and (B) the first against the third Principal Component of the caudal plastral region. The separation of the adult individuals into two groups is shown by means of the circle on the graph. Results of (C) Regression analysis and (D) Canonical Variate Analysis. The three groups separated on the graph represent the adults, split into groups I and II, and the juveniles. *Proterochersis robusta* is represented by stars, *P. porebensis* by dots. Juvenile specimens are represented by green points, sex groups are indicated by blue and red points. Representations of scute shapes not to scale.

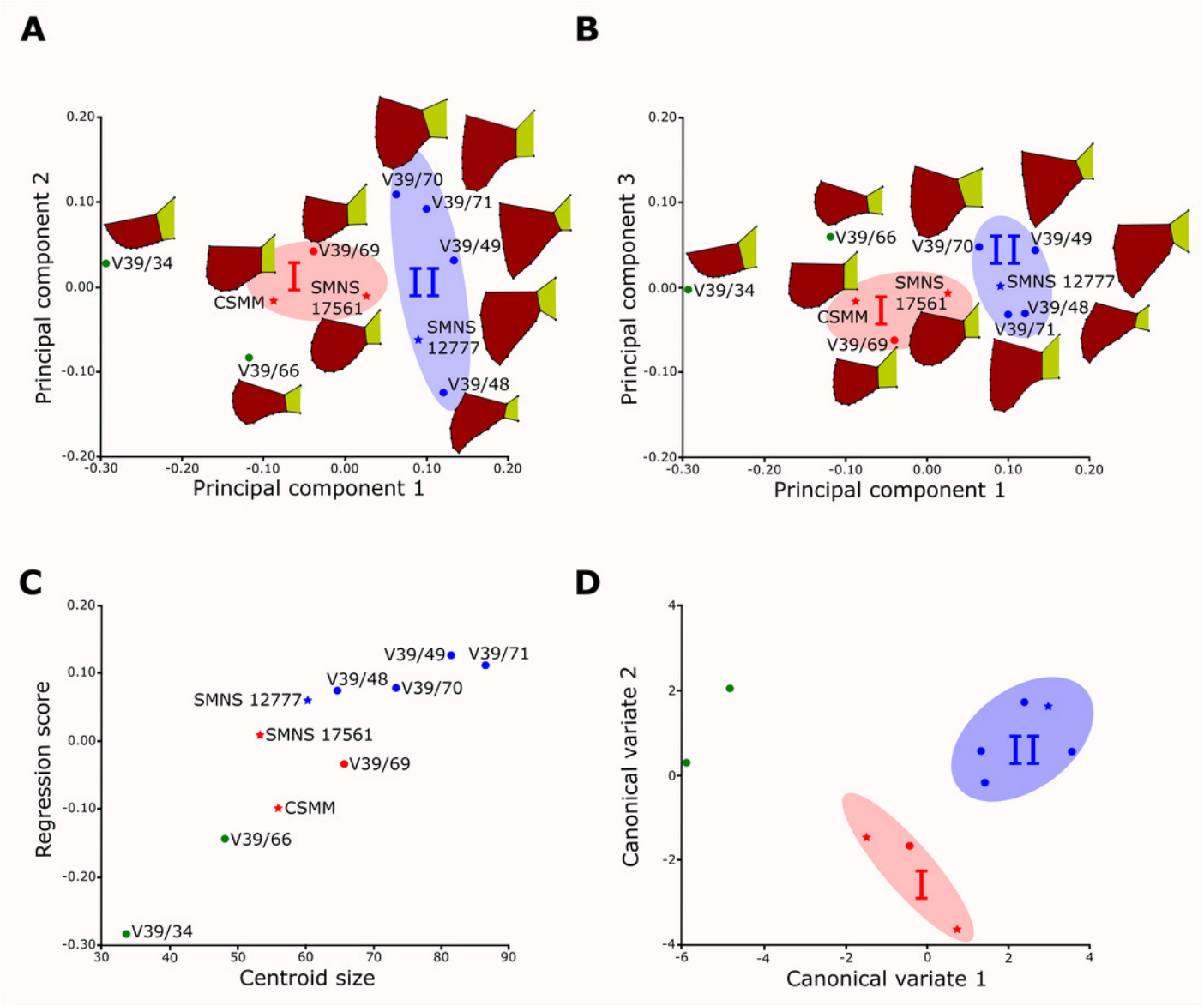
A
Principal component 2
Principal component 1
V39/34
V39/66
V39/69
V39/70
V39/71
V39/49
V39/48
CSMM
SMNS 17561
SMNS 12777
I
II
B
Principal component 3
Principal component 1
V39/34
V39/66
V39/70
V39/49
SMNS 12777
SMNS 17561
CSMM
V39/48
V39/71
V39/69
C
Regression score
Centroid size
V39/49
V39/71
V39/48
V39/70
SMNS 12777
SMNS 17561
V39/69
CSMM
V39/66
V39/34
D
Canonical variate 2
Canonical variate 1
II
I

SHELL VARIABILITY IN THE BASAL TURTLES *PROTEROCHERSIS* SPP.

SUPPLEMENTARY INFORMATION:

MATERIAL,

EXTENDED METHODS,

SUPPLEMENTARY TABLES,

SUPPLEMENTARY FIGURES,

AND

SUPPLEMENTARY REFERENCES

TOMASZ SZCZYGIELSKI[1,*], JUSTYNA SŁOWIAK[1], AND DAWID DRÓŻDŻ[1]

[1]Institute of Paleobiology, Polish Academy of Sciences, Twarda 51/55, 00-818 Warsaw, Poland

*E-mail: t.szczygielski@twarda.pan.pl

MATERIAL

It should be noted that some of the specimens described here (SMNS 17755, SMNS 17756, SMNS 18440, SMNS 50917, SMNS 56606, SMNS 81917, ZPAL V.39/164, ZPAL V.39/197, ZPAL V.39/277, ZPAL V.39/378, ZPAL V.39/381, ZPAL V.39/383, and ZPAL V.39/384), including the ontogenetically youngest individuals, lack any diagnostic characters that would unambiguously support their identification as *Proterochersis robusta* or *P. porebensis*. They all come, however, from Poręba and Murrhardt – the localities which thus far yielded numerous diagnostic specimens referable only to *P. porebensis* and *P. robusta*, respectively, we therefore refer them to these taxa. This identification is tentative, but in the light of current knowledge seems to be probable.

PROTEROCHERSIS ROBUSTA

The specimens informative for this study are:

CSMM uncat. The holotype of "*Murrhardtia staeschei*" Karl & Tichy, 2000. Found in Mettelberg Quarry, near Murrhardt, Germany. A mostly complete shell (Figs 2A–B, 3A, 8A, S3A, S5A), missing the marginal sections of the carapace (including the anterior edge of the cervical region, but not the last two right marginal scute areas), parts of the first three and of the fifth vertebral scute, pleurals, inframarginals, right bridge and right part of the anterior lobe of the plastron. Figured by Wild (Wild 1987), described and figured by Karl and Tichy (Karl & Tichy 2000) and Szczygielski and Sulej (2016). Carapace approximately 36.5 cm long.

SMNS 11396. The holotype of "*Proterochersis intermedia*" Fraas, 1913. Found in Stuttgart-Rohracker, Germany. A fragment of the right side of the plastron (Fig. 3B), with partial areas of the first and second abdominal and femoral, and sutures visible, a natural mold of the visceral surface of the same fragment, a partial natural internal mold of the carapace with impressions of the fourth to 10th dorsal rib, with corresponding rib heads and vertebrae embedded in matrix, and fragments of carapace. The carapace shows no discernible external characters and thus is not informative for this study. Described and figured by Fraas (1913) and Szczygielski and Sulej (2016).

SMNS 12777. The holotype of *Proterochersis robusta*. Found in Rudersberg, Germany. A natural mold of the shell, with small fragment of the ninth marginal scute area, complete right side of the pelvis and posterior right side of the plastron preserved (areas of the second abdominal, femoral, anal, intercaudal, base of the caudal, damaged third and fourth inframarginal, fragments of the left anal and caudal scute), and some sutures visible as impressions (Figs 3C, 8B). Figured by Stromer (Stromer 1912) and (in part) by Młynarski (Młynarski 1976). Figured and described in detail by Fraas (1913) and Szczygielski and Sulej (2016).

SMNS 16442. Found in Murrhardt, Germany. A damaged anterior part of the carapace (apparently corresponds to the area of the first, and anterior and medial parts of the second vertebral scute, Fig. 2C), an anterior lobe of the plastron (humeral scute area and entoplastron, bearing the medial parts of gular scutes, with epiplastra missing, Fig. 3D), a rock impression of the latter, a posterior lobe of the plastron (area of femorals and anals with a base of the right caudal process, Fig. 3D), a damaged part of the carapace margin with a fragment of the anterior part of the bridge, and some difficult to interpret fragments and impressions in plaster (one of them probably of a marginal sulci), some of these elements with traceable sutures. Due to extensive damage, the fragments of the carapace show little surficial characters. The plastron is better preserved. Described and figured by de Broin (1984) and Szczygielski and Sulej (2016). Histological sections from that specimen were examined by Scheyer and Sander (2007).

SMNS 16603. Found in the vicinity of Lorch, Germany. An internal mold of a shell of a young specimen, with a posterior right part of the carapace (Fig. 2D–E), a pelvis, a part of the right axillary buttress and an anterior fragment of the plastron (consisting of the area of the right extragular and gular, a part of the left extragular, and medial parts of humeral scutes, Figs 3E, S5B) preserved. Described and figured by de Broin (1984) and Szczygielski and Sulej (2016).

SMNS 17561. Found in Murrhardt, Germany. A virtually complete shell (2F–G, 3F, 10C, S2B, S3C–D), but with substantial parts restored or filled with plaster and paint. The areas of the left extragular, the last pair of inframarginals, right parts of the third and fourth vertebral, posterior part of the second right pleural, right third and fourth pleural, parts of the right supramarginals, right second to fifth and possibly ninth to 12th marginal, left third marginal, and posterior part of the right bridge seem to be at least partially restored. Based on our observations, however, these repairs seem to even out some minor surficial damage suffered by this specimen rather than to fill for any large missing areas of the shell, but their extent is difficult to evaluate. In any case, the morphology is consistent with other specimens of *Proterochersis robusta* and *P. porebensis*, so no major errors were made during that treatment. Carapace approximately 35 cm long. This specimen was described and figured by Gaffney (1986),

Karl and Tichy (Karl & Tichy 2000), and Szczygielski and Sulej (2016). The line drawing of the shell of *Proterochersis robusta* that was first presented in Gaffney (1990), and has frequently been used since, is based mainly on that specimen.

SMNS 17755. Found in Murrhardt, Germany. A left bridge and most of the left half of the plastron, consisting of the areas of the sixth to ninth (and part of the 10th) marginal, second third, and part of the first supramarginal, second and third inframarginal, fragment of the humeral scute, most of the pectoral, both abdominals, femoral and fragment of anal scute, with visible sutures (Fig. 3G). Large part of this specimen is relatively well-preserved, although the lateral surface is heavily damaged and significant area, especially in anterior section, is restored with plaster. This specimen was described and figured by Szczygielski and Sulej (2016).

SMNS 17755a. Found in Murrhardt, Germany. A fragment of carapace, consisting of the areas of the last vertebral scute, a broken off and dislocated fragment of the fourth vertebral scute area, a part of the third and complete fourth left pleural, a fragment of the 10th, most of the 11th, full 12th, and most of the 13th left marginal, with sacrum and dorsal parts of both ilia preserved inside and with visible sutures (Figs 2H, S3C).

SMNS 17930. Found in Oberbrüden, Germany. An internal mold of the carapace with embedded right part of the pelvis and small parts of the right bridge, and a large part of the carapace (Figs 2I–J, 6), including the areas of the cervical scute, complete first vertebral and increasingly more fragmentary second, third, fourth, and small fragment of the fifth vertebral scute, complete first pair of pleurals, fragmentary second, third, and fourth right pleural, damaged right supramarginals, and marginal scutes: the first and the second, a fragment of the third, complete fourth, fragmentary fifth and 10th, complete 11th, and a fragment of the 12th. Part of the mid-section and fragments near the right anterior and posterior margin are restored with plaster. Carapace approximately 36 cm long.

SMNS 18440. Found in Murrhardt, Germany. A left bridge fragment, comprising the area of small posterior fragments of the pectoral scute, nearly complete first and complete second abdominal scute, most of the femoral scute, a part of the first and complete second, third, and (poorly preserved) fourth inframarginal, a fragment of the fifth and 10th marginal scute, and complete sixth, seventh, eighth, and ninth marginals, complete three supramarginals, and fragments of the second and third pleural scute, with sutures visible (Figs 2K, 3H). Apart from several breaks, it is well-preserved.

SMNS 50917. Found in Murrhardt, Germany. A fragmentary plastron consisting of an area of complete left femoral scute and fragments of the left pectoral, the first and the second left abdominal, the right femoral and right and left anal scutes (Fig. 3I). Viscerally, a base of the pelvis and the epipubic process are preserved. Associated is an unspecified, poorly-preserved shell fragment, possibly from the bridge area.

SMNS 56606. Found in Murrhardt, Germany. A mostly complete pelvis of a young individual with attached badly damaged posterior part of the carapace (natural surface preserved only in the partial area of the last and the second-to-last left marginal scute and in some places along the rim of the caudal notch), at least one sacral vertebra and rib pair, posterior segment of the dorsal vertebral column (approximately two complete and posterior half of the third centrum with associated rib heads), and poorly preserved posterior part of the plastron, consisting of the areas of mostly intact intercaudal scute and damaged posterior sections of the anal scutes, with caudal processes broken off (Fig. 3J).

SMNS 81917. Found in Murrhardt, Germany. A partially preserved plastral bone (hypoplastron or hypoplastron) of a juvenile exposed in visceral view (Fig. S4A).

PROTEROCHERSIS POREBENSIS

All of the existing specimens (ZPAL V.39/1–28, ZPAL V.39/34, ZPAL V.39/48–72, ZPAL V.39/155–300, ZPAL V.39/331–366, ZPAL V.39/367–392, and uncatalogued) were studied. The specimens informative for this study are:

ZPAL V.39/1. A fragment of a middle right section of a carapace consisting of partial areas of the first and the second vertebral scute, including proximal parts of three ribs (Fig. S2G–H).

ZPAL V.39/2. A fragment of a middle left section of a carapace, consisting of partial areas of the second and the third vertebral scute, including proximal parts of five ribs (Fig. S2A–B).

ZPAL V.39/3. A large part of an isolated costal with sutural edges.

ZPAL V.39/4. An isolated neural bone with transverse, ω-shaped sulcus.

ZPAL V.39/6. Posterior right section of a carapace, including partial area of the fifth vertebral scute, two last marginal scute areas, and partial area of the third-to-last marginal scute, with part of the posterior process of ilium (Fig. S3D).

ZPAL V.39/8. A fragment of a left bridge region, consisting of the areas of complete first and anterior part of the second supramarginal scute, a part of the fifth, complete sixth, and part of the seventh marginal scute, a fragment of the first pleural scute, and minute fragments of the axillary and the first two inframarginal scutes.

ZPAL V.39/18. Posterior right part of the carapace, consisting of the last marginal scute area, partial area of the second-to-last and third-to-last marginal scute, partial fourth and fifth vertebral scute areas, and partial area of the fourth right pleural, with part of the posterior process of ilium (Fig. S3E).

ZPAL V.39/23. A fragment of the posterior left carapacial rim, consisting of the area of the last marginal, a posterior part of the preceding marginal, and a small fragment of the last vertebral scute, with sutural edge (Fig. S3F).

ZPAL V.39/34. A nearly complete shell of a juvenile (Figs 4A–B, 5A, 8K, S2C, S3G, S5E–G). Carapace approximately 28 cm long. This specimen was described and figured by Sulej et al. (2012) and Szczygielski and Sulej (2016).

ZPAL V.39/48. The holotype of *Proterochersis porebensis*. A nearly complete shell (Figs 4C–D, 5B, 8G, S3H, S5H–J), pelvis, left scapulocoracoid, and right femur. Carapace approximately 42.5 cm long. This specimen was described and figured by Szczygielski and Sulej (2016) and Szczygielski (2017).

ZPAL V.39/49. A mostly complete shell (Figs 4E–F, 5C, 8D, S3I, S5K–M) and pelvis. Carapace approximately 49 cm long. This specimen was described and figured by Szczygielski and Sulej (2016) and Szczygielski (2017).

ZPAL V.39/56. Left caudal process of plastron (Fig. 8L–N).

ZPAL V.39/57. Anterior left part of the carapace, consisting of partial areas of the cervical scute, first vertebral, first left pleural, and marginal scute areas: complete first, fragmentary second, complete third and fourth, and partial fifth (Fig. S1N).

ZPAL V.39/59. Posterior left part of the carapace, consisting of two last marginal scute areas and partial last vertebral scute area, with part of the posterior process of ilium (Fig. S3J).

ZPAL V.39/60. A fragment of a carapace, consisting of a complete ninth scute area and fragmentary areas of the third supramarginal scute and the third pleural scute (Fig. S1O–P).

ZPAL V.39/63. Posterior right part of the carapace, consisting of partial areas of the fourth and fifth vertebral scutes, and a posterodorsal part of the fourth pleural scute area, with attached dorsal section of the right ilium (Fig. S1A–B).

ZPAL V.39/66. Posterior plastral lobe consisting of the area of the posterior part of the anal scutes, nearly complete intercaudal scute, proximal part of the right and complete left caudal scute, with the basal part of the ischia attached to the visceral surface (Fig. 8J).

ZPAL V.39/68. Posterior plastral lobe consisting of the area of the posterior part of the anal scutes, the complete intercaudal scute, and proximal parts of caudal scutes, with the basal part of the ischia attached to the visceral surface (Fig. 8H). Although the caudal scutes are broken at the base, it is clear that they were elongated and aligned posteriorly.

ZPAL V.39/69. Posterior plastral lobe consisting of the area of the anal, intercaudal, and caudal scutes, with bases of the lateral pubic processes and basal part of the ischia and pubis attached to the visceral surface (Fig. 8F).

ZPAL V.39/70. Posterior plastral lobe consisting of the area of the posterior part of the anal scutes, nearly complete intercaudal scute, proximal part of the left and complete right caudal scute, with the basal part of the ischia attached to the visceral surface (Fig. 8I).

ZPAL V.39/71. Posterior plastral lobe consisting of the area of the posterior part of the anal scutes, nearly complete intercaudal scute, proximal part of the left and complete right caudal scute, with the basal part of the ischia attached to the visceral surface (Fig. 8E).

ZPAL V.39/72. A mostly complete carapace, missing only parts of the areas of the third, fourth, and fifth vertebral scute, fragments of the second left and third and fourth right pleural scute, part of the second and most of the third right supramarginal scute, as well as the eighth and anterior part of the ninth right marginal scute (Figs 4G–H, S2D,

S2K). Associated with a proximal caudal vertebra. Carapace approximately 44.5 cm long. This specimen was described and figured in Szczygielski and Sulej (2016) and Szczygielski (2017).

ZPAL V.39/157. A fragmentary plastron, consisting of partial sections of the right femoral and right anal scute areas with attached right lateral pubic process.

ZPAL V.39/165. A partially preserved plastral bone (likely right hyoplastron) of a juvenile.

ZPAL V.39/169. A fragment of the dorsal vertebral column consisting of one complete and small fragments of two surrounding vertebrae and an attached part of a carapace with intervertebral sulcus (Fig. S2E–F).

ZPAL V.39/176. A fragment of a costal with sutural edges (Fig. S1E).

ZPAL V.39/186. Left gular tubercle of a large specimen (Fig. S5N–Q).

ZPAL V.39/187. A fragment of the anterior plastral lobe consisting of the area of the right gular and extragular (Fig. S5R–T).

ZPAL V.39/189. A fragment of the anterior plastral lobe consisting of the area of the right gular and medial part of the right extragular (Fig. S5U–X).

ZPAL V.39/197. A partially preserved plastral bone (likely right hyoplastron) of a juvenile (Fig. S4C).

ZPAL V.39/199. Left caudal process of plastron (Fig. 8O–Q).

ZPAL V.39/200. (?)Left caudal process of plastron (Fig. 8R–T).

ZPAL V.39/213. A fragment of the posterior left carapacial rim, consisting of the area of the last marginal, a posterior edge of the preceding marginal, and a small fragment of the last vertebral scute, with suture running at the base of the peripheral (Fig. S3L).

ZPAL V.39/277. A partially preserved plastral bone of a juvenile (Fig. S4B).

ZPAL V.39/333. A fragment of the right part of the anterior plastral lobe, consisting of the complete right gular, extragular, and an anterior part of the right humeral scute area, and small fragment of the left humeral scute area (Fig. S5Y–A').

ZPAL V.39/377. An unankylosed fragment of the dorsal vertebral column of a young specimen, consisting of one complete vertebra and an anterior half of a succeeding vertebra (Fig. S1H–K).

ZPAL V.39/378. An ankylosed fragment of the dorsal vertebral column, consisting of one complete vertebra and fragments of a preceding and succeeding vertebra with associated rib heads (Fig. S1F–G).

ZPAL V.39/379. A fragment of the right part of the anterior plastral lobe, consisting of the complete right gular, extragular, and an anterior part of the right humeral scute area (Fig. S5B'–D').

ZPAL V.39/380. Posterior right part of the carapace, consisting of two last marginal scute areas and partial last vertebral scute area, with part of the posterior process of ilium (Fig. S3M).

ZPAL V.39/381. A fragmentary costal of a hatchling (Fig. S1C–D).

ZPAL V.39/382. A fragment of a large costal.

ZPAL V.39/383. A partially preserved plastral bone of a juvenile.

ZPAL V.39/384. A partially preserved plastral bone of a juvenile (Fig. S4D).

ZPAL V.39/385. A nearly complete anterior plastral lobe with bases of the dorsal processes of the epiplastra and complete posterior process of the entoplastron preserved on the visceral side, and areas of both gular, both extragular, two supernumerary, right humeral and right pectoral scutes, as well as partially preserved left humeral and pectoral, and the first pair of abdominals (Figs 7, S5E'–G').

ZPAL V.39/386. Posterior left part of the carapace, consisting of partial area of the last and third-to-last marginal scute, complete area of the second to last marginal scute, and partial fourth and fifth vertebral scute areas, with part of the posterior process of ilium (Fig. S3N).

ZPAL V.39/387. A fragment of the anterior plastral lobe consisting of the area of the left gular and extragular, and an anterior part of the left humeral scute area (Fig. S5H'–J').

ZPAL V.39/388. A fragment of the anterior plastral lobe consisting of the area of the right gular and extragular (Fig. S5K'–M').

ZPAL V.39/390. Anterior left part of carapace consisting of partial areas of the cervical scute, the first vertebral scute, and damaged two anteriormost left marginal scutes (Fig. S1L–M).

PRINCIPAL COMPONENT ANALYSES

The shape analysis was performed for the gular and anal regions of the plastron. The sample of gular regions includes nine specimens of *Proterochersis porebensis* (ZPAL V.39/34, ZPAL V.39/48, ZPAL V.39/49, ZPAL V.39/187, ZPAL V.39/333, ZPAL V.39/379, ZPAL V.39/385, ZPAL V.39/387, and ZPAL V.39/388) and one *P. robusta* individual (SMNS 17561). We took photographs of articulated and most complete anterior tips of plastra (areas of gular and extragular scutes) in ventral view. Additionally the shape of the extragulars of *P. porebensis* was analyzed based on the veritcal sections of their 3D models. Models were generated photogrammetrically using freeware programs Visual SFM and MeshLab for the specimens ZPAL V.39/48, ZPAL V.39/187, ZPAL V.39/333, ZPAL V.39/379, ZPAL V.39/385, ZPAL V.39/387, ZPAL V.39/388 (Cignoni et al. 2008; Wu 2011) and Agisoft Photoscan for ZPAL V.39/34 and ZPAL V.39/49. In the case of the *P. robusta* specimen SMNS 17561 (the only specimen of that species fully preserving that region) the 3D modeling was impossible to perform because the specimen is not sufficiently prepared and the extragulars are only exposed ventrally. To create the models with Visual SFM and MeshLAB, around 100 photos from angles of 0º, 15º, and 40º were taken. To speed up the process of the model generation, the photographs were scaled down to resolution 800x600 px by the freeware program FastStone Photo Resizer (with the exception of ZPAL V.39/385, for which photographs of resolution 6000x4000 px were used). For the specimens ZPAL V.39/34 and ZPAL V.39/49, around 200 of 6000x4000 px photos were used to obtain models of whole shells, and then the anterior plastral sections were separated using MeshLab. Model of each specimen was then scaled in MeshLab to match its original size and the extragulars were digitally sectioned in sagittal plane. For sectioning the best preserved extragulars were chosen: right extragulars of ZPAL V.39/49, ZPAL V.39/187, ZPAL V.39/333, ZPAL V.39/379, ZPAL V.39/388, left extragulars of ZPAL V. 39/34, ZPAL V.39/387, right and left extragulars of ZPAL V.39/48 and ZPAL V.39/387. The 3D models used for the analysis are shown in the online appendix Article S2.

For the anal region, we took photographs of the best preserved posterior tips of plastra (caudal processes and intercaudal scute) in ventral view. We analyzed seven *P. porebensis* (ZPAL V.39/34, ZPAL V.39/48, ZPAL V.39/49, ZPAL V.39/66, ZPAL V.39/69, ZPAL V.39/70, and ZPAL V.39/71) and three *P. robusta* individuals (CSMM uncat., SMNS 12777, and SMNS 17561).

A set of five landmarks on the gular region in ventral view, two in the vertical section of the extragulars, and another five on the anal region were digitalized using tpsDig software (Rohlf 2015). All landmarks are of Bookstein's (1997) first type, they point the intersections between element boundaries – herein, the landmarks mark intersections between the interscutal sulci (see Table S5). In order to analyze the shape of curves, we used eight semilandmarks along the anterior curve of gularium and extragularium, thirteen along the curve of cross-sectioned extragularium, and twelve semilandmarks along the edge of caudal process. The semilandmarks were also taken using tpsDig. In case of minor incompleteness of the element, several semilandmarks were estimated, using the opposite side whenever possible. In four cases (SMNS 17561, ZPAL V.39/49, ZPAL V.39/69, ZPAL V.39/385), complete data from opposite sides of a single individual were averaged. The gular and the anal regions were digitized twice.

Significance of differences in shape between *Proterochersis porebensis* and *P. robusta* was assessed using Procrustes Analysis of Variance (ANOVA) in MorphoJ software (analogous to MANOVA) and Canonical Variate Analysis (CVA) with 10 000 permutations (Klingenberg 2009, 2011). First, Procrustes analysis was performed to remove the information related to size, position, and orientation. Wireframe graphs, Principal Component Analyses (PCA) and Canonical Variate Analysis were used to visualize shape differences. The regression analyses were performed to show the influence of size on shape.

TABLES

Table S1. *Proterochersis robusta*, carapace scutes. **+** – preserved whole or nearly whole; **P** – partially preserved; ***** – preserved only as an impression or damaged bone but providing at least partial data about the outline; **-** – not preserved or insignificant part preserved. X indicates lack of the fifteenth marginal. **R** means right, **L** means left side of the body. Note that the numbering of posteriormost marginals is uncertain if the twelfth one is not preserved at least in most part. SMNS 17561 has most of its scutes restored – these restorations seem to be mostly superficial and close to the original shape of the elements, but their extent is difficult to evaluate.

Specimen	Side	Cervical	Vertebral					Pleural				Supramarginal			Marginal													
			1	2	3	4	5	1	2	3	4	1	2	3	1	2	3	4	5	6	7	8	9	10	11	12	13	14	15
CSMM	R	P	P	P	P	+	+	-	-	-	P	-	-	-	-	-	-	-	-	-	-	-	-	-	-	-	-	-	?
	L	P	+	P	P	+	P	-	-	-	-	-	-	-	-	P	P	-	-	-	-	-	-	-	-	?P	?+	?+	?X
SMNS 11396	R	-	-	-	P	P	-	-	-	-	-	-	-	-	-	-	-	-	-	-	-	-	-	-	-	-	-	-	?
	L	-	-	-	P	-	-	-	-	-	-	-	-	-	-	-	-	-	-	-	-	-	-	-	-	-	-	-	?
SMNS 16442	R	-	P	P	P	-	-	-	-	-	-	-	-	-	-	-	-	-	-	-	-	-	-	-	-	-	-	-	?
	L	-	P	P	-	-	-	-	-	-	-	-	-	-	-	-	-	-	-	-	-	-	-	-	-	-	-	-	?
SMNS 16603	R	-	-	-	-	P	P	-	-	P	P	-	-	-	-	-	-	-	-	-	-	-	-	-	-	-	-	-	?
	L	-	-	-	-	-	-	-	-	-	-	-	-	-	-	-	-	-	-	-	-	-	-	-	-	-	-	-	?
SMNS 17561	R	+	+	+	+	+	+	+	+	+	+	+	+	+	P	+	P	+	+	+	+	+	+	+	+	P	P	+	X
	L	+	+	+	+	+	+	+	+	+	+	+	+	+	+	+	+	P	P	+	+	+	P	P	+	P	P	P	X
SMNS 17755	R	-	-	-	-	-	-	-	-	-	-	-	-	-	-	-	-	-	-	-	-	-	-	-	-	-	-	-	?
	L	-	-	-	-	-	-	-	-	-	-	P	P	P	-	-	-	-	*	P	P	P	P	P	-	-	-	-	?
SMNS 17755a	R	-	-	-	-	P	P	-	-	-	-	-	-	-	-	-	-	-	-	-	-	-	-	-	-	-	-	-	?
	L	-	-	-	-	-	P	-	-	P	+	-	-	-	-	-	-	-	-	-	-	-	-	P	P	+	+	-	?
SMNS 17930	R	+	P	P	P	P	P	P	+	P	P	P	P	P	+	+	P	+	P	-	-	-	-	P	+	P	-	-	?
	L	P	+	P	P	-	-	-	-	-	-	-	-	-	P	-	-	-	-	-	-	-	-	-	-	-	-	-	?
SMNS 18440	R	-	-	-	-	-	-	-	-	-	-	-	-	-	-	-	-	-	-	-	-	-	-	-	-	-	-	-	?
	L	-	-	-	-	-	-	-	P	P	-	P	+	P	-	-	-	-	P	+	+	+	P	P	-	-	-	-	?
SMNS 56606	R	-	-	-	-	-	*	-	-	-	-	-	-	-	-	-	-	-	-	-	-	-	-	-	-	-	-	-	?
	L	-	-	-	-	-	*	-	-	-	-	-	-	-	-	-	-	-	-	-	-	-	-	-	-	-	-	-	?

Table S2. *Proterochersis robusta*, plastron scutes. **+** – preserved whole or nearly whole; **P** – partially preserved; ***** – preserved only as an impression or damaged bone but providing at least partial data about the outline; **-** – not preserved or insignificant part preserved. **R** means right, **L** means left side of the body. SMNS 17561 has most of its scutes restored – these restorations seem to be mostly superficial and close to the original shape of the elements, but their extent is difficult to evaluate.

Specimen	Side	Extragular	Gular	Humeral	Pectoral	Abdominal		Femoral	Anal	Caudal	Intercaudal	Axillary	Inframarginal			
						1	2						1	2	3	4
CSMM	R	-	P	P	P	P	P	+	+	+	+	-	-	-	-	-
	L	P	+	+	+	+	+	+	+	+		+	-	P	-	-
SMNS 11396	R	-	-	-	-	P	P	P	-	-	-	-	-	-	-	-
	L	-	-	-	-	-	-	-	-	-		-	-	-	-	-
SMNS 12777	R	-	-	-	-	-	+	+	+	P	+	-	-	-	-	*
	L	-	-	-	-	-	-	-	*	*		-	-	-	-	-
SMNS 16442	R	-	P	P*	*	-	-	P	+	-	-	-	-	-	-	-
	L	-	P	P*	*	-	-	P	+	P		-	-	-	-	-
SMNS 16603	R	+	P	P	-	-	-	-	-	-	-	P	-	-	-	-
	L	-	-	P	-	-	-	-	-	-		-	-	-	-	-
SMNS 17561	R	P	+	+	+	+	P	+	+	+	+	+	+	+	+	*
	L	+	+	+	+	+	+	+	+	+		+	+	+	+	*
SMNS 17755	R	-	-	-	-	-	-	-	-	-	-	-	-	-	+	+
	L	-	-	P	P	P	+	+	P	-		-	-	-	-	-
SMNS 18440	R	-	-	-	-	-	-	-	-	-	-	-	-	-	-	-
	L	-	-	-	-	P	+	P	-	-		-	P	+	+	+
SMNS 50917	R	-	-	-	-	-	-	-	P	-	-	-	-	-	-	-
	L	-	-	-	-	P	P	+	P	-		-	-	-	-	-
SMNS 56606	R	-	-	-	-	-	-	-	P	-	+	-	-	-	-	-
	L	-	-	-	-	-	-	-	P	P		-	-	-	-	-

Table S3. *Proterochersis porebensis*, carapace scutes. **+** – preserved whole or nearly whole; **P** – partially preserved; ***** – preserved only as an impression or damaged bone but providing at least partial data about the outline; **-** – not preserved or insignificant part preserved. X indicates lack of the fifteenth marginal. **R** means right, **L** means left side of the body. Note that the numbering of posteriormost marginals is uncertain if the twelfth one is not preserved at least in most part. See text for discussion on ZPAL V.39/34 marginal scutes.

Specimen	Side	Cervical	Vertebral					Pleural				Supramarginal			Marginal													
			1	2	3	4	5	1	2	3	4	1	2	3	1	2	3	4	5	6	7	8	9	10	11	12	13	14	15
ZPAL V.39/1	R	-	P	P	-	-	-	-	-	-	-	-	-	-	-	-	-	-	-	-	-	-	-	-	-	-	-	-	?
	L	-	-	-	-	-	-	-	-	-	-	-	-	-	-	-	-	-	-	-	-	-	-	-	-	-	-	-	?
ZPAL V.39/2	R	-	-	-	-	-	-	-	-	-	-	-	-	-	-	-	-	-	-	-	-	-	-	-	-	-	-	-	?
	L	-	-	P	P	P	-	-	-	-	-	-	-	-	-	-	-	-	-	-	-	-	-	-	-	-	-	-	?
ZPAL V.39/5	R	-	-	-	-	-	-	-	-	-	-	-	-	-	-	-	-	-	-	-	-	-	-	-	-	-	-	-	?
	L	-	-	-	-	-	-	-	-	-	-	-	-	P	-	-	-	-	-	-	-	+	P	-	-	-	-	-	?
ZPAL V.39/6	R	-	-	-	-	-	P	-	-	-	-	-	-	-	-	-	-	-	-	-	-	-	-	-	-	?P	?+	?+	?X
	L	-	-	-	-	-	-	-	-	-	-	-	-	-	-	-	-	-	-	-	-	-	-	-	-	-	-	-	?
ZPAL V.39/8	R	-	-	-	-	-	-	-	-	-	-	-	-	-	-	-	-	-	-	-	-	-	-	-	-	-	-	-	?
	L	-	-	-	-	-	-	-	-	-	-	+	P	-	-	-	-	-	P	+	P	-	-	-	-	-	-	-	?
ZPAL V.39/18	R	-	-	-	-	P	P	-	-	-	P	-	-	-	-	-	-	-	-	-	-	-	-	-	-	P	P	+	X
	L	-	-	-	-	-	-	-	-	-	-	-	-	-	-	-	-	-	-	-	-	-	-	-	-	-	-	-	?
ZPAL V.39/21	R	-	-	-	-	-	-	-	-	-	-	-	-	-	-	-	-	-	P	P	-	-	-	-	-	-	-	-	?
	L	-	-	-	-	-	-	-	-	-	-	-	-	-	-	-	-	-	-	-	-	-	-	-	-	-	-	-	?
ZPAL V.39/22	R	-	-	-	-	-	-	-	-	-	-	-	-	-	-	-	-	-	-	-	-	-	-	-	-	-	-	-	?
	L	+	P	-	-	-	-	-	-	-	-	-	-	-	P	P	-	-	-	-	-	-	-	-	-	-	-	-	?
ZPAL V.39/23	R	-	-	-	-	-	-	-	-	-	-	-	-	-	-	-	-	-	-	-	-	-	-	-	-	-	-	-	?
	L	-	-	-	-	-	P	-	-	-	-	-	-	-	-	-	-	-	-	-	-	-	-	-	-	-	?P	?+	?X
ZPAL V.39/34	R	+	+	P	P	P	P	P	P	P	P	*	P	+	?	+	P	P	P	P	+	+	+	+	+	P	+	P	X
	L	+	+	P	P	P	P	P	P	P	+	*	+	+	?	+	P	P	P	P	P	P	+	P	+	P	+	+	X
ZPAL V.39/48	R	+	+	P	+	+	+	+	+	+	+	+	+	+	P	P	P	P	P	P	+	+	+	+	P	P	P	+	+
	L	+	+	+	+	+	+	+	+	+	+	P	+	+	P	+	P	P	P	+	+	+	+	P	P	P	P	+	+
ZPAL V.39/49	R	+	+	+	+	P	P	+	+	+	P	+	+	+	+	+	P	+	P	P	+	+	+	+	P	P	P	P	X
	L	+	+	P	P	P	P	+	P	P	P	+	+	P	P	+	P	P	+	+	P	P	+	+	+	P	+	+	X
ZPAL V.39/54	R	-	-	-	-	-	-	-	-	-	-	-	-	-	-	-	-	-	-	-	-	-	-	-	-	-	-	-	?
	L	-	-	-	-	-	-	-	-	-	-	-	-	-	-	-	-	-	-	-	-	-	-	-	-	-	-	?+	?X

Specimen	Side	Cervical	Vertebral					Pleural				Supramarginal			Marginal													
			1	2	3	4	5	1	2	3	4	1	2	3	1	2	3	4	5	6	7	8	9	10	11	12	13	14	15
ZPAL V.39/57	R	-	-	-	-	-	-	-	-	-	-	-	-	-	-	-	-	-	-	-	-	-	-	-	-	-	-	-	?
	L	P	P	-	-	-	-	P	-	-	-	-	-	-	+	P	+	+	P	-	-	-	-	-	-	-	-	-	?
ZPAL V.39/59	R	-	-	-	-	-	-	-	-	-	-	-	-	-	-	-	-	-	-	-	-	-	-	-	-	-	-	-	?
	L	-	-	-	-	-	P	-	-	-	-	-	-	-	-	-	-	-	-	-	-	-	-	-	-	-	?P	?+	?X
ZPAL V.39/60	R	-	-	-	-	-	-	-	-	-	-	-	-	-	-	-	-	-	-	-	-	-	-	-	-	-	-	-	?
	L	-	-	-	-	-	-	-	-	P	-	-	-	P	-	-	-	-	-	-	-	-	+	-	-	-	-	-	?
ZPAL V.39/63	R	-	-	-	-	P	P	-	-	-	P	-	-	-	-	-	-	-	-	-	-	-	-	-	-	-	-	-	?
	L	-	-	-	-	-	-	-	-	-	-	-	-	-	-	-	-	-	-	-	-	-	-	-	-	-	-	-	?
ZPAL V.39/67	R	-	-	-	-	-	-	-	-	-	-	-	-	-	-	-	-	-	-	-	-	-	-	-	-	-	-	-	?
	L	-	-	-	-	-	-	-	-	P	-	-	-	P	-	-	-	-	-	-	-	-	+	-	-	-	-	-	?
ZPAL V.39/72	R	P	+	+	P	P	P	+	+	P	P	+	+	P	+	+	+	+	+	P	P	-	P	P	P	P	+	+	X
	L	P	+	+	P	P	P	+	P	+	+	+	P	+	P	P	+	P	P	P	+	P	+	+	P	P	+	+	X
ZPAL V.39/158	R	-	-	-	-	-	-	-	-	-	-	-	-	-	-	-	-	-	-	-	-	-	-	-	-	-	-	-	?
	L	-	P	-	-	-	-	P	-	-	-	-	-	-	-	-	P	+	P	-	-	-	-	-	-	-	-	-	?
ZPAL V.39/160	R	-	-	-	-	-	-	-	P	-	-	P	+	P	-	-	-	-	-	P	+	P	-	-	-	-	-	-	?
	L	-	-	-	-	-	-	-	-	-	-	-	-	-	-	-	-	-	-	-	-	-	-	-	-	-	-	-	?
ZPAL V.39/161	R	-	-	-	-	-	-	-	-	-	-	-	-	-	-	-	-	-	-	-	-	-	-	-	-	-	-	-	?
	L	+	P	-	-	-	-	-	-	-	-	-	-	-	P	-	-	-	-	-	-	-	-	-	-	-	-	-	?
ZPAL V.39/167	R	-	-	-	-	-	-	-	-	-	-	-	-	-	-	-	-	-	-	-	-	-	-	P	P	-	-	-	?
	L	-	-	-	-	-	-	-	-	-	P	-	-	-	-	-	-	-	-	-	-	-	-	-	-	-	-	-	?
ZPAL V.39/168	R	-	-	-	-	-	-	-	-	-	-	-	-	-	-	-	-	-	-	-	-	-	-	-	-	-	-	-	?
	L	-	-	-	-	-	-	-	-	-	-	-	P	-	-	-	-	-	-	P	P	-	-	-	-	-	-	-	?
ZPAL V.39/173	R	-	-	-	-	-	-	-	-	-	-	-	-	-	-	-	-	-	-	-	-	-	-	-	-	-	-	-	?
	L	-	-	-	-	-	-	-	-	-	-	-	-	-	-	-	-	-	-	-	-	P	P	-	-	-	-	-	?
ZPAL V.39/213	R	-	-	-	-	-	-	-	-	-	-	-	-	-	-	-	-	-	-	-	-	-	-	-	-	-	-	-	?
	L	-	-	-	-	-	P	-	-	-	-	-	-	-	-	-	-	-	-	-	-	-	-	-	-	-	-	?+	?X
ZPAL V.39/370	R	-	-	-	-	-	-	-	-	-	-	-	-	-	-	-	-	-	-	-	-	-	-	-	-	-	-	-	?
	L	-	-	-	-	-	P	-	-	-	-	-	-	-	-	-	-	-	-	-	-	-	-	-	-	-	-	-	?
ZPAL V.39/380	R	-	-	-	-	-	P	-	-	-	-	-	-	-	-	-	-	-	-	-	-	-	-	-	-	-	?+	?+	?X
	L	-	-	-	-	-	-	-	-	-	-	-	-	-	-	-	-	-	-	-	-	-	-	-	-	-	-	-	?
ZPAL V.39/386	R	-	-	-	-	-	-	-	-	-	-	-	-	-	-	-	-	-	-	-	-	-	-	-	-	-	-	-	?
	L	-	-	-	-	-	P	-	-	-	-	-	-	-	-	-	-	-	-	-	-	-	-	-	-	P	+	P	X

Specimen	Side	Cervical	Vertebral					Pleural				Supramarginal			Marginal													
			1	2	3	4	5	1	2	3	4	1	2	3	1	2	3	4	5	6	7	8	9	10	11	12	13	14	15
ZPAL V.39/390	R	P	-	-	-	-	-	-	-	-	-	-	-	-	-	-	-	-	-	-	-	-	-	-	-	-	-	-	?
	L	+	P	-	-	-	-	-	-	-	-	-	-	-	-	-	-	-	-	-	-	-	-	-	-	-	-	-	?
ZPAL V.39/394	R	-	-	-	-	-	-	-	-	-	-	-	-	-	-	-	-	-	-	-	-	-	-	-	-	-	-	-	?
	L	-	P	-	-	-	-	P	-	-	-	-	-	-	-	-	P	+	P	-	-	-	-	-	-	-	-	-	?
ZPAL V.39/395	R	-	-	-	-	-	-	-	-	-	-	-	-	-	-	-	-	-	-	-	-	-	-	-	-	-	-	-	?
	L	-	P	-	-	-	-	P	-	-	-	-	-	-	-	-	P	+	P	-	-	-	-	-	-	-	-	-	?
ZPAL V.39/396	R	-	-	-	-	-	-	-	-	-	-	-	-	-	-	-	-	-	-	-	-	-	-	-	-	-	-	-	?
	L	-	P	P	P	-	-	+	P	-	-	P	-	-	-	P	+	+	P	P	-	-	-	-	-	-	-	-	?
ZPAL V.39/397	R	-	-	-	-	-	-	-	-	-	-	-	-	-	-	-	-	-	-	-	-	-	-	-	-	-	-	-	?
	L	-	-	-	-	-	-	-	-	-	-	-	-	-	-	-	-	-	-	-	-	-	+	-	-	-	-	-	?
ZPAL V.39/399	R	-	-	-	-	-	-	-	-	-	-	-	-	-	-	-	-	-	-	-	-	-	-	-	-	-	-	?+	?X
	L	-	-	-	-	-	-	-	-	-	-	-	-	-	-	-	-	-	-	-	-	-	-	-	-	-	-	-	?
ZPAL V.39/400	R	-	-	-	-	-	-	-	-	-	-	-	-	-	-	-	-	-	-	-	-	-	-	-	-	-	-	-	?
	L	-	-	-	-	-	-	-	-	-	-	-	-	+	-	-	-	-	-	-	-	+	P	-	-	-	-	-	?
ZPAL V.39/402	R	-	-	-	-	-	P	-	-	-	-	-	-	-	-	-	-	-	-	-	-	-	-	-	-	-	-	-	?
	L	-	-	-	-	-	P	-	-	-	-	-	-	-	-	-	-	-	-	-	-	-	-	-	-	-	-	-	?

Table S4. *Proterochersis porebensis*, plastron scutes. **+** – preserved whole or nearly whole; **P** – partially preserved; **-** – not preserved or insignificant part preserved. **R** means right, **L** means left side of the body.

Specimen	Side	Extragular	Gular	Humeral	Pectoral	Abdominal		Femoral	Anal	Caudal	Intercaudal	Axillary	Inframarginal			
						1	2						1	2	3	4
ZPAL V.39/8	R	-	-	-	-	-	-	-	-	-	-	-	-	-	-	-
	L	-	-	-	-	-	-	-	-	-		-	P	P	P	-
ZPAL V.39/13	R	-	-	-	-	-	-	P	P	-	P	-	-	-	-	-
	L	-	-	-	-	-		P	P	-		-	-	-	-	-
ZPAL V.39/21	R	-	-	-	-	-	-	-	-	-	-	-	P	P	-	-
	L	-	-	-	-	-	-	-	-	-		-	-	-	-	-
ZPAL V.39/34	R	-	-	P	P	P	P	P	P	+	+	P	P	P	P	P
	L	+	P	P	P	P	P	P	+	P		P	+	+	+	P
ZPAL V.39/48	R	P	P	P	+	+	+	+	+	P	+	+	+	+	+	+
	L	+	+	P	+	+	+	+	+	+		P	+	+	P	+
ZPAL V.39/49	R	+	+	+	+	P	P	+	+	P	+	P	+	+	+	+
	L	P	+	+	+	+	+	+	+	+		+	P	+	+	P
ZPAL V.39/56	R	-	-	-	-	-	-	-	-	-	-	-	-	-	-	-
	L	-	-	-	-	-	-	-	-	+		-	-	-	-	-
ZPAL V.39/62	R	-	-	-	P	-	-	-	-	-	-	-	-	-	-	-
	L	-	-	-	P	-	-	-	-	-		-	-	-	-	-
ZPAL V.39/64	R	-	-	-	-	-	-	-	-	-	-	-	-	-	-	-
	L	-	-	P	P	-	-	-	-	-		-	-	-	-	-
ZPAL V.39/66	R	-	-	-	-	-	-	-	P	P	P	-	-	-	-	-
	L	-	-	-	-	-	-	-	P	+		-	-	-	-	-
ZPAL V.39/68	R	-	-	-	-	-	-	-	P	P	+	-	-	-	-	-
	L	-	-	-	-	-	-	-	P	P		-	-	-	-	-
ZPAL V.39/69	R	-	-	-	-	-	-	-	+	+	+	-	-	-	-	-
	L	-	-	-	-	-	-	-	+	+		-	-	-	-	-
ZPAL V.39/70	R	-	-	-	-	-	-	-	P	+	+	-	-	-	-	-
	L	-	-	-	-	-	-	-	P	P		-	-	-	-	-
ZPAL V.39/71	R	-	-	-	-	-	-	-	P	+	+	-	-	-	-	-
	L	-	-	-	-	-	-	-	P	P		-	-	-	-	-
ZPAL V.39/157	R	-	-	-	-	-	-	P	P	-	-	-	-	-	-	-
	L	-	-	-	-	-	-	-	-	-		-	-	-	-	-
ZPAL V.39/159	R	-	-	-	P	P	P	P	-	-	-	-	-	-	-	-
	L	-	-	-	-	-	-	-	-	-		-	-	-	-	-
ZPAL V.39/160	R	-	-	-	-	-	-	-	-	-	-	-	-	P	P	P
	L	-	-	-	-	-	-	-	-	-		-	-	-	-	-
ZPAL V.39/170	R	-	-	-	-	-	-	-	-	-	-	-	-	-	-	-
	L	-	-	-	-	-	-	P	P	-		-	-	-	-	-
ZPAL V.39/172	R	-	-	P	-	-	-	-	-	-	-	-	-	-	-	-
	L	-	-	P	-	-	-	-	-	-		-	-	-	-	-
ZPAL V.39/185	R	-	-	-	-	-	-	-	-	-	-	-	-	-	-	-
	L	-	-	-	P	-	-	-	-	-		-	-	-	-	-
ZPAL V.39/186	R	-	-	-	-	-	-	-	-	-	-	-	-	-	-	-
	L	-	P	-	-	-	-	-	-	-		-	-	-	-	-
ZPAL V.39/187	R	+	P	-	-	-	-	-	-	-	-	-	-	-	-	-
	L	-	-	-	-	-	-	-	-	-		-	-	-	-	-

Specimen	Side	Extragular	Gular	Humeral	Pectoral	Abdominal		Femoral	Anal	Caudal	Intercaudal	Axillary	Inframarginal			
						1	2						1	2	3	4
ZPAL V.39/189	R	P	P	-	-	-	-	-	-	-	-	-	-	-	-	-
	L	-	-	-	-	-	-	-	-	-		-	-	-	-	-
ZPAL V.39/194	R	-	-	P	P	-	-	-	-	-	-	-	-	-	-	-
	L	-	-	-	-	-	-	-	-	-		-	-	-	-	-
ZPAL V.39/199	R	-	-	-	-	-	-	-	-	-	-	-	-	-	-	-
	L	-	-	-	-	-	-	-	-	+		-	-	-	-	-
ZPAL V.39/200	R	-	-	-	-	-	-	-	-	-	-	-	-	-	-	-
	L	-	-	-	-	-	-	-	-	?+		-	-	-	-	-
ZPAL V.39/333	R	+	P	P	-	-	-	-	-	-	-	-	-	-	-	-
	L	-	-	P	-	-	-	-	-	-		-	-	-	-	-
ZPAL V.39/343	R	-	-	-	-	-	-	-	-	-	-	-	-	-	-	-
	L	-	-	-	P	P	P	-	-	-		-	-	-	-	-
ZPAL V.39/379	R	+	+	P	-	-	-	-	-	-	-	-	-	-	-	-
	L	-	-	-	-	-	-	-	-	-		-	-	-	-	-
ZPAL V.39/385	R	P	+	P	P	P	-	-	-	-	-	-	-	-	-	-
	L	+	+	P	P	P	-	-	-	-		-	-	-	-	-
ZPAL V.39/387	R	-	-	-	-	-	-	-	-	-	-	-	-	-	-	-
	L	+	+	P	-	-	-	-	-	-		-	-	-	-	-
ZPAL V.39/388	R	P	P	-	-	-	-	-	-	-	-	-	-	-	-	-
	L	-	-	-	-	-	-	-	-	-		-	-	-	-	-
ZPAL V.39/389	R	-	-	-	-	-	-	-	-	-	-	-	-	-	-	-
	L	-	-	-	-	-	-	-	-	+		-	-	-	-	-
ZPAL V.39/400	R	-	-	-	-	-	-	-	-	-	-	-	-	-	-	-
	L	-	-	-	-	-	-	-	-	-		-	-	-	P	-
ZPAL V.39/404	R	P	P	-	-	-	-	-	-	-	-	-	-	-	-	-
	L	-	-	-	-	-	-	-	-	-		-	-	-	-	-

Table S5. Definition of landmarks.

Plastron region	Plane	Landmark	Definition
Gular	**Ventral**	**1**	Caudal end of the intergular sulcus
		2	Caudal end of the sulcus between the gular and extragular scute
		3	Laterocaudal tip of the extragular scute
		12	Cranial end of the sulcus between the gular and extragular scute
		21	Cranial end of the intergular sulcus
	Vertical cross-section	**1**	Sulcus between the extragular and humeral scute
		15	Posterodorsal edge of the extragular scute
Anal	**Ventral**	**1**	Cranial tip of the intercaudal scute
		2	Caudal edge of the intercaudal scute
		3	Cranial end of the caudointercaudal sulcus
		4	Caudal end of the caudointercaudal sulcus
		17	Lateral end of the caudoanal sulcus

Table S6. MANOVA of size variation in the anal plastral region.

Effect	SS	MS	df	F	p-value
Species (centroid size)	551.44	551.44	1	2.22	> 0.3
Species (shape)	0.01	0.0005	30	0.33	1
Sex (centroid size)	644.52	644.52	1	4.15	> 0.2
Sex (shape)	0.04	0.001	30	2.51	< 0.01

Table S7. Mahalanobis distances among groups based on the anal plastral region, p-values from permutation tests in brackets.

	Juveniles	Group II (“Females”)
Juveniles	-	6.1 (0.03)
Group I (“Males”)	7.8 (0.04)	4.2 (< 0.02)

Table S8. Examples of sexual dimorphism in extant and fossil turtles.

Body section		Feature	References
Limbs		Feet wideness	Keswick & Hofmeyr 2015
		Rugose surfaces on male hindlimbs	Berry & Shine 1980
		Size and shape of claws on forelimbs	Wibbels *et al.* 1991; Wyneken 2001
Pelvis		Size of pelvic aperture	Cordero 2018
Shell	**Whole shell**	Kinesis	Pritchard 2008; Keswick & Hofmeyr 2015
		Presence or absence of particular shell scutes	Lichtig & Lucas 2017
		Relative shape and size of particular shell scutes or bones	Brophy 2006; Leuteritz & Gantz 2013; Lichtig & Lucas 2017
		Shape and size of posterior aperture of the shell	Pritchard 2008; Leuteritz & Gantz 2013; Keswick & Hofmeyr 2015
		Shell height	Brophy 2006; Pritchard 2008; Keswick & Hofmeyr 2015
		Shell length	Chiari & Claude 2011
		Shell width	Brophy 2006; Chiari & Claude 2011; Keswick & Hofmeyr 2015
		Time of fontanelle retention	Pritchard 2008
	Carapace	Allometric growth dynamic	Chiari & Claude 2011; Keswick & Hofmeyr 2015
		Degree of saddling	Pritchard 2008
		Shape of the posterior part	Wibbels *et al.* 1991; Pritchard 2008
		Plastron length	Brophy 2006
	Plastron	Seasonal plastron de-ossification and scute softening in males	Wibbels *et al.* 1991; Wyneken 2001; Pritchard 2008
		Shape and size of anal notch	Brophy 2006; Pritchard 2008; Cadena *et al.* 2013; Leuteritz & Gantz 2013; Sullivan & Joyce 2017
		Shape and size of gular processes	Pritchard 2008
		Ventral concavity	Wyneken 2001; Pritchard 2008; Cadena *et al.* 2013; Leuteritz & Gantz 2013
Tail		Cloacal position	White & Murphy 1973; Wyneken 2001
		Tail length	Berry & Shine 1980; Wibbels *et al.* 1991; Wyneken 2001; Sullivan & Joyce 2017
Whole body		Body size	Berry & Shine 1980; Brophy 2006; Pritchard 2008; Leuteritz & Gantz 2013; Ceballos & Iverson 2014; Keswick & Hofmeyr 2015; Lichtig & Lucas 2017; Cordero 2018

FIGURES

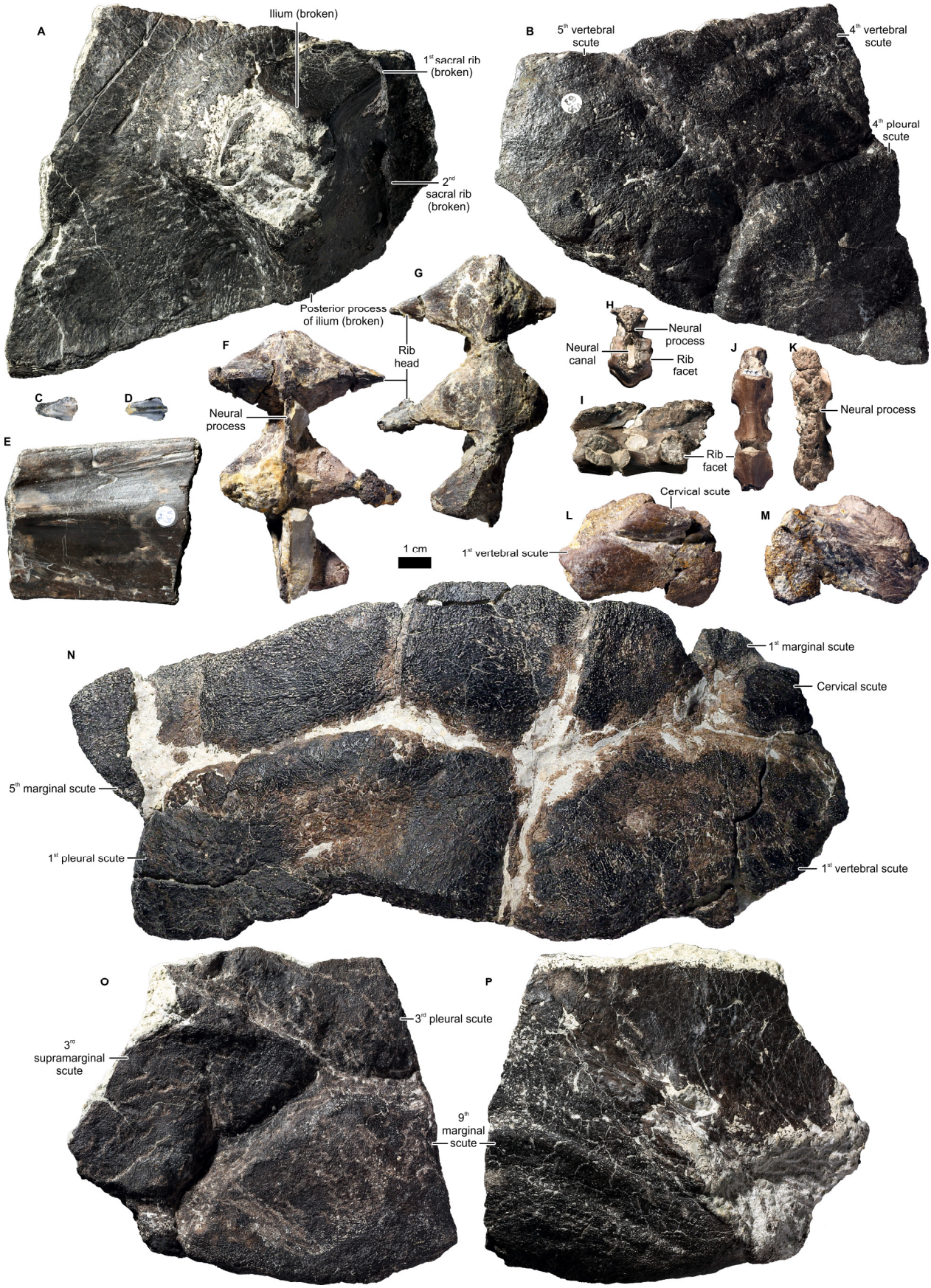

Fig. S1. Carapace variability of *Proterochersis porebensis*.

A–B: ZPAL V.39/63, carapace fragment of a large specimen with attached ilium in (**A**) visceral and (**B**) external view.

C–D: ZPAL V.39/381, fragmentary costal of a (?)hatchling in (**C**) external and (**D**) visceral view.

E: ZPAL V.39/176, costal fragment of a large specimen in visceral view.

F–G: ZPAL V.39/378, fragmentary dorsal vertebral column in (**F**) dorsal and (**G**) ventral view.

H–K: ZPAL V.39/377, fragmentary dorsal vertebral column of a juvenile in (**H**) cross-section (posterior view at a broken vertebra), (**I**) lateral right, (**J**) ventral, and (**K**) dorsal view.
L–M: ZPAL V.39/390, anterior part of a carapace in (**L**) external and (**M**) visceral view.
N: ZPAL V.39/57, anterior part of a carapace in external view.
O–P: ZPAL V.39/60, carapace fragment in (**O**) external and (**P**) visceral view.

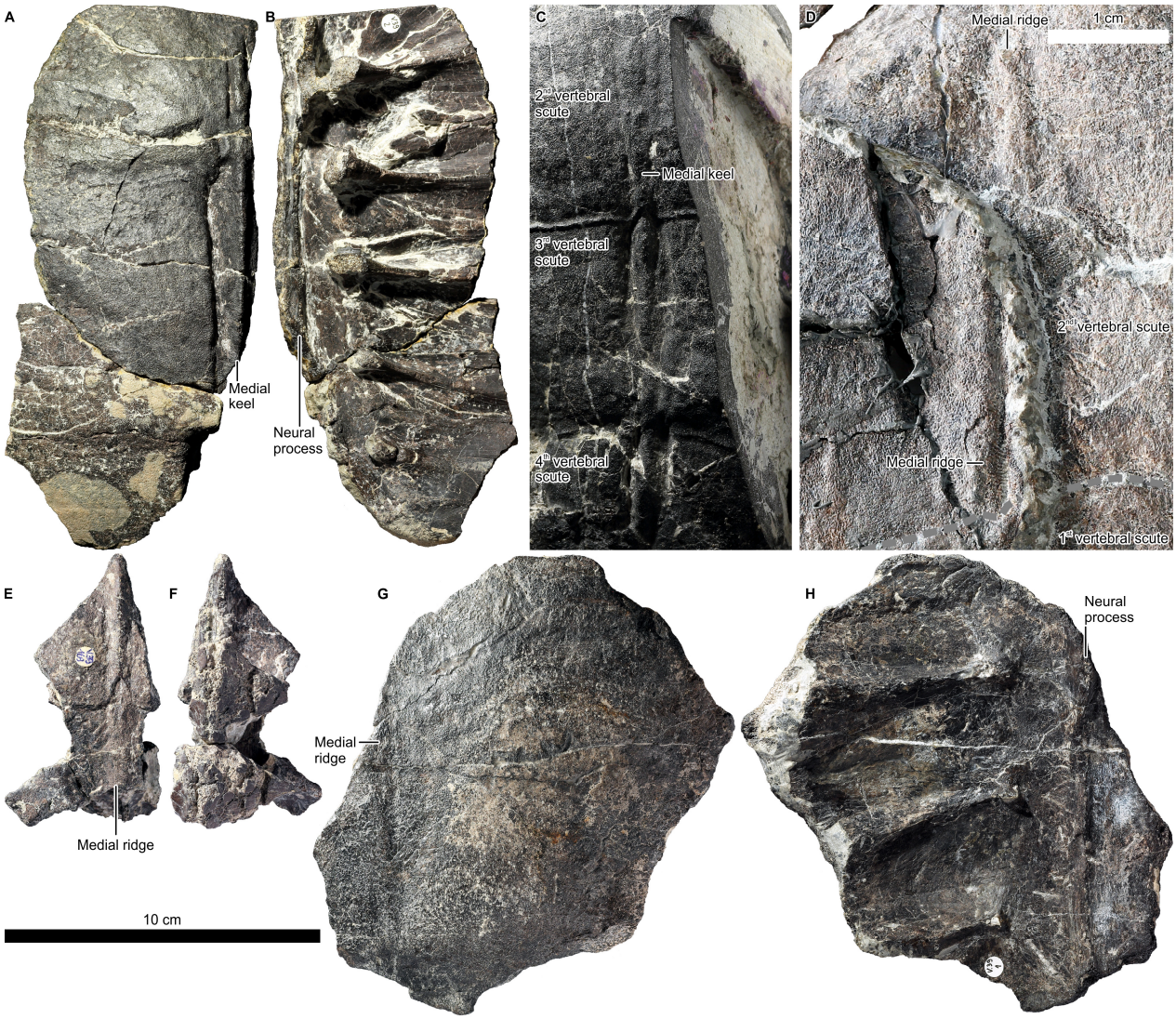

Fig. S2. Middorsal structures of *Proterochersis porebensis*.

A–B: ZPAL V.39/2, carapace fragment in (**A**) external and (**B**) visceral view.

C: ZPAL V.39/34, close-up on middorsal carapacial keel in dorsal view.

D: ZPAL V.39/72, close-up on middorsal carapacial ridge in anterodorsal view.

E–F: ZPAL V.39/169, carapace fragment with part of dorsal vertebral column in (**E**) dorsal and (**F**) ventral view.

G–H: ZPAL V.39/1, carapace fragment in (**G**) external and (**H**) visceral view.

A–B and **E–H** in the same scale.

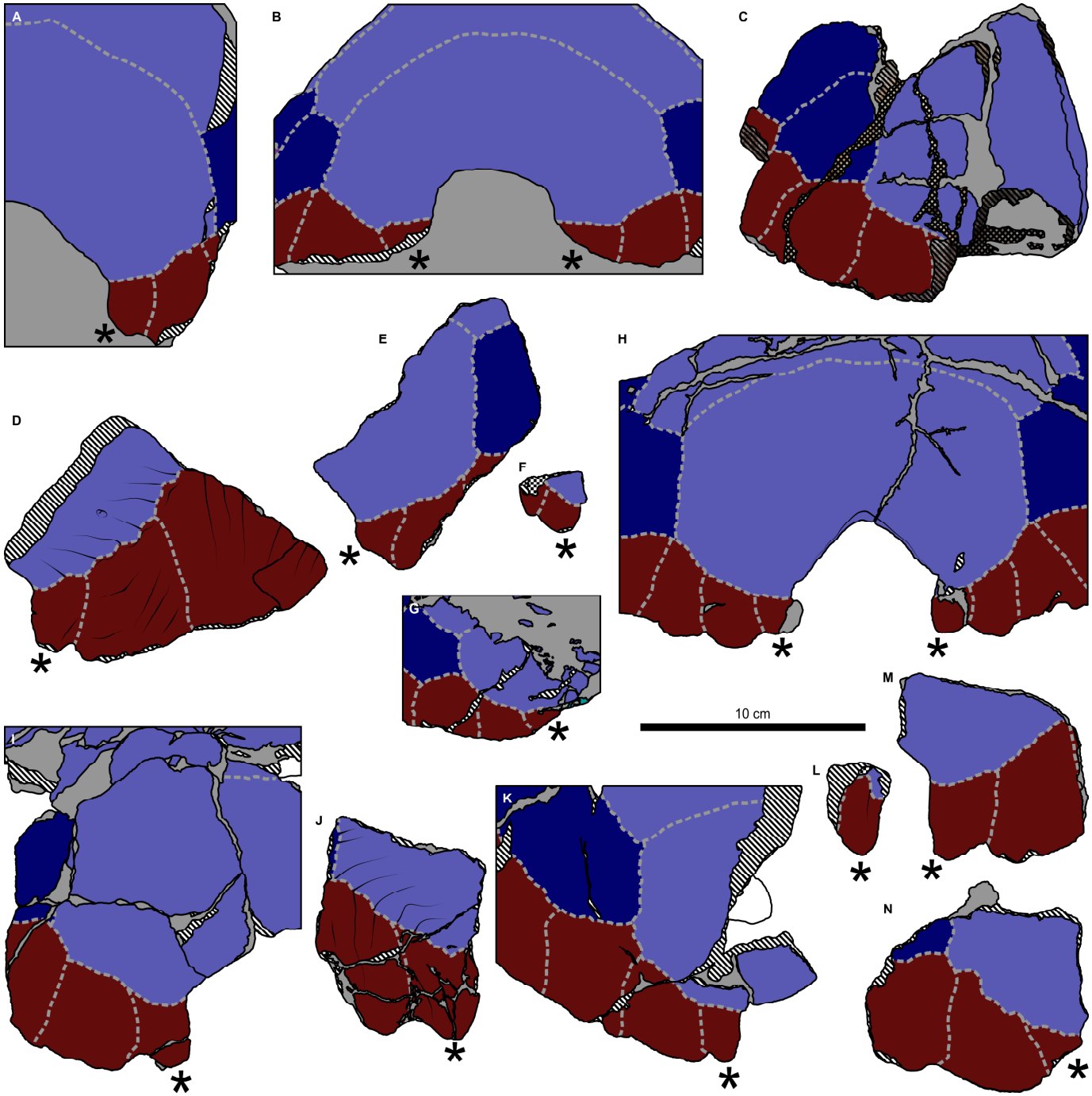

Fig. S3. Posterior regions of carapace of (**A–B**) *Proterochersis robusta* and (**C–M**) *P. porebensis* in external view.

A: CSMM uncat.
B: SMNS 17561.
C: SMNS 17755a.
D: ZPAL V.39/6.
E: ZPAL V.39/18.
F: ZPAL V.39/23.
G: ZPAL V.39/34.
H: ZPAL V.39/48.
I: ZPAL V.39/49.
J: ZPAL V.39/59.
K: ZPAL V.39/72.
L: ZPAL V.39/213.
M: ZPAL V.39/380.
N: ZPAL V.39/386.

Last marginals indicated by **asterisk**.

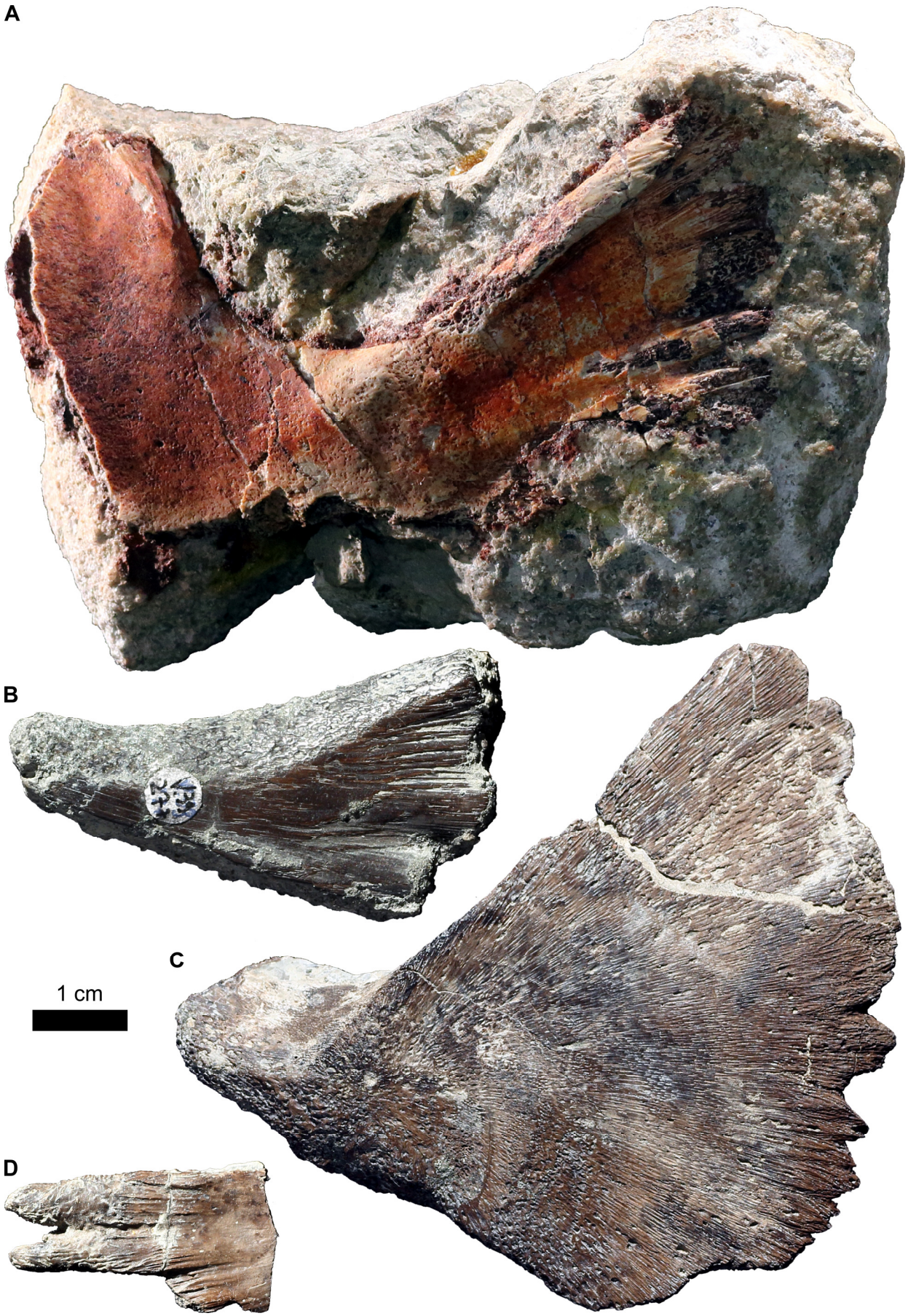

Fig. S4. Plastral bones of young individuals of (**A**) *Proterochersis robusta* and (**B–D**) *P. porebensis*.
A: SMNS 81917, hyoplastron or hypoplastron.
B: ZPAL V.39/277, xiphiplastron or mesoplastron.
C: ZPAL V.39/197, hyoplastron in external view.
D: ZPAL V.39/384

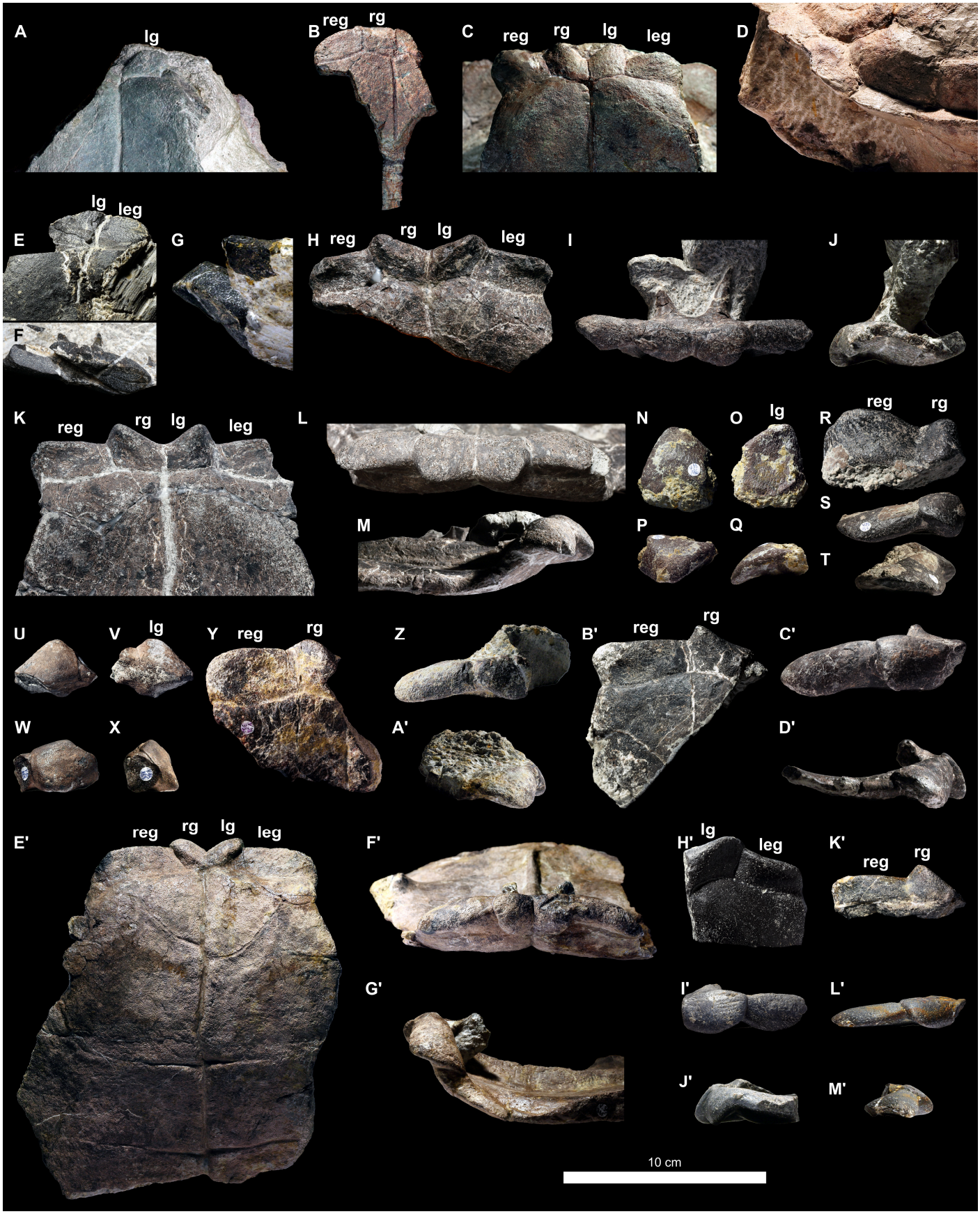

Fig. S5. Gular plastral regions of (**A–D**) *Proterochersis robusta* and (**E–M'**) *P. porebensis*.

A: CSMM uncat. in ventral view.

B: SMNS 16603, plastron in ventral view.

C–D: SMNS 17561 in (**C**) ventral and (**D**) lateral left view.

E–G: ZPAL V.39/34 in (**E**) ventral, (**F**) anterior, and (**G**) lateral left view.

H–J: ZPAL V.39/48 in (**H**) ventral, (**I**) anterior, and (**J**) lateral left view.

K–M: ZPAL V.39/49 in (**K**) ventral, (**L**) anterior, and (**M**) lateral right view.

N–Q: ZPAL V.39/186, gular tubercle in (**N**) dorsal, (**O**) ventral, (**P**) anterior, and (**Q**) lateral left view.

R–T: ZPAL V.39/187 in (**R**) ventral, (**S**) anterior, and (**T**) lateral right view.
U–X: ZPAL V.39/189, gular tubercle in (**U**) dorsal, (**V**) ventral, (**W**) anterior, and (**X**) lateral right view.
Y–A′: ZPAL V.39/333 in (**Y**) ventral, (**Z**) anterior, and (**A′**) lateral right view.
B′–D′: ZPAL V.39/379 in (**B′**) ventral, (**C′**) anterior, and (**D′**) lateral right view.
E′–G′: ZPAL V.39/385 in (**E′**) ventral, (**F′**) anterior, and (**G′**) lateral left view.
H′–J′: ZPAL V.39/387 in (**H′**) ventral, (**I′**) anterior, and (**J′**) lateral left view.
K′–M′: ZPAL V.39/388 in (**K′**) ventral, (**L′**) anterior, and (**M′**) lateral right view.

Abbreviations:

leg – left extragular scute.
lg – left gular scute.
reg – right extragular scute.
rg – right gular scute.

REFERENCES

Berry, J. F. & Shine, R. 1980. Sexual size dimorphism and sexual selection in turtles (order Testudines). *Oecologia*, **44**, 185–191.

Bookstein, F. L. 1997. *Morphometric tools for landmark data: Geometry and biology*. Cambridge University Press.

Brophy, T. R. 2006. Allometry and sexual dimorphism in the snail-eating turtle *Malayemys macrocephala* from the Chao Phraya River Basin of central Thailand. *Chelonian Conservation and Biology*, **5**, 159–165, doi: 10.2744/1071-8443(2006)5[159:AASDIT]2.0.CO;2.

Cadena, E. A., Jaramillo, C. A. & Bloch, J. I. 2013. New material of the platychelyid turtle *Notoemys zapatocaensis* from the Early Cretaceous of Colombia; Implications for understanding Pleurodira evolution. *In*: Brinkman, D. B., Holroyd, P. A. & Gardner, J. D. (eds) *Morphology and Evolution of Turtles*. Springer Science+Business Media, Dordrecht, 105–120.

Ceballos, C. P. & Iverson, J. B. 2014. Patterns of sexual size dimorphism in Chelonia: Revisiting Kinosternidae. *Biological Journal of the Linnean Society*, **111**, 806–809, doi: DOI 10.1111/j.1095-8312.2012.02015.x.

Chiari, Y. & Claude, J. 2011. Study of the carapace shape and growth in two Galápagos tortoise lineages. *Journal of Morphology*, **272**, 379–386, doi: 10.1002/jmor.10923.

Cignoni, P., Callieri, M., Corsini, M., Dellepiane, M., Ganovelli, F. & Ranzuglia, G. 2008. MeshLab: An open-source mesh processing tool. In: *Sixth Eurographics Italian Chapter Conference*. 129–136, doi: 10.2312/LocalChapterEvents/ItalChap/ItalianChapConf2008/129-136.

Cordero, G. A. 2018. Is the pelvis sexually dimorphic in turtles? *The Anatomical Record*, 1–22, doi: 10.1002/ar.23831.

de Broin, F. 1984. *Proganochelys ruchae* n.sp., chélonien du Trias supérieur de Thaïlande. *Studia Palaeocheloniologica*, **1**, 87–97.

Fraas, E. 1913. *Proterochersis*, eine pleurodire Schildkröte aus dem Keuper. *Jahreshefte des Vereins für Vaterlandische Naturkunde in Württemberg*, **69**, 13–30.

Gaffney, E. S. 1986. Triassic and Early Jurassic turtles. *In*: Padian, K. (ed.) *The Beginning of the Age of Dinosaurus. Faunal Change across the Triassic-Jurassic Boundary*. Press Syndicate of the University of Cambridge, Cambridge, 183–187.

Gaffney, E. S. 1990. The comparative osteology of the Triassic turtle *Proganochelys*. *Bulletin of the American Museum of Natural History*, **194**, 1–263.

Karl, H.-V. & Tichy, G. 2000. *Murrhardtia staeschei* n. gen. n. sp. – eine neue Schildkröte aus der Oberen Trias von Süddeutschland. *Joannea Geologie und Paläontologie*, **2**, 57–72.

Keswick, T. & Hofmeyr, M. D. 2015. Sexual dimorphism and geographic variation in the morphology of a small southern African tortoise *Psammobates oculifer*. *Amphibia-Reptilia*, **36**, 55–64, doi: 10.1163/15685381-00002976.

Klingenberg, C. P. 2009. Morphometric integration and modularity in conFigurations of landmarks: Tools for evaluating a priori hypotheses. *Evolution and Development*, **11**, 405–421, doi: 10.1111/j.1525-142X.2009.00347.x.

Klingenberg, C. P. 2011. MorphoJ: An integrated software package for geometric morphometrics. *Molecular Ecology Resources*, **11**, 353–357, doi: 10.1111/j.1755-0998.2010.02924.x.

Leuteritz, T. E. J. & Gantz, D. T. 2013. Sexual Dimorphism in Radiated Tortoises (*Astrochelys radiata*). *Chelonian Research Monographs*, **6**, 105–112, doi: 10.3854/crm.6.a18p105.

Lichtig, A. J. & Lucas, S. 2017. Sutures of the shell of the Late Cretaceous-Paleocene baenid turtle *Denazinemys*. *Neues Jahrbuch für Geologie und Paläontologie - Abhandlungen*, **283**, 1–8, doi: 10.1127/njgpa/2017/0622.

Młynarski, M. 1976. *Encyclopedia of Paleoherpetology. Part 7. Testudines*. Gustav Fischer Verlag, Stuttgart and New York, 130 pp.

Pritchard, P. C. H. 2008. Evolution and structure of the turtle shell. *In*: Wyneken, J., Godfrey, M. H. & Bels, V. (eds)

Biology of Turtles. CRC Press, Boca Raton, London & New York, 46–83.

Rohlf, F. J. 2015. The tps series of software. *Hystrix*, **26**, 1–4, doi: 10.4404/hystrix-26.1-11264.

Scheyer, T. M. & Sander, P. M. 2007. Shell bone histology indicates terrestrial palaeoecology of basal turtles. *Proceedings of the Royal Society of London B: Biological Sciences*, **247**, 1885–1893.

Stromer, E. F. 1912. *Lehrbuch Der Paläozoologie. II. Teil: Wirbeltiere*. B.G. Teubner, Leipzig and Berlin, 325 pp.

Sulej, T., Niedźwiedzki, G. & Bronowicz, R. 2012. A new Late Triassic vertebrate fauna from Poland with turtles, aetosaurs, and coelophysoid dinosaurs. *Journal of Vertebrate Paleontology*, **32**, 1033–1041, doi: 10.1080/02724634.2012.694384.

Sullivan, P. M. & Joyce, W. G. 2017. The shell and pelvic anatomy of the Late Jurassic turtle *Platychelys oberndorferi* based on material from Solothurn, Switzerland. *Swiss Journal of Palaeontology*, **136**, 323–343.

Szczygielski, T. 2017. Homeotic shift at the dawn of the turtle evolution. *Royal Society Open Science*, **4**, 160933, doi: http://dx.doi.org/10.1098/rsos.160933.

Szczygielski, T. & Sulej, T. 2016. Revision of the Triassic European turtles *Proterochersis* and *Murrhardtia* (Reptilia, Testudinata, Proterochersidae), with the description of new taxa from Poland and Germany. *Zoological Journal of the Linnean Society*, **177**, 395–427, doi: 10.1111/zoj.12374.

White, J. B. & Murphy, G. G. 1973. The reproductive cycle and sexual dimorphism of the common snapping turtle, *Chelydra serpentina serpentlna*. *Herpetologica*, **29**, 240–246.

Wibbels, T., Owens, D. W. & Rostal, D. C. 1991. Soft plastra of adult male sea turtles: An apparent secondary sexual characteristic. *Herpetological Review*, **22**, 47–49.

Wild, R. 1987. Die Tierwelt der Keuperzeit (unter besonderer Berücksichtigung der Wirbeltiere. *Natur an Rems und Murr*, **6**, 17–43.

Wu, C. 2011. VisualSFM: A visual structure from motion system. Available at http://ccwu.me/vsfm/ (acessed 22 June 2018).

Wyneken, J. 2001. *The Anatomy of Sea Turtles*. U.S. Department of Commerce NOAA Technical Memorandum NMFS-SEFSC-470, 172 pp.

MPEG 0451

MPEG 0459

MPEG 0464

Laboratório de Paleontologia de
Ribeirão Preto - FFCLRP-USP

0 5 cm